universität wien

MASTERARBEIT / MASTER'S THESIS

Titel der Masterarbeit / Title of the Master's Thesis

„How muscular characteristics of the Greenland shark could give insight into the outstanding aging abilities of the Greenland shark- a comparison with the small-spotted catshark"

verfasst von / submitted by

Marlene Luisa Musial, BSc

angestrebter akademischer Grad / in partial fulfilment of the requirements for the degree of

Master of Science (MSc)

Wien, 2022 / Vienna, 2022

Studienkennzahl lt. Studienblatt / degree programme code as it appears on the student record sheet:	UA 066 834
Studienrichtung lt. Studienblatt / degree programme as it appears on the student record sheet:	Molekulare Biologie
Betreut von / Supervisor:	Dr. Dea Slade, PhD

Acknowledgements

I would like to thank everybody who supported me during the thesis. This project would not have been possible without the support of many people. First of all, I want to thank my two supervisors from the University of Copenhagen Robert Seaborne, PhD, and my group leader and main supervisor at the University of Copenhagen, Associate Prof. Julien Ochala, PhD, MSc who guided me through my thesis, mentored me and always offered advise and encouragement. Besides that, I am also incredibly thankful for the support of my lab colleagues, especially Jenni Laitila, PhD, MSc who guided me through the Cryosection experiment and Elise Thomsen, MSc, who helped me with the Mant-ATP chase experiment. Also Anders Karlsen, PhD, MSc from the Xlab assisted me with his expertise. Finally, I would also like to thank Dr. Dea Slade, PhD for supervising my thesis.

Overall, the project also would not have been possible without the samples for the small-spotted catshark that were nicely provided by the Fiskeri- og Søfartsmuseet i Esbjerg and the Greenland shark samples that were kindly provided by Prof. Holly Shiels BSc, MSc, PhD.

Zusammenfassung

Gesundes Altern, Langlebigkeit und steigende Lebenserwartung sind Themen, die immer bedeutender werden. Der Grönlandhai (*Somniosus microcephalus*) hat eine Lebenserwartung von mindestens 272 Jahren hat, was ihn zum Wirbeltier mit der höchsten Lebenserwartung macht. Trotz dessen sind Studien über den *Somniosus microcephalus* beschränkt auf Verbreitung, Lebenszyklus, Verhalten, Migration, Ernährung, Phylogenie, sensorische Fähigkeiten und das mitochondriales Genom. Forschung zur potenziellen Einzigartigkeit der Organe dieser Spezies (inklusive Skelettmuskel) und ihrer spezifischen metabolischen Regulation wurden bisher noch nicht durchgeführt.

Deshalb werde ich im Zuge meiner Masterarbeit versuchen Anpassungen der Skelettmuskulatur des *Somniosus microcephalus*, zu erforschen. Der Fokus liegt auf Myosin, dem häufigsten Protein, seiner Funktionalität und metabolischen Kraft. Die Ergebnisse werden mit einem Hai mit normaler Lebenserwartung verglichen (Kleingefleckter Katzenhai *Scyliorhinus canicula,* erwartete durchschnittliche Lebenserwartung von 17 Jahren). Dafür werde ich Muskelgewebe analysieren, und morphologische Versuche an roten und weißen Muskeln, sowie funktionelle/metabolische Versuche (Mant-ATP Chase Experiments), durchführen.

Diese Masterarbeit wird von Julien Ochala und Robert Seaborne der Universität Kopenhagen, sowie Dea Slade der Universität Wien betreut. Julien Ochala und Robert Seaborne sind führende Wissenschaftler im Bereich der Muskelphysiologie und der Genomsequenzierung. Die Arbeit wird durchgeführt am Departement für Biomedizin der Universität Kopenhagen.

Abstract

Healthy aging, longevity and increasing life expectancy are topics that become more and more important over time. Interestingly, the Somniosus microcephalus (Greenland Shark) defies such topics as it can live on average 272 years, which makes it the world's longest-lived vertebrate on the planet. Despite its extreme life expectancy, studies on the Somniosus microcephalus have been limited to its demographics, life history, behaviour/interactions, movement ecology, diet/trophic ecology, phylogeny, sensory abilities and mitochondrial genome. Hence, research on the potential uniqueness of this species organs (including skeletal muscle) and its specific metabolic regulation have been overlooked.

In line with this, my Master's thesis will aim to explore skeletal muscle adaptations in Somniosus microcephalus, by focussing on the most abundant protein, myosin, its functionality and metabolic power and by comparing the data to a shark species with normal life expectancy (small-spotted catshark, lifespan estimation of 17 years). For that, I will dissect muscle tissue from these vertebrate animals and will run morphological assays of red and white muscles as well as functional/metabolic assays (Mant-ATP Chase Experiments).

To achieve this Master's project, I will be supervised by Julien Ochala and Robert Seaborne from the University of Copenhagen, who are leading scientists in the field of muscle physiology and genome sequencing, as well as Dea Slade from the University of Vienna. All the work will be run at the Department of Biomedical sciences at the University of Copenhagen.

Outline

Introduction

Muscles

Muscle structure

Skeletal muscle tissue is largely comprised of assembled muscle cells (myofibers), as well as other cellular and tissue material, such as connective tissue. The size of a skeletal muscle is mostly determined by the number and size of individual myofibers, however fat and connective tissue may lead to an altered ratio (FORTIN et al., 2014, Javan et al., 2013).

Myofibers are the largest cells in the body (Hansson et al., 2020). They are a relatively unique type of cell, and, unlike traditional cells, have multiple nuclei (myonuclei) and are post-mitotic (S. Hikida, 2011). These nuclei are responsible for protein synthesis control in the region of the muscle, the nuclear domain, and have a regulated but not constant size (S. Hikida, 2011). The myonuclear domain theory proposes that myonuclei are added to muscle fibers when the fiber cross-sectional area increases (ConceiÇÃO et al., 2018). Another study proposes that the number of myonuclei in a fiber segment is determined by growth signals during development and hypertrophy. It states that the number of nuclei and a setpoint *a* determine cellular dimensions and the number of nuclei scales invariably sub linearly to cell volume ($b < 1$), but linearly to cell surface ($b = 1$) (Hansson et al., 2020).

The protein production in the nuclear domains is normally coordinated, which leads to similar protein production across the length of the fiber. However, non-uniformity in the production of contractile properties in adjacent segments sometimes can occur (Wilkins et al., 2001). Muscle growth, repair and regeneration mostly works through satellite cells (adult stem cells of skeletal muscle), that are located between the sarcolemma and the basal lamina (Macaluso and Myburgh, 2012, S. Hikida, 2011). The proliferation and differentiation of these stem cells into new myofibers occurs after activation through myogenic factors (Bareja et al., 2014). The muscle structure is shown in figure 1. The epimysium, a layer of connective tissue, surrounds individual muscles. Muscles are arranged in bundles of grouped myofibers and surrounded by another layer of connective tissue, the perimysium. Every myofiber is surrounded by a cell membrane or sarcolemma. The internal myofilament structure and the sarcolemma are physically connected through several proteins. The connection mostly occurs at the actin proteins in the thin filament. Lack of, or defunct,

connective proteins may lead to damage of the sarcolemma, muscle weakness, and atrophy (Frontera and Ochala, 2015).

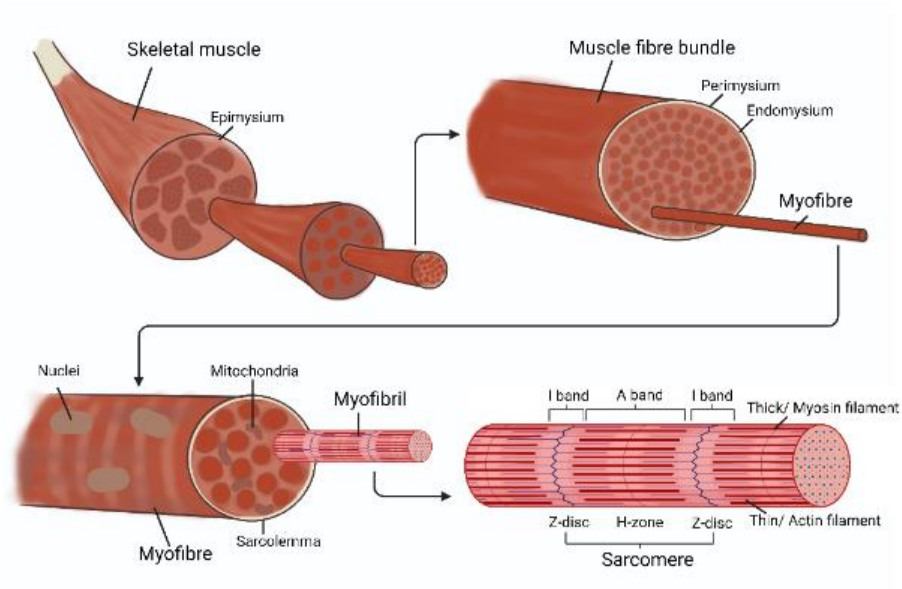

Figure 1: Skeletal muscle structure. *Skeletal muscle is comprised of muscle fiber bundles, comprised of myofibers/ muscle fibers. Muscles are covered by the epimysium, muscle fiber bundles are covered by the perimysium and muscle fibers are covered by the endomysium. A skeletal muscle fiber is surrounded by the sarcolemma, containing sarcoplasm. Each muscle fiber is composed of many myofibrils, having sarcomeres as contractile units. Created with Procreate, Adobe Illustrator and Biorender.com.*

The cytoskeleton determines the shape and length of myofibers and transmits force generated by the actin-myosin interaction to the extracellular skeleton. Myofibrils run along the fiber major axis from one end to the other and end with the myotendinous junction that transfers tension to the tendons. They are a specialized component of the cytoskeleton. The cytoskeleton contains several signalling proteins (Schiaffino and Reggiani, 2011).

Without the water content, single myofibers are comprised of ~80% protein (contractile, regulatory, cytoskeletal) and ~8% sarcoplasm (Hoppeler et al., 1973). Myofibers are comprised of myofibrils, containing myofilaments (Frontera and Ochala, 2015). The contractile machinery of skeletal muscles is comprised of sarcomeres that form myofibrils. This creates the striated pattern of myofibers (Schiaffino and Reggiani, 2011). The sarcomere is made up of many proteins that contribute to excitation-contraction coupling, energy release, and force and power generation (Ottenheijm and Granzier, 2010). Figure 2 shows the main components of the striated muscle sarcomere. In each sarcomere thin (actin) and thick (myosin) filaments overlap. Additionally, the cytoskeleton is formed of transversal structures, the Z-disc and M-bands and longitudinal filaments composed of the giant proteins

titin and nebulin, running in parallel with thin and thick filaments (Schiaffino and Reggiani, 2011). Actin and myosin are the most abundant myofilaments (proteins). They form ~70-80% of the total protein content of a single myofiber. Myosin is a motor protein (Frontera and Ochala, 2015). Many contractile and cytoskeletal proteins exist as multiple isoforms, which leads to different mechanical properties of the myofibrils in different types of myofibers (Schiaffino and Reggiani, 2011). Myosin, as well as myosin genes in mammals and humans are described below. Other important proteins are the regulatory proteins of the calcium-dependent troponin complex (troponins C, I, and T), and tropomyosin. They are associated with the actin filament and are important in the activation process of myofilament sliding and force generation (Frontera and Ochala, 2015). The interaction of actin and myosin filaments mediate the contractile function of the sarcomere and is controlled by calcium through the troponin-tropomyosin complex. The thin filament components are very similar in all myofibers. Actin is the main component of the thin filaments. α-skeletal and α-cardiac isoforms of actin exist (Gunning et al., 1983). The Z-disc provides a mechanical link to transmit force longitudinally between adjacent sarcomeres and transversally through the extra myofibrillar cytoskeleton to adjacent myofibrils and costameres. They are also responsible for detecting force and link tension along the myofibrils through signalling (Pyle and Solaro, 2004). A network of α-actinin filaments links thin filaments, and binds titin and nebulin (Schiaffino and Reggiani, 2011). It is known that some molecular components of the sarcomere exist as multiple isoforms. They are differentially distributed in slow and fast fibers. Isomers occurring in slow fibers are tropomyosin α-slow, TnC-slow, TnI-slow, TnT-slow, myomesin-1 EH, MyHC-1 or β/slow, MyLC-1s, MyLC-2s, MBP-C-slow, Titin long isoforms, α-actinin-slow, etc.. Isomers that occur in fast fibers are α-actintin-fast, Tropomyosin- α-fast, TnC-fast, TnI-fast, TnT-fast, Myomesin-1 and 3, MyHC 2A, 2B and 2X, MyLC-2f, MyLC-1f/3f, MBP-C-fast, Titin short isoforms, etc.. There are also some general isoforms, such as actin, Myomesin-1, etc. (Schiaffino and Reggiani, 2011, Luther, 2009).

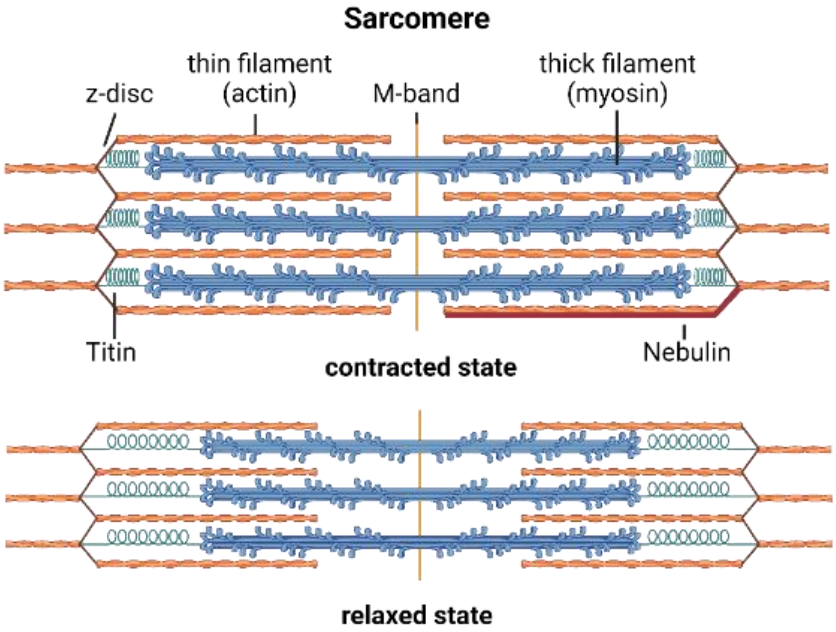

Figure 2: Schematic of the striated muscle sarcomere. *The thick filament (actin) is shown in orange, the thin filament (myosin) in blue, Titin is shown in green, and Nebulin in red. Created with Biroender.com.*

The sarcoplasm of myofibers contains a transverse tubular system (T-tubule), the sarcoplasmic reticulum and a mitochondrial network. The amount of these elements depends largely on the fiber type of myofiber (see `myofiber types`). The inward folded sarcolemma forms the T-tubule system, which conducts the nerve action potential to the interior of the cell (Jayasinghe and Launikonis, 2013). It is in contact with the cell exterior and helps to spread the excitation interval uniformly throughout the myofiber (Frontera and Ochala, 2015). The sarcoplasmic reticulum stores, releases and reuptakes calcium after activation (Lamboley et al., 2014). The sarco/endoplasmic reticulum Ca^{2+}-ATPase (SERCA) and calsequestrin help to maintain calcium homeostasis in the sarcoplasmic reticulum (Frontera and Ochala, 2015). Mitochondria generate the energy for muscle actions. They form a three-dimensional network throughout the cell and need oxygen (Dahl et al., 2015). Between the mitochondria and the sarcolemma, oxygen is transported. The distance between these two is important, especially during aerobic exercise. Also in the inter-myofibrillar space mitochondria are located (Frontera and Ochala, 2015). Stimuli, such as exercise, neuromuscular pathologies or aging can lead to structural and functional changes of the muscular elements (Yan et al., 2012). For example aging that can lead to a fragmented sarcoplasmic reticulum with impaired calcium release and muscle activation, which can lead to muscle weakness (Weisleder et al., 2006).

Myofiber types

Historically, until around 1968–1970, mammalian skeletal muscles were classified as either 'fast' or 'slow' twitch muscles. Fast ones were the white muscles, characterized by glycolytic metabolism and specialized for phasic activity, and slow ones the red muscles, rich in myoglobin and oxidative enzymes and specialized for more continuous activity (Needham, 1926). However, fast myofibers are heterogenous and enzyme histochemical procedures for myosin ATPase led to the identification of two fiber populations, called type 2A and 2B fibers. Type 1 fibers are predominant in slow-twitch muscles (Brenner and Eisenberg, 1986, Guth and Samaha, 1969). 2A and 2B fibers have high levels of glycolytic enzymes. Therefore the fibers are classified into slow oxidative (type 1), fast-twitch oxidative glycolytic (2A), and fast-twitch glycolytic fibers (2B) (Peter et al., 1972). Single fiber microdissection made precise analyses of metabolic properties possible (Essén et al., 1975, Lowry et al., 1978, Spamer and Pette, 1977). Different fiber populations have a wide variation in enzyme activities. 1988–1994, 2X fibers were detected (Wada M., Schiaffino et al., 1988, Schiaffino et al., 1989) with a resistance to fatigue intermediate between that of 2A and 2B units (Larsson et al., 1991). Immunohistochemical and in situ hybridization analyses of muscle sections (DeNardi et al., 1993, Gorza, 1990) and biochemical and physiological studies of single fibers (Bottinelli et al., 1994, Pette and Staron, 1990) found the spectrum of fiber types with pure or hybrid MyHC composition: 1 ↔ 1/2A ↔ 2A ↔ 2A/2X ↔ 2X ↔ 2X/2B ↔ 2B. The four major fiber types are variously distributed in body muscles of mammals with varying relative proportions of any fiber type according to species and anatomical site (Schiaffino et al., 1989). For example, in leg muscles, slow type 1 fibers are more abundant in the posterior compartment. In many species, type 2 fibers are more numerous in forelimbs than in hindlimbs. Besides that, humans upper limb muscles are faster than lower limb muscles (McComas and Thomas, 1968, Harridge et al., 1996).

Mammalian skeletal muscle- myosin isoforms and fiber types

Myosin heavy chain isoforms are used as a marker for myofiber types, as described above (Schiaffino and Reggiani, 2011). Mammalian, skeletal muscles contain four major myosin heavy-chain (MHC) isoforms. MHC I is the "slow" or beta myosin heavy chain. The fast ones are IIa-, IIx- and IIb- MHCs. Additionally, mammalian skeletal muscle also contains myosin light chains. The MLC isoforms are

the “slow” MLC1 and the “fast” MLC1f and MLC3f (Schiaffino and Reggiani, 1994). All sarcomeric myosins are hexamers that consist of two MyHC and two pairs of MyLC (Schiaffino and Reggiani, 2011). Myosin is the molecular motor of muscle cells. Sarcomeric myosins are elongated molecules with two globular domains, heads and one long filamentous domain, the tail. Each head consists of a NH_2-terminal domain of the MyHC comprised of ~840 amino acids. ATP- and actin-binding sites are located in the myosin head. The motor domain is able to hydrolyze ATP and generate force and displace the myosin. At the COOH terminus, the head has a long α-helix, containing two IQ domains that bind two MyLCs (one essential and one regulatory per head). MyHC molecule stretches to an α-helical domain of ~1,100 amino acids, containing heptad repeat sequences that form an α-helical coiled coil for heavy chain dimerization. Through self-assembly, the myosin tails create the “thick” or myosin filament. On the myosin filament, hundreds of myosin heads are located that are responsible for force generation and movement. The tail is responsible for dimerization of the MyHC, thick-filament assembly, and MyBP aggregation (Schiaffino and Reggiani, 1994). The MHC isoforms can be differentially distributed in myofibers, which determines the different myofiber types. Type I, IIa, IIb and IIx fibers contain the respective MHC only. On the other hand also intermediate hybrid fibers that contain both beta/slow- and IIa-MHC, IIa- and IIx-MHC, or IIx- and IIb-MHC, exist (Schiaffino and Reggiani, 1994). The mammalian genomes contains 11 sarcomeric *MYH* genes, six of them in skeletal muscle, two in cardiac muscle and three in other muscles, shown in table 1 (Schiaffino and Reggiani, 2011, Rossi et al., 2010), that are highly conserved in vertebrate evolution and each code for a different MyHC isoform (Berg et al., 2001). In adult skeletal myofibers, MyHC-2A, MyHC-2X, and MyHC-2B, coded by *MYH2*, *MYH1*, and *MYH4* are expressed (Schiaffino, 1996, Bicer and Reiser, 2004, Timson, 2003). The myosin molecule can also be post translationally modified (PTM). Phosphorylation is the most well characterised PTM of the myosin molecule at the MyLC (Blumenthal et al., 1985) which enhances force development at submaximal calcium concentration (Sweeney and Stull, 1990). The level of phosphorylation is higher in fast than slow muscles (Moore and Stull, 1984). MHCs can be also be glycosylated leading to adjustments of the maximum shortening velocity and speed of actin filament translocation in in vitro motility assay (Ramamurthy et al., 1999).

Table 1: Sarcomeric MYH genes in mammals, corresponding protein products and expression pattern. *Adjusted from (Schiaffino and Reggiani, 2011, Rossi et al., 2010).*

	Gene	Protein	Expression
Skeletal muscle	MYH1	MyHC-2X	Fast 2X fibers
	MYH2	MyHC-2A	Fast 2A fibers
	MYH3	MyHC-emb	Developing muscle
	MYH4	MyHC-2B	Fast 2B fibers
	MYH8	MyHC-neo	Developing muscle
	MYH13	MyHC-EO	Extraocular muscle
Cardiac muscle	MYH6	MyHC-α	Jaw muscle and heart
	MYH7	MyHC-β/slow	Slow muscle and heart
Others	MYH7b*	MyHC-slow/tonic	Extraocular muscle
	MYH15	MyHC-15	Extraocular muscle
	MYH16	MyHC-M	Jaw muscle

Muscle function

Excitation–Contraction Coupling: Physiology of Muscle Activation

To generate muscle force, two processes need to be coordinated through the excitation-contraction (EC) coupling principle. The nerve stimulus is transmitted to the triad. After that, calcium gets released by the cisternae of the sarcoplasmic reticulum. Actin and myosin interact and form cross-bridges. The action potential spreads from the myofiber membrane to the inside of the muscle cell via the transverse tubular system, close to the terminal cisternae of the sarcoplasmic reticulum. After a voltage sensor on the T tubule opens, calcium that is stored in the sarcoplasmic reticulum flows inwards (Rebbeck et al., 2014). Through the calcium current, the ryanodine receptors in the terminal cisternae of the sarcoplasmic reticulum, open and release calcium into the sarcoplasm. There, the calcium binds to troponin C on the actin, which initiates some events that lead to release of the tropomyosin from the active site on the actin filament. Actin and the head of the myosin molecule can then bind via the active site on actin. In the myosin head, Adenosine tri-phosphate (ATP) and ATPase are located. They help with forming a new cross-bridge with actin and releasing the old one. Then, the actin and myosin filaments are able to slide into each other and generate force (Frontera and Ochala, 2015). In skeletal muscle, calcium is used as intracellular messenger. This triggers contractions via binding to troponin and is also can activate protein phosphorylation or dephosphorylation via binding to calmodulin, as well as activate proteolysis via calcium-dependent proteases. Therefore, the concentration of intracellular cytosolic free calcium needs to be controlled precisely through the SR (Schiaffino and Reggiani, 2011).

Energy Production and Release

Muscle actions need ATP to provide energy. The metabolic energy pathway that is used to produce and sustain muscle actions is dependent on the duration and intensity of activities. Common energy pathways in the myofiber are using stores of ATP and creatine phosphate (CP), anaerobic glycolysis, and oxidative phosphorylation. Due to the small reserves in myofibers, the ATP and CP energy pathway is used for high intensity short duration (few seconds) activities. The anaerobic glycolysis pathway is responsible for muscle actions lasting for a couple of minutes. ATP quickly gets produced. However, the end products, such as H^+ or lactate, impair muscle function and are associated with muscle fatigue (Frontera and Ochala, 2015). Oxidative phosphorylation within the mitochondrial network, however, provides energy for exercises with low intensities over a longer duration (minutes to hours). Capillaries are ordered in a network and transport oxygen to active myofibers (Weibel, 2013). These energy pathways overlap, and the contribution of each pathway depends on the intensity and duration of contraction and movement (Frontera and Ochala, 2015). Carbohydrates (plasma glucose and muscle glycogen) and fats (plasma free fatty acids and muscle triglycerides) mainly fuel muscle cells (Romijn et al., 1993), however, amino acid metabolism contributes in a small fraction to the total energy production. At high intensities, mostly muscle glycogen stores are used for muscle actions. At lower intensities and and long duration exercise, mainly the metabolism of free fatty acids is used to generate muscle energy (Frontera and Ochala, 2015).

Types of muscle actions

One functional unit of the mammalian skeletal muscle is composed of a motor neuron and myofibers. Many motor units work together to create movement. Due to the heterogeneity of myofibers they can create different movements as continuous low-intensity activity, repeated submaximal contractions, or fast and strong maximal contractions (Schiaffino and Reggiani, 2011). Muscle actions can be classified into static, dynamic concentric and dynamic eccentric activation of the muscle. Static, or isometric, muscle action does not create movement in the joint or limb although force is generated. Dynamic actions need force generation and joint movement and can be concentric or eccentric, which are normally combined in one movement. In concentric ones, the muscle gets shortened and origin and insertion come closer together.

Eccentric ones lengthen the muscle and origin and insertion move away from each other (Frontera and Ochala, 2015).

Motor neurons and muscle spindles

In mammals, motor units, comprised of a motor neuron and all the innervated myofibers, build the units of the neuromuscular system. Muscle spindles are proprioceptive sensory organs that act as stretch-sensitive mechanoreceptors and detect changes in skeletal muscle length. They consist of a few short and thin myofibers, intrafusal fibers. Afferent neurons transmit the signals to the spinal cord, followed by contractile responses (Schiaffino and Reggiani, 2011). They are innervated by sensory neurons and by γ-motor neurons. Schwann cells wrap the spindles. Motor neurons and myigureofibers are linked through the neuromuscular junction (NMJ) that transmits the nerve impulses to the myofibers (Schiaffino and Reggiani, 2011).

Force Generation and Movement

In 1954, the theory of force generation of myofibers, the sliding filament theory, was published (Huxley and Niedergerke, 1954, Huxley and Hanson, 1954). This theory is still widely accepted. Individual actin-myosin cross-bridges generate force that is transmitted longitudinally and laterally within the fiber. When the produced force reaches the myotendinous junction, tendons, and joints, movement is created (Frontera and Ochala, 2015). The amount of generated force depends on the degree of activation by the nervous system, its structure, the muscle size, the space between myofilaments, the number of actin-myosin cross-bridges, the generated force per cross-bridge and the interaction between cellular elements (Frontera and Ochala, 2015). The process of generating force in the muscle begins when ATP binds to the myosin head. In the myosin head, an ATPase is positioned that hydrolyzes the ATP to ADP and Pi. The existing cross-bridge detaches. This leads to a movement of the myosin head and binding to a new actin molecule. When Pi gets released, force is generated, followed by a conformational change, and a power stroke, which leads to pushing of the actin filament alongside myosin. The process ends with ADP release and myosin bound to actin (rigor state). The formed cross-bridges can be of different strength. ATP-consumption depends on the expressed myosin heavy chain isoforms, on the number of myosin heads, the fraction of myosin heads forming cross-bridges, as well as the rate for cross-bridge detachment (Frontera and Ochala, 2015). In humans, the rate of ATP consumption is the lowest in type I fibers, intermediate in IIa

fibers, and the biggest in IIx fibers (Larsson and Moss, 1993). Furthermore, the generated force is also dependent on biomechanical properties of the musculoskeletal system, as for example, the length of the muscle or sarcomere. Besides that, it also depends on the velocity of the movement (Frontera and Ochala, 2015). Also the concentration of calcium in the sarcoplasm and the sensitivity of the thin filament influence the level of generated force (Frontera and Ochala, 2015). The relative role of glycolysis and oxidative phosphorylation is different in slow and fast muscles. In slow muscles, all the needed ATP is generated by oxidative mitochondrial processes. In fast muscles, glycolytic processes are needed to generate ATP rapidly (Ogata and Mori, 1964, Padykula and Gauthier, 1967). Based on biochemical properties, fibers can be classified as S (slow), FOG (fast oxidative glycolytic), and FG (fast glycolytic) (Barnard et al., 1971, Peter et al., 1972). In humans, different fiber types consume ATP at a different speed. During maximal exercise, ATP declines at a different speed in different human muscle fibers. The mean ATP concentration values at 10s exercise time are 0 for Type 1 fibers, -10 mmol (kg dm) $^{-1}$ ATP for Type 2A fibers, and ~-17,5 mmol (kg dm) $^{-1}$ ATP for type 2A-2X fibers. At 25s exercise time, the mean ATP concentration are -5 mmol (kg dm) $^{-1}$ ATP for Type 1 fibers, -15 mmol (kg dm) $^{-1}$ ATP for Type 2A fibers, and ~-19 mmol (kg dm) $^{-1}$ ATP for type 2A-2X fibers (Schiaffino and Reggiani, 2011, Karatzaferi et al., 2001).

Muscles and metabolic activities

Dependent on their metabolic activities, myofibers are able to adapt their size or thickness, internal structure (relative abundance of relevant intracellular components), and extracellular surroundings (for example capillary density). Fiber thickness is inversely related to aerobic oxidative activity or mitochondrial density. The same fiber type with identical metabolic properties may have different size in different muscles (Andersen, 1975, Sjøgaard, 1982, Dawson et al., 1987, Acevedo and Rivero, 2006, Behnke et al., 2003). In humans, type 2 fibers are larger than type 1 fibers (Saltin, 1983). In slow myofibers, the number of capillary vessels surrounding a myofiber is higher than for fast fibers (Andersen, 1975, Sjøgaard, 1982, Dawson et al., 1987, Acevedo and Rivero, 2006, Behnke et al., 2003). The mitochondrial content of myofibers varies significantly in relation to fiber type. In human, the mitochondrial volume is 6% in type 1 fibers, 4.5% in type 2A fibers and 2.3% in type 2X fibers (Howald et al., 1985). Besides that, the ultrastructure between slow and fast

myofibers differs (Jackman and Willis, 1996, Gauthier, 1979) as well as their enzyme activity. Fast fibers have a higher glycogen content at rest than slow fibers (Greenhaff et al., 1993, Vøllestad et al., 1984). Intracellular substrate stores can only support the regeneration of a limited amount of ATP. Therefore, myofiber energy metabolism depends on the transport of substrate trans-sarcolemma. Fast and slow fibers have different characteristics in this case. Slow fibers have greater abundance of transport mechanisms for lactate, glucose, and fatty acids (FA). In slow muscles, lactate and glucose uptake is about 2-fold greater, and FA transport threefold bigger, than in fast muscles (Chabowski et al., 2006, Kraegen et al., 1993, Juel and Pilegaard, 1998).

Myosin head conformations- SRX/DRX

Myosin exists in three different functional states in the sarcomere (figure 3A): The active cycling state of myosin (actin-activated ATP hydrolysis and rapid ATP turnover time of <1 s), the disordered relaxed (DRX) state (ATP turnover state of myosin in the absence of actin, very slow ATP turnover time of <30 s) and the super-relaxed (SRX) state (ATP turnover times of more than 100 s). Energy (ATP) utilization is different between myosin states, as shown in figure 3B and 4. When muscles contract, myosin states continuously change between the actin-bound state and the actin-free DRX state (Nag and Trivedi, 2021). Myosin in the SRX state is held 'in-reserve' and in skeletal and cardiac myofibers, ~ 50–60% of the myosin heads are in the SRX state (Stewart et al., 2010, Hooijman et al., 2011). Physiological, pathophysiological, and non-physiological factors can modulate the SRX state of myosin. In 2010, the new functional SRX state of myosin has been discovered in rabbit skeletal myofibers (Stewart et al., 2010). It has a 10-fold slower ATP turnover rate than the non-actin-bound state, the DRX state. The SRX and DRX state exist in a dynamic equilibrium under resting muscle conditions and are thought to be significant contributors to adaptive thermogenesis in skeletal muscle. They can act as a reserve pool and may be recruited when the cardiac muscle power increases. Striated muscle contraction is regulated by modulating the myosin DRX↔SRX state equilibrium. The ratio of the SRX state can be measured kinetically by following the release of fluorescent ATP hydrolysis products from myosin. The SRX state has a very slow release of the ATP hydrolysis products relative to myosin in other states. In relaxed skeletal muscle, ~50% of the myosin remains in the SRX state, whereas the other 50% are in DRX state (Cooke, 2011, Stewart et al., 2010). With aging, muscle strength can progressively be lost (dynapenia), which happens more often in post-

menopausal women than in men of the same age. This occurs independent of muscle size or the presence of neurological or muscular diseases. Studies on possible changes of aging and sex on the myosin DRX↔SRX state equilibrium or changes on the properties of the SRX state, have been done. In mice, female individuals showed significantly faster ATPase cycling time of myosin in both the DRX and SRX states with age, which might be due to the ovarian hormone estradiol, which is the key hormonal signal to skeletal muscle in females. This could result in a buildup of weakly bound actomyosin complexes, slowing down the cross-bridge kinetics and leading to increased weakness with age. Another explanation could be a compensation for the loss of myofibers through the shift towards more DRX heads (Colson et al., 2015, Phung et al., 2018).

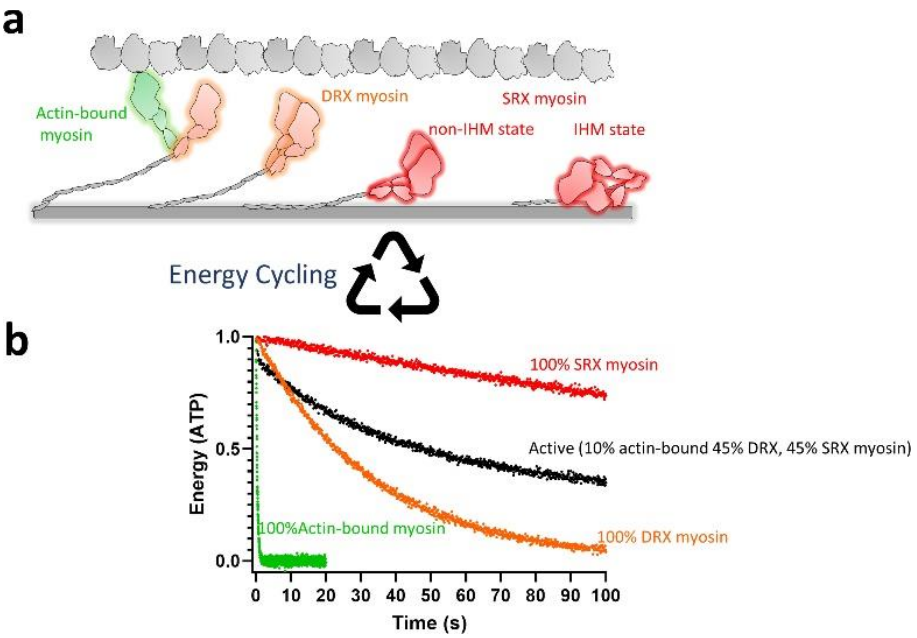

Figure 3: Possible different functional states of myosin. *(a) Actin-bound myosins are shown in green. They are most active and utilize maximum ATP. This myosin state is in equilibrium with an off-actin state, the DRX state of myosin (orange). It has 100-fold less activity than the actin-interacting form. DRX state myosins are in equilibrium with those in the SRX state (red), which has a further 10-fold less activity than the DRX state. The SRX state of myosin exists in IHM state or non-IHM state. Actin is shown in grey, myosin thick-filament shaft as grey cylindrical rod; (b) Energy (ATP) utilization by different myosin states is shown. The ATP turnover rate for the actin-bound myosin, DRX myosin, and SRX myosin was assumed to be 3 s−1, 0.03 s−1, and 0.003 s−1, respectively. A standard deviation of 0.1 units was used to generate random Gaussian noise. The simulated curves were generated using the GraphPad Prism software. (From: (Nag and Trivedi, 2021)).*

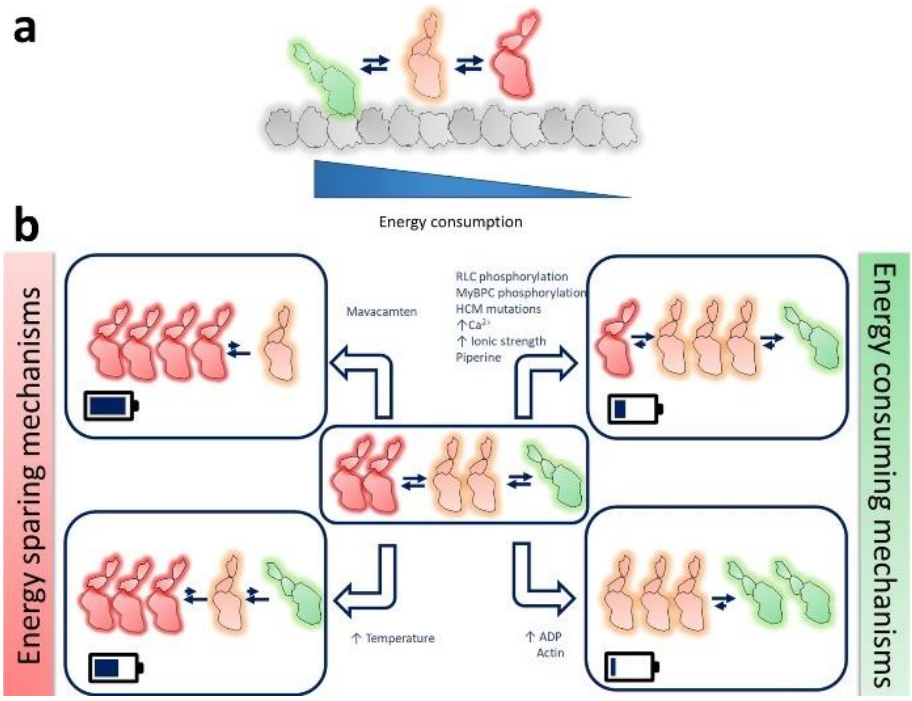

Figure 4: Possible different functional states of myosin- energy utilization and alteration of the states. *(a) States of myosins are arranged in the order of their energy utilization - actin-bound myosin (green), DRX myosin (orange), and SRX myosin (red); (b) Graphical representation of alteration of the myosin population through different physiological, pathophysiological, and non-physiological perturbations. (From: (Nag and Trivedi, 2021)).*

Aging

In humans, sex is the strongest predictor of lifespan, and women on average live longer than men (Tower, 2017). Countries have different life expectancies possibly due to healthcare expenditures, but also environmental factors (Bein et al., 2017). Diseases that are non-communicable are responsible for 63% of all deaths worldwide, of which three quarters were incurred by individuals over 60 years old (organization). The highest cause of death worldwide are ischemic heart disease and stroke, as determined 2016 with a combined 15.2 million deaths out of 56.9 million total deaths. Chronic obstructive pulmonary disease, Alzheimer's disease and other dementias, lung and tracheal cancers and diabetes are the next high causes, with another 8.3 million deaths (organization, 2019b). These age-related diseases often come with prolonged disability and reduced productivity, and a negative financial impact within families and heavy demands on healthcare systems (organization, 2019a). Therefore, increasing human longevity and extending the period of health/healthy aging are among the most difficult challenges facing modern medicine. Due to advances in medical support, the life expectancy has more than doubled in the last hundred years and the age group over 85 is the fastest growing across all age groups (Hill et al., 2016). In industrialized countries the life expectancy of humans was 30 and 45 years at the beginning of the 20th century. Improvements in health care, nutrition, and standards of living led to an increase in life expectancy. In the early 21st century it was suggested that life expectancy would still increase with a healthy lifestyle (Leonard P. Guarente, 2022). This suggests that besides environmental conditions, other factors regulate lifespan. The molecular mechanisms by which longevity has evolved are still mostly unexplained (Guest, 2019). Today, the aging research is looking for geroprotectors, pharmacological or nutraceutical compounds that prevent aging. Treatment in animals has already managed to expand lifespan. Nevertheless, testing the findings on humans is not an option (Stenvinkel and Shiels, 2019).

Aging can be defined in different ways. Countless theories try to explain how and why we age, but the definition of aging/senescence has been uncertain for a long time (da Costa et al., 2016). Overall, aging simply refers to the changes that occur during an organisms' life-span (Kirkwood, 2005). The rate at which these take place varies widely (Kirkwood, 2005). This definition also contains changes occurring through aging, that do not affect the individual's viability. The phenotype is the end

result of the interaction between genotype and external factors: [phenotype] = [genotype] + [(diet, lifestyle and environment)] (Anton et al., 2005). Biogerontologists rather use the term senescence, than aging to differentiate innocuous changes from those leading to increased risk of disease, disability or death (Dollemore, 2002). In this context senescence is defined as the progressive deterioration of bodily functions over time (Goldberger et al., 2002). Human aging is associated with a loss of complexity in a wide range of physiological processes and anatomic structures (Goldberger et al., 2002). This includes blood pressure (Kaplan et al., 1991), stride intervals (Hausdorff et al., 1997, Terrier and Dériaz, 2011), respiratory cycles (Peng et al., 2002, Schumann et al., 2010), vision (Azemin et al., 2012), postural dynamics (Manor et al., 2010), decreased fertility and increased risk or mortality (Chesser, 2015, López-Otín et al., 2013). Aging is defined as the breakdown of self-organizing systems and reduced ability to adapt to the environment (Vasto et al., 2010). Explanations of the aging mechanisms have become unexpectedly complicated. Gerontologists discovered that multiple processes, at a cellular and molecular level, but also on tissues and organ systems, combining and interacting on many levels, are the basis of the aging process (Guarente, 2014, Dollemore, 2002). Biochemical mechanisms cause or react to aging (Yin and Chen, 2005). To completely understand the underlying molecular pathways of aging, as well as for potential lifespan extending therapeutics, new synthetic and medicinal chemistry methodologies are yielding small molecule tools (Ostler, 2012). To better understand how these could contribute, it is important to look at the theories of aging, as well as why and how we age.

Associated molecular mechanisms

Differentiated human adult cells age via several mechanisms, as for example, damage to DNA molecules, perturbations in proteostasis, mitochondrial dysfunction, inappropriate insulin/IGF-1 signalling, and damage resulting from oxidative stress (Guest, 2019). Most model organisms for aging research with long lifespans have the capacity to reduce the effects of one or more of these pathways. For aging research these pathways first needed to be investigated in detail. There are many potential circulating biomarkers that are associated with aging, longevity and age-related diseases. These biomarkers are involved in the pathways of calcium homeostasis, cytoskeleton and hormones, fibrosis, inflammation, mitochondria and apoptosis, neuromuscular junction and others. For this project the biomarkers involved in the cytoskeleton and hormones, neuromuscular junction pathway, as well as the calcium homeostasis (calreticulin, regucalcin, S100 calcium binding protein B) are the most interesting ones (Guest, 2019). Most of the pathways were studied in detail in long-lived rodent and worm mutants. Short- and long-lived species showed differences in these pathways, which further helped with understanding longevity. Altogether, this helped to understand longevity regulation and to potentially maximise the human lifespan in the future (Guest, 2019).

The Hallmarks of Aging

Findings from short-lived, canonical model organisms, led to a classification system of the hallmarks of aging (López-Otín et al., 2013), shown in figure 5. The “primary” hallmarks describe molecular damages during the aging process and comprise genomic instability, telomere attrition, epigenetic alteration, and loss of proteostasis. “Antagonistic” hallmarks are deregulated nutrient sensing, mitochondrial dysfunction, and cellular senescence. They have protective and beneficial hormetic effects at low dose, but detrimental effects at high levels. The ‘Integrative hallmarks’ are composed of stem cell exhaustion and altered intercellular communication, leading to loss of reserve capacity or resilience (Holtze et al., 2021).

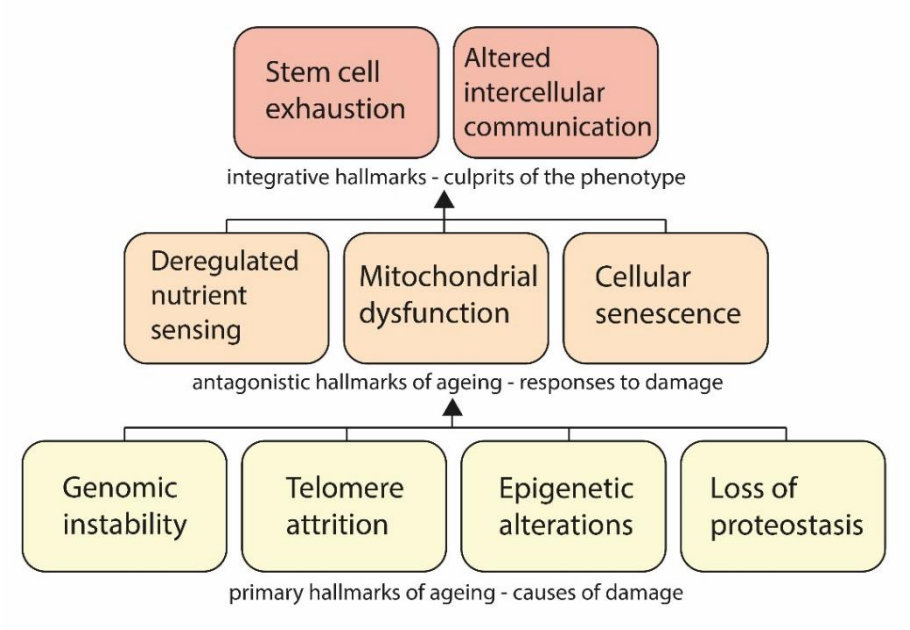

Figure 5: The Hallmarks of Aging, grouped into three categories. *The hallmarks of aging are grouped into three categories, the primary, antagonistic and integrative hallmarks. Compensatory or antagonistic responses to the damage initially mitigate the damage, but can potentially become deleterious themselves. Integrative hallmarks are ultimately responsible for the functional decline associated with aging. Created with Adobe Illustrator.*

Theories of aging

To date, and with the help of model organisms, several theories of aging have been suggested. These theories refer to different characteristics of these organisms or the metabolism in general. These characteristics are 1) the growth of organisms, 2) the reproductive strategy, 3) the lifespan and body size correlation, 4) a correlation between genome size and aging of an organism, 5) mitochondrial oxidative stress theory and 6) caloric restriction to delay the aging process.

1) Aging is correlated with the growth of organisms. For example fishes which rapidly grow to a definite size are short-lived, whilst steadily and slowly growing ones, as sharks, tend to live longer (Goss, 1974, C., 1881).

2) However, also the general reproductive strategy of species can have an influence on its longevity. A continuum of reproductive strategies can be distinguished. They range from r, the production of large numbers of offspring provided with minimal care, to K, the production of few offspring nurtured intensively (Rushton, 1987). The species are called R- and K-selective species. Species belong in a continuum between these groups, according to their life history traits. These groups predict, how well animal populations effectively respond to environmental and/or anthropogenic disturbance (Pianka, 1970, Edwards et al., 2019). Higher order

vertebrates with extreme longevity, often have K-selected life history traits that influence the maximum intrinsic population growth rates (rmax), such as slow growth, late maturity, and relatively low recruitment rates (McCann and Shuter, 1997). These traits limit the ability of populations to sustain high levels of mortality (Simpfendorfer and Kyne, 2009, Norse et al., 2012, Musick, 1999, Adams, 1980). Chondrychthian deep water species show significantly lower rates of population increase, as the frequency of K-selected traits become more with increasing depth, in chondrichthyans (Russell et al., 2011). They also have a heightened vulnerability to exploitation and incidental mortality relative to their shallow-water counterparts (García et al., 2008, Simpfendorfer and Kyne, 2009). Most bony fish have a `R-selected` reproductive strategy that is characterised through the production of many young that do not cost much energy and of which only few will survive. The interval between birth and maturity is short and the potential for the population to recover from depletion is high, as well as relatively adaptable to environmental changes. Sharks belong to the species with a `K-selected` reproductive strategy and have only small numbers of young at a relatively high cost. They are more likely to survive until adulthood. In this case the offspring is relatively large. Additionally, sharks grow slowly, which means that they will only be able to produce offspring after some years (especially the species living in cold, low-energy deep-ocean). Also the gestation period is long, in some species several years. In general, sharks are long-lived species that produce small numbers of offspring in their lifetime, which is a good reproduction strategy for apex predators to maintain a stable population since they do not have many predators. However, fisheries threaten these species, especially larger sharks since smaller ones grow more quickly and reach maturity sooner (Ebert et al., 2021).

3) Furthermore, lifespan and body size are positively related, which explains 63% of the variation in maximum longevity across mammals, birds, amphibians and reptiles (de Magalhães et al., 2007, Fushan et al., 2015). Mice and rats are negative outliers, since they only live half the time than expected (Prothero and Jürgens, 1987, de Magalhães et al., 2007). Mammals and birds have the highest correlation, reptiles slightly lower. In amphibians the correlation is even lower. Longevity is positively correlated with captivity, nocturnal lifestyle, a low ambient temperature, poison defense (Stark and Meiri, 2018). Fish and invertebrates have a similar positive allometric relationship (Holm et al., 2016).

4) Besides that, another theory of aging says that longevity of animals is determined by genetically preprogrammed manner, in which animals try to avoid aging (Partridge and Barton, 1993). According to this theory, there is a correlation between the size of the genome and the aging process of an organism. Nevertheless, the aging process is also influenced by external factors, as for example the breeding structure, environmental conditions, disease and others. One genetical aspect that affects longevity is the quantity of DNA per cell, or C-value (Monaghan and Metcalfe, 2000). However, it is unknown how genome size affects phenotype and longevity. During evolution, DNA steadily accumulated, which led to merely coincidental cellular and organismal relationships with genome size (Ohno, 1972, Pagel and Johnstone, 1992). Furthermore, genome size shifts induce direct changes in cellular parameters, which makes them be selected for (or against) by natural selection (Roth et al., 1994, Cavalier-Smith, 1982, Vinogradov, 1997). Indirectly, a bigger genome size, causing slower cell growth and metabolic rate, could lead to a longer lifespan. The genome size is measured as C-value, is highly variable across different species and taxa and is independent of organismal complexity or the number of coding genes(Griffith et al., 2003).

5) Another possible explanation for human aging is the mitochondrial oxidative stress theory. "*The Mitochondrial Free Radical Theory of Aging (MFRTA) proposes that mitochondrial free radicals, produced as by-products during normal metabolism, cause oxidative damage. According to MFRTA, the accumulation of this oxidative damage is the main driving force in the aging process*." (Sanz and Stefanatos, 2008). According to this theory, short-lived species should be less resistant to oxidative damage, than long-lived species. This theory is supported by many studies. However, it is not valid for all species (Costantini et al., 2017). Negligible or extremely rapid senescence in mammals can also lead to new targets in human aging, if one considers that lifespan and aging rates vary across taxa. Greenland sharks, among other species, such as naked mole rats, the ocean quahog or rockfish, can have negligible senescence and can therefore be extremely resistance to diseases that are related to aging. They are thought to be extremely stress-resistant due to maintenance of protein homeostasis and robust mitochondrial functions. Human health span could for example extended through treatments that target protein modification or the upregulation of matrix antioxidants (Stenvinkel and Shiels, 2019). Human aging processes can be arrested through senolytic drugs, as quercetin and

navitoclax (Patnaik et al., 1994). Overall, three types of senescence exist in fish. These are rapid senescence, which appears in eels, killi fish and the pacific salmon, gradual senescence, which appears in guppy and platy fish, and negligible senescence, in sturgeons and rockfish (Patnaik et al., 1994). Therefore, it would be good to also do comparative studies in fish with rapid or negligible senescence (Mikhailova et al., 2017). The aging process can be retarded in species showing gradual senescence, through lower environmental temperature and dietary restriction. Nevertheless, it is unknown why only some species of fish exhibit negligible senescence (Mikhailova et al., 2017). Cellular, genetic and biochemical characteristics of slow aging can be studied due to the fact that fish with negligible senescence exist. Furthermore, muscle extracts from fish with negligible senescence, such as sturgeon, have protective effects on senescence induced by oxidative stress (Hua et al., 2015). It would be also interesting to study, if long-lived fish have an increased capacity to repair DNA damage, protect protein function or have a continued turnover of tissue (Stenvinkel and Shiels, 2019).

6) Furthermore, since energy excess is the main cause of accelerated aging in mammals, one of the best ways to delay aging phenotypes in mammals is caloric restriction without malnutrition (Pifferi et al., 2019, Lian et al., 2018). In humans, caloric restriction may have adverse effects and reduce the quality of life (Pifferi et al., 2019). Also drugs could be used to arrest aging by having caloric restriction mimetic effects (Handschin, 2016). It is believed, that Sirtuins mediate the longevity effect of calorie restriction. Therefore activators of Sirtuins are an important field of research. Humans age over a slow and gradual process. Therefore, clinical trials of anti-senescence drugs (Zhu et al., 2015), nuclear factor erythroid 2-related factor 2 (NRF2)-agonists (Stenvinkel et al., 2021), NAD-dependent deacetylase sirtuin-1 (SIRT1) agonists (Lee et al., 2019) and/or dietary interventions that prolong lifespan in animals, such as caloric (Pifferi et al., 2019) and methionine (Lee et al., 2016) restriction, would need to be extremely long (Stenvinkel and Shiels, 2019).

7) Nowadays, Antagonistic Pleiotropy (Williams, 1957, Rose, 1991) is the best accepted explanation for the evolution of aging. According to this theory, there are genes, or evolved patterns of gene expression, for essential elements of individual fitness, as for example fertility, that are “*so closely tied to loss of homeostasis and self destruction late in life that natural selection has been compelled to accept the*

latter as a necessary cost of the former" (Mitteldorf, 2019). The AP theory resolves the dilemma of senescence within the context of uncontroversial selection mechanisms due to individual competition (Mitteldorf, 2017). Senescence has a conserved genetic basis (Guarente and Kenyon, 2000) although it has a negative impact on individual fitness.

Metabolism and aging

The effects of aging and metabolism are linked. However, both are not fully related via a action and reaction pattern. Low levels of metabolic impairment can decrease the effects of aging through the stimulation of repair systems (hormesis). Severe metabolic injury, on the other hand, accelerates aging (Catic, 2018). Besides that, the ecology and the metabolic rate of organisms are closely linked. The metabolic rate provides information on behaviour, life history, population dynamics and trophic impact. For sharks, like the Greenland sharks, it can be measured through field respirometry (Ste-Marie et al., 2020). The "*Field metabolic rate (FMR) is a holistic measure of metabolism representing the routine energy utilization of a species living within a specific ecological context, thus providing insight into its ecology, fitness and resilience to environmental stressors.*" (Ste-Marie et al., 2022). It helps to understand food webs and trophic systems (Ste-Marie et al., 2022). To understand an organism´s ecology it is important to understand and study its metabolism, which includes gathers all reactions taking place in the cell of an organism and are responsible for anabolism and catabolism. Anabolic processes enable the organism to synthesize organic material, whereas catabolism enables it to break down molecules to provide energy. Metabolic studies study locomotion, growth, feeding rates, as well as activity patterns of organisms (Pinte et al., 2021). As previously highlighted, skeletal muscle is a major site of energy production and metabolic activity, processing a number of metabolites and substrates including glucose, fatty acids and lactate (Schiaffino and Reggiani, 2011).

Substrate is used in aerobic and anaerobic pathways to produce adenosine triphosphate (ATP) and other metabolic building blocks. In the aerobic pathway ATP is generated via oxidation of nicotinamide adenine dinucleotide (NADH). In the anaerobic pathway the ability to maintain ATP production depends on lactate dehydrogenase oxidizing glycolytic NADH. The aerobic pathway produces more ATP

per glucose molecule than the anaerobic one but requires a higher concentration of oxygen and is slower than the anaerobic pathway (Pinte et al., 2021).

Fast and slow myofibers have differences in their glucose, lactate, and fatty acid metabolism. The rate and capacity of ATP generation through different types of metabolism (glycolytic anaerobic or oxidative aerobic) is different. Some enzymes have similar activity in anaerobic and aerobic metabolism in slow and fast fibers (Schiaffino and Reggiani, 2011). The activity of some key enzymes is different in fast and slow fibers (Vøllestad et al., 1992, Greenhaff et al., 1993). The prevalent steps of energy generation in fast myofibers are anaerobic glycolysis from glucose to pyruvate generation (catabolic pathway), in which ATP is generated, and conversion of pyruvate to lactate by lactate dehydrogenase (LDH) with reoxidation of NADH, or the rapid oxidation of NADH produced by glycolysis through lactate dehydrogenase activity and the glycerol-3-phosphate shuttle (Schiaffino and Reggiani, 2011). LDH isoenzymes distribution varies according to fiber type (Leberer and Pette, 1984, Peter et al., 1971). In fast fibers there is a tendency for the conversion of pyruvate to lactate, whereas in slow fibers lactate rather gets converted to pyruvate. For glycolysis, the biggest amount of glucose comes from trans-sarcolemmal transport in slow fibers, and from glycogen stores in fast fibers. In slow myofibers the prevalent metabolic pathways are lactate to pyruvate conversion, and the entering of pyruvate into the citric acid cycle via the pyruvate dehydrogenase (PDH) complex, which leads to oxidative phosphorylation (Schiaffino and Reggiani, 2011). Fast fibers have higher phosphorylase content and more effective stimulation (Greenhaff et al., 1993). Furthermore, in human muscles, glycogen decrease is the fastest in type 1 and type 2A fibers and then in type 2X fibers (Gollnick et al., 1974, Vøllestad et al., 1984). In glycogen resynthesis, phosphofructokinase (PFK) is rate-limiting and has a higher activity in fast-glycolytic than in slow-oxidative fibers (Spamer and Pette, 1977). Fast fibers have three additional mechanisms in glycolysis (Schiaffino and Reggiani, 2011).

Muscles during aging

During aging of an organism, sarcopenia can occur. Sarcopenia is defined as the loss of muscle mass without the loss of body weight in elder people (Cruz-Jentoft and Sayer, 2019, Rolland et al., 2011). The muscle atrophies, the cross section of muscle-fibers can be reduced, and muscle cells die (Kamel, 2003, Welle, 2002). Muscle size, number and type, as well as strength, can be affected through sarcopenia (Pascual-Fernández et al., 2020, Cruz-Jentoft and Sayer, 2019, Rolland et al., 2011, Welle, 2002, Kamel, 2003). Rosenberg used the term sarcopenia for the first time (Rosenberg, 1997). He defined it as the loss of lean body mass with aging (Rosenberg, 1997). The European Working Group on Sarcopenia in Older People defined it as a lower muscle mass and muscle weakness and/or impaired muscle function (Cruz-Jentoft et al., 2010). Due to the number of affected people worldwide, sarcopenia is a very important topic to investigate. In elder humans, muscle weakness, atrophy or sarcopenia is one of the main reasons for a decrease in life quality (Frontera and Ochala, 2015). People suffering from sarcopenia also lose muscle power (Reid et al., 2014). 40-50% of over 80 year olds, have sarcopenia (Barbosa-Silva et al., 2016, Iannuzzi-Sucich et al., 2002). Men lose more muscle mass and strength than women, which preferentially occurs in the lower limbs compared to the upper limbs (Yamada et al., 2014, Frontera et al., 2000a). Since the world population is growing and the life expectancy of humans increases steadily, sarcopenia grows as a problem. Sarcopenia is characterized by reduction in muscle size, but more important is the change in myofiber quality (Frontera et al., 2000b). Most studies show that older humans have reduced single fiber maximal force for type I and type II fibers (Miller and Toth, 2013). Since the gene expression patterns in the skeletal muscle change over time, the proteins can be implicated in age-related processes. Impacted proteins are for example those involved in cellular senescence, insulin signalling or myogenesis (Tumasian et al., 2021, Dao et al., 2020).

Sarcopenia does not have any underlying disease and the exact molecular mechanisms still remain unknown (Christian and Benian, 2020). Nonetheless, proposed molecular mechanisms explaining the dysfunction are (Frontera and Ochala, 2015) 1) a reduction in myosin protein content (D'Antona et al., 2003), due to an aberrated gene transcription of the myostatin gene or a decreased translation and protein synthesis causing a lower myosin concentration per unit of muscle cell area, and 2) a myofilament dysfunction through post-translational modifications of myosin

via oxidation or glycosylation. Through oxidative modification of myosin, the binding of the myosin head to the actin filament can get disrupted and therefore lead to a reduced number of actin–myosin cross-bridges in the strong-binding state (Moen et al., 2014). Force and power generation will therefore be limited (Frontera and Ochala, 2015). The remaining fibers that are not lost during the aging process help to compensate for age-related differences in fiber size and quality (Frontera et al., 2008, Reid et al., 2012, Reid et al., 2014).

Skeletal muscles change with age. Mostly, these changes come from alternated interactions of factors, included in several different pathways. The factors are involved in the neuromuscular junction, endocrine system, growth factors, muscle protein turnovers, as well as behaviour- and disease related factors (Curcio et al., 2016). Sarcopenia is a “multifactorial” pathogenesis and has a multitude of pathways, with more than one biomarker involved (Lauretani et al., 2014, Santilli, 2014). The pathophysiology of sarcopenia is comprised of endocrine dysfunctions, inflammatory conditions, and glucose, glycogen, and lipid metabolism alterations (Malafarina et al., 2012, Pedersen and Febbraio, 2012). Muscle-related cytokines fulfil auto-, para- and endocrine actions between muscle and bone- fatty- and liver tissue. Furthermore, other factors that favour the development of sarcopenia are chronic diseases, anorexia, obesity, or low physical activity (Biolo et al., 2014, Sakuma et al., 2015). A series of biomarkers may be found in tissue and blood samples of sarcopenia (Kalinkovich and Livshits, 2015).

The applicability or interest in using other animal species as models to study successful aging

Model organisms for aging research are chosen for different characteristics of the species. They have special features according to some hallmarks of aging. There are traditional model species for aging research, canonical species, and less common ones, non-canonical species (Holtze et al., 2021). In this chapter the advantages and disadvantages of using different models, as well as pathways of interest for aging research that can be studied with them, are discussed. Several features of species or populations make them interesting for research, as for example the lifespan, genetic variation within a population or immortality. Human live more than 4.5 times longer than expected (Holtze et al., 2021). Knowledge about the molecular aging mechanisms obtained in canonical model organisms could be potentially used to elongate it even further (Tacutu et al., 2018).

Different characteristics to choose model organisms for aging research are (Holtze et al., 2021) 1) species with extreme long lifespans, related to their body size, mass or in general, as for example ant queens that reach extreme long lifespans (up to 45 years), compared to their size and to other individuals of the same species (Giraldo and Traniello, 2014), 2) variable lifespans in different populations within the same genotype which gives the possibility to look at the underlying mechanisms leading to longevity within the same genotype. Examples are Chameleons of the genus *Furcifer* with highly variable lifespans between 4-5 months and 10 times the length (Eckhardt et al., 2017, Karsten et al., 2008, Tacutu et al., 2018). Another interesting feature of species used for aging research is 3) immortality, as for example the “immortal jellyfish” *Turritopsis dohrnii* that has immortal features and undergoes a reverse development from the medusa to the polyp stage in case of injuries or age weakness due to transdifferentiation, possibly repeatable indefinitely because it is not intrinsically limited (Piraino et al., 1996).

Traditional, canonical model species for aging research include the laboratory mouse (Mus musculus), rat (*Rattus norvegicus domestica*), the common fruit fly (*Drosophila melanogaster*) and the roundworm (*Caenorhabditis elegans*). Most of what we know today has been established in these species (Holtze et al., 2021). Canonical species have some common characteristics, they mature rapidly and it is possible to breed them economically in captivity (Holtze et al., 2021). Advantages of using these models are the access to strains with known genetic properties, high-quality genomic and transcriptomic sequencing data, versatile experimental manipulation capabilities including well-established genome editing tools, as well as extensive experience in husbandry. Furthermore, they are easy to handle, have short generation times, normed strains, as well as standardized husbandry, and information on genomic and transcriptomic sequencing data is known. In these species the underlying mechanisms of aging can be studied with knock-in and knock-out models, cell lines comprising embryonic stem cells, and genetic engineering tools such as CRISPR/Cas systems (Holtze et al., 2021). However, only using a few model species also comes with some disadvantages: 1) it makes it impossible to gain a broad and general understanding of mechanisms and biological processes during aging (Holtze et al., 2021), and 2) it is unclear to what extent information obtained in short-lived model organisms can be transferred to long-lived species (Holtze et al., 2021). Flies and nematodes have maximum lifespans of up to a few months (Tacutu et al., 2018), mice and rats of up to 4 years and zebrafishes up to 5.5 years (Tacutu et al., 2018), which makes them short-lived species (Holtze et al., 2021).

However, there are also other model organisms to study aging besides the traditional ones, the non-canonical species. With non-canonical model organisms one can study relevant mechanisms for extended lifespans that do not occur in canonical ones. The highlighted non-canonical species for example have exceptional lifespans, an enormous regeneration potential or a remarkable resistance to aging-related diseases. The mechanisms are the same in canonical and non-canonical species. In non-canonical ones, various known aging-related signalling pathways have different weighting. Some intriguing, life-prolonging mechanisms only work in non-canonical model organisms, which can be advantageous (Holtze et al., 2021). Experimentally prolonged lifespans in short-lived species often have many side-effects (Folch et al., 2018) as for example decreased fertility or reduced pathogen resistance (Fontana et al., 2010). Long-lived species are good models to study aging. They either have long

lifespans by themselves or elongated lifespans through targeting of molecular pathways that slow down the aging process (Holtze et al., 2021). Regularly manipulated lifespan extending effects in short-lived model organisms are for example the growth hormone/insulin-like growth factor 1 (GH/IGF1) system or the mechanistic target of rapamycin (mTOR) pathway or sirtuins (Fontana et al., 2010, Duran-Ortiz et al., 2021, Longo et al., 2015, Pan and Finkel, 2017, Laplante and Sabatini, 2012, Junnila et al., 2013). Gaining more knowledge in this field, will also help to contribute to the development of interventions for longer and healthier lifespans in humans (Holtze et al., 2021). Alternative long-lived model organisms also can show enhanced DNA repair (extreme long-lived mammals, turtles, and Planaria), a potential critical factor in longevity, or mitonuclear balance (in mole-rats, bats, killifishes and clownfishes). Also enhanced proteasome activity is studied, as it contributes to the long life and health span of two long-lived social mole-rat genera (*Heterocephalus* and *Fukomys*). Impact of oxidative stress and telomere maintenance on aging are controversial in both, non-canonical species, and traditional ones (Holtze et al., 2021). Examples for non-canonical model organisms are the Greenland shark, the short-lived killifish (*Nothobranchius furzeri*), long-lived primates (*Callithrix jacchus, Cebus imitator, Macaca mulatta*), bathyergid mole-rats (*Heterocephalus glaber, Fukomys spp.*), bats (*Myotis spp.*), birds, olms (*Proteus anguinus*), turtles, bivalves *(Arctica islandica*), and potentially non-aging ones such as *Hydra* and *Planaria.*

By current knowledge, one of the longest lived vertebrates are a species of shark, Greenland Shark, making it a very interesting model for aging research. Not many studies have been done on longevity and lifespan in sharks yet. However, some have been published, as for example a study on the age and growth of the Scalopped hammerhead shark (Kotas et al., 2011), the minimum longevity of the lemon shark (Brooks et al., 2016), vertical radiocarbon measurements in white sharks (Hamady et al., 2014), as well as the age and growth of the tiger shark (Holmes et al., 2015). Nevertheless, the age at which sharks mature, their growth rates, as well as their lifespan is unknown for most sharks (Ebert et al., 2021). Also, for some species it is easier to determine the age of the individuals than for others, depending on the handling and size of the animal. Age determination in sharks can be done via several methods (Ebert et al., 2021). The two most common ways to determine the age of sharks are the analysis of distinct growth rings of vertebrae centra, dorsal fin

spines and caudal thorns of sharks and the bomb radiocarbon method (Cressey, 2017). The growth ring method works via counting of annually, seasonally or even less frequent laid down growth rings. The frequency is unknown which could lead to underestimation of the actual sharks age since vertebrae sometimes stop growing at the same time the shark stops to grow (Ebert et al., 2021). Growth rates for sharks kept in captivity are different from those in the wild, because they are fed freely and are not exposed to seasonal changes (Ebert et al., 2021). The second method to determine the age of sharks uses traces of 1950s nuclear-bomb tests to estimate the age (Cressey, 2017). In vertebrates, the eye lens nucleus is composed of metabolically inert crystalline proteins. The centre forms during prenatal development (Lynnerup et al., 2008, Bassnett et al., 2011) and the tissue retains proteins that are synthesized at age 0, which is a feature of vertebrates that are difficult to age (Lynnerup et al., 2008, Bada et al., 1987, George et al., 1999). Radiocarbon (^{14}C) levels (percent of modern carbon (pMC)) are used to estimate ages and stable isotopes ^{13}C and ^{15}N, to evaluate the carbon source. Depleted $\delta^{13}C$ and enriched $\delta^{15}N$ levels represents a high trophic level. Isotope signatures develop because of the diet of the sharks mother, not the animal itself (Nielsen et al., 2016). Either vertebrae or eye lenses are used as time stamps to evaluate the age of marine mammals (Francis et al., 2007, Campana et al., 2002, Kalish, 1993, Hamady et al., 2014), testing the periodicity of increment formation and age (Campana, 2001, Goldman et al., 2012). Many original life span estimates for sharks have been re-evaluated using the bomb radiocarbon method and have often been raised (Brooks et al., 2016), which leads to confusion about how threatened species are (Cressey, 2017). This method already confirmed that some sharks only reach maturity at an age of 40 years and can live for over 100 years (Ebert et al., 2021). Since the productivity of populations is negatively correlated with maximum reproductive age, in sharks (Smith et al., 1998), an increase in the known maximum age within a population therefore means that is more vulnerable than expected (Brooks et al., 2016).

The Greenland Shark is an excellent species to study aging. The biology of Greenland sharks is described in a separate chapter. It is one of the animals that are more successful at aging than humans. It is the longest lived vertebrate species currently living (Nielsen et al., 2016, Ebert et al., 2021). The life expectancy is even longer than the one of the bowhead whale (*Balaena mysticetus*, estimated longevity of 211 years) (George et al., 1999). Only the ocean quahog A*rctica islandica*, lives longer, with 507 years (Butler et al., 2013). Greenland sharks grow with a slow rate and (Ebert et al., 2021) it is estimated that Greenland Sharks only reach maturity at 150 years (Nielsen et al., 2016). Nielsen et al. tried to determine the age of Greenland sharks using radiocarbon dating techniques on eye lens nuclei, as described above. The oldest animal of this study was nearly 400 years old. The study suggests a lifespan of at least 272 years for Greenland sharks with more than 500 cm in length. The largest animal (502 cm) was 392 ± 120 years old (Nielsen et al., 2016).

The shark species

In order to conduct the experiments, we used the Greenland shark (*Somniosus microcephalus*) and the small-spotted Catshark (*Scyliorhinus canicula)*. There are key similarities and differences, as explained later in detail, that make these shark species interesting to study and relevant for this thesis. This chapter covers information about the phylogeny, taxonomy, biology, metabolism, behaviour, feeding, trophic ecology and distribution of these species.

Phylogenetic classification and taxonomy of sharks

Taxonomy of the cartilaginous fishes- Chondrichthyes

Sharks belong to the taxonomic class of chondrichthyans, cartilaginous fishes (Ebert et al., 2021). Chondrichthyans are vertebrates which can be divided into two subclasses, elasmobranchs (Elasmobranchii ('elasmo' means plate and 'branchii' means gills) (Ebert et al., 2021, Vélez-Zuazo and Agnarsson, 2011), including sharks and rays) and chimaeras (Holocephali), which had their last common ancestor with the rest of jawed vertebrates around 450 million years ago (Hara et al., 2018). Figure 6 shows a simplified phylogenetic tree of vertebrates, including elasmobranchs and bony fish. Chondrichthyes fish have a simple cartilaginous internal skeleton. Their unique features are placoid scales and rows of teeth that are continually replaced. Main features of sharks are their jaws, nostrils on the underside of the head and claspers in mature males (Ebert et al., 2021). One other main characteristic of the Elasmobranchs subclass are the multiple (five to seven gill openings on the head (Ebert et al., 2021). In 2021 there were 536 valid species of Elasmobranchs known (Ebert et al., 2021). Chimeras, the second subclass of chondrichthyans, belong to the subclass Holocephali ('holo': whole, 'cephali': head). They have soft gill covers with one opening on the head protecting four gills (Ebert et al., 2021). Common body characteristics of sharks are a cylindrical shape (sometimes flattened), five to seven gill openings on the side of the head and pectoral fins that are not attached to the head above the gill openings (Ebert et al., 2021). Their vertebral column extends into the top lobe of the large caudal fin, which usually is asymmetrical. They have one or two dorsal fins. A few species are flattened (Ebert et al., 2021). All living orders of sharks are shown in figure 6.

Orders and families of living sharks

Living sharks are classified into nine orders by their topography and general body features (figure 6). The Greenland Shark (*Somniosus microcephalus)* belongs to the order of Squaliformes (dogfish sharks) and the family of Somniosidae (sleeper sharks). Whereas the small-spotted Catshark (*Scyliorhinus canicula)* belongs to the order of Carcharhiniformes (ground sharks) and the family of Scyliorhinidae (catsharks.) Figure 6 shows the phylogeny of sharks, including the families of the Greenland shark and small-spotted Catshark (Ebert et al., 2021, Vélez-Zuazo and Agnarsson, 2011).

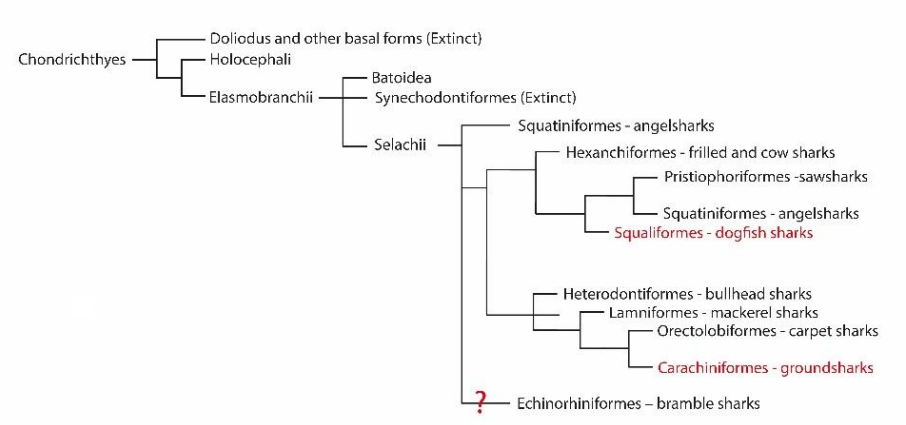

Figure 6: Phylogenetic tree of chondrichthyes with focus on the orders of sharks. *There are 14 living orders of Chondrichthyan fishes, nine of them are sharks. Sharks belong to the Selachii. The orders of sharks to which the Greenland shark and the small-spotted Catshark belong, are marked in red. Created with Adobe Illustrator.*

Phylogenetic classification and topography of the Greenland shark

The family of Squalidae, dogfish sharks, consists of 135 species in six families. The sleeper sharks (Somniosidae), to which the Greenland shark belongs, is one of these families (Ebert et al., 2021) with sixteen deep sea benthic and oceanic species in six genera (Ebert et al., 2021). Greenland Sharks, shown in figure 7A, have a gigantic, heavy, cylindrical body. They have a short, rounded snout, spear-like upper teeth and slicing lower teeth with low, bent cusps and high roots. They have small precaudal fins, and spineless, equal-sized, low dorsal fins with the distance between the fin bases being equal from the snout to the first gill slits. They have a short caudal peduncle. The upper lobe is slightly longer than the lower lobe. They have a rough skin with denticles with strong, hook-like, erect cusps. They appear to be mid-grey to brown in colour, sometimes with transverse dark bands, small dark spots and blotches, and small light spots (Ebert et al., 2021). At birth they measure ~40-50cm, and mature males reach ~300cm, females ~450cm, maximum at least 640cm, possibly 756cm (Ebert et al., 2021).

Phylogenetic classification and topography of the small-spotted Catshark

The small-spotted catshark *Scyliorhinus canicula* belongs to the order of Ground sharks *Caracharhiniformes* and family of Catsharks *Scyliorhinidae* (Ebert and Fowler, 2014). The group of ground sharks is the largest, most diverse and widespread group of sharks (Ebert et al., 2021). Small-spotted catsharks belong to the Catsharks, *Scyliorhinidae*, that contain about 50 species in seven genera (Ebert and Fowler, 2014). Small-spotted catshark, *Scyliorhinus* were known as “sea dogs” and “dog-fishes” because of their ferocious pack-like feeding behaviour (Soares and Carvalho, 2019). The lifespan of the species in unknown. However, for a male the longest recorded lifespan was 8.6 years and for a female 7 years. Based on growth estimates the maximum lifespan was estimated with at least 17 years for this species (Rodriguez-Cabello et al., 2005). They have a large, slender body and greatly expanded anterior nasal flaps that reach mouth and cover shallow nasoral grooves (figure 7B). They only have labial furrows on their lower jaw and their second dorsal is much smaller than their first. Their body covered in numerous small, dark spots on light background, sometimes with scattered white spots (Ebert et al., 2021). At birth they measure 9-10cm. Mature sharks differ in size depending on their habitat. In the north Atlantic males are 52-56cm in size, females 54-60cm and in the Mediterranean sea males get 37-40cm long and females 37-47cm. At max males get 65cm, females 71cm, rarely 80cm, and the record is 100cm for this species (Ebert et al., 2021). Small-spotted catsharks have 40-61 upper teeth and 39-50 lower teeth (Ebert et al., 2021). Benthic species, such as the small-spotted catshark mostly rest on the seabed and therefore have an adapted body shape and are less “cigar-shaped” as pelagic sharks that are faster (Ebert et al., 2021).

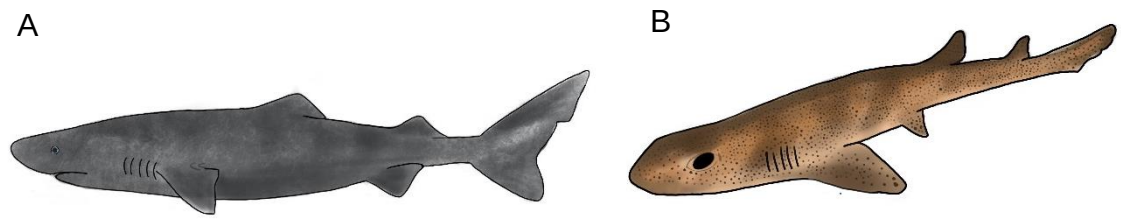

Figure 7: Appearance of A) the Greenland shark *(From: (Ebert et al., 2021) p.191)* **and B) the small-spotted catshark.** *Created with Procreate.*

Distribution

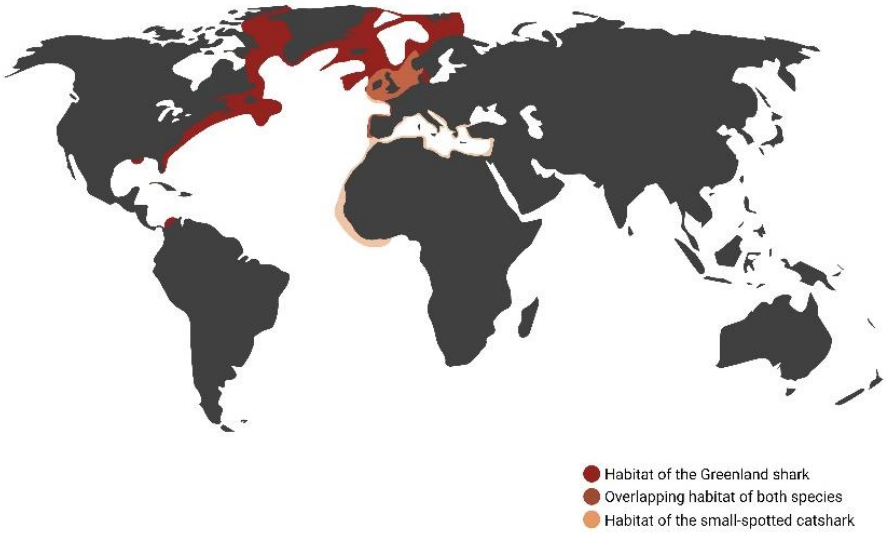

Figure 8: Distribution of the Greenland shark of the small-spotted catshark. *Habitat of the Greenland shark is shown in red, overlapping habitat of both species in orange and habitat of the small-spotted catshark is shown in yellow. Created with BioRender.com and Procreate.*

The distribution of the Greenland sharks is shown in figure 8. Greenland Sharks are distributed in the North Atlantic and Arctic, and occasionally can be found around Portugal, the Gulf of Mexico and off the Caribbean coast of Colombia (Ebert et al., 2021). Preferably, they inhabit deep-water and coastal regions of the Arctic and North Atlantic (Yano et al., 2007). However, they could live everywhere where deep water temperatures are <5°C (MacNeil et al., 2012) and also have been seen at the surface and at depths up to 1,816 m (Porteiro et al., 2017, Herdendorf and Berra, 1995, Campana et al., 2015). There are regional differences in the relative abundance of Greenland Sharks by life stage, size and sex. Adult females appear to be often in southwestern Greenland, Iceland and Newfoundland (Campana et al., 2015, Nielsen et al., 2014, McMeans et al., 2010, Yano et al., 2007). Juvenile sharks often occur in inshore and offshore waters (Hussey et al., 2015), especially in longline, trawl, and camera surveys within Scott Inlet, Baffin Island, and in offshore waters >1000 m depth (Devine et al., 2018, Fisk et al., 2002, Hussey et al., 2015, Nielsen et al., 2014, Yano et al., 2007). Greenland shark movements have been recorded using a variety of telemetry technologies. Vertical movements into shallow and warmer water coincided with the pre-dawn high tide, as acoustic tracking in the St.Lawrence Estuary revealed (Gallant et al., 2016). Greenland sharks prefer greater depths at lower latitudes. They also undergo long-distance horizontal movements, one individual for example swam 1015km in 125 days (Campana et al., 2015). The

knowledge on the distribution and population abundances of the Greenland shark are based on fishery surveys, stock assessments of commercial species, and bycatch reports from fisheries (Edwards et al., 2019). Greenland sharks that are caught as commercial bycatch, are often misidentified for other large shark species for example the basking shark (Cetorhinus maximus) (Campana et al., 2008, Edwards et al., 2019). The bycatch is estimated to be 1000 tons/yr in one district in north-western Greenland alone (Gunnarsdottir and Jørgensen, 2008, Edwards et al., 2019).

Small-spotted catsharks are distributed in the Northeast Atlantic from Norway and the British Isles to western Mediterranean, Morocco, Sahara Republic, and Mauritania to Senegal, Ivory Coast (figure 8) (Ebert et al., 2021). The small-spotted catshark is the most common catshark in coastal waters of Europe (Ellis and Shackley, 1997). The species lives in continental shelves and uppermost slopes on sandy, coralline, algal, gravel or muddy bottoms. In the northeast Atlantic they mainly live between 10-100 m depth, whereas they live in up to 400 m depth in the Mediterranean Sea (Muus et al., 1999) and from 288-780 m in the eastern Ionian Sea (Mytilineou et al., 2005). They are nocturnal and during the day males rest on the ground and females hide in the shallows, at 0.5-1.5 m depth and in caves and crevices (Sims et al., 2001, Soares and Carvalho, 2019).

Biology of sharks

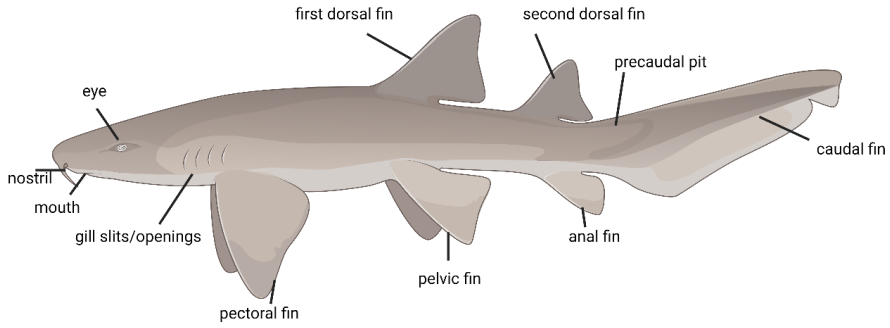

Figure 9: Body features of a shark. *Lateral view of a nurse shark. Created with BioRender.com.*

A shark´s body has three main sections: head, trunk, and tail (figure 9). Although these features are constant there is a great variation in shark size and shape dependent on habitat and feeding strategy. The body shape of most sharks is cylindrical. Nonetheless, there can be variations depending on the lifestyle of the species. Sharks that are hard swimmers have a large, stiff, lower caudal fin lobe. Sharks do not have gas-filled swim bladders that would provide them with natural

buoyancy, as teleost fishes like for example Bluefin tuna or marlins have. Therefore sharks need very broad pectoral fins to produce lift that, together with the pelvic fins, control the angle of pitch, the up and down movement, and prevent falling to the side (Ebert et al., 2021). The skeleton of sharks is made out of cartilage, which unlike bone, does not contain nerves or blood vessels. Cartilage is a strong and flexible material mostly made out of proteins containing fewer materials than bone. In older individuals the cartilage can be partly calcified, harder and more similar to bone. This light, manoeuvrable skeleton assists them with efficient swimming. The skeleton of sharks consists of only a few individual parts (Ebert et al., 2021).

Feeding of sharks

Most shark species are specialized on food and only eat a small range of prey animals. Information on which food sharks eat, and what their feeding methods are, can be obtained through examining their teeth. Many sharks have different teeth with different roles, for example to hold or crush prey. Sharks have two main hunting strategies: active searching for prey or the `sit and wait` strategy [90]p.42. Ambushing is common in species that lie on the seabed. They lie motionless on the seabed and wait for their prey to come by [90]p.44. However, sharks have different feeding strategies. Some species bite out parts of living animals, as for example the cookiecutter shark, and others `ram-feed` as the Basking shark [90]p.42. Several species feed cooperatively, including the Whitetip Reef Shark, and hunt in groups to capture their prey. Many deep-sea squaloid dogfishes are migratory, in order to find new food sources in their low productive environment. After capturing and swallowing their prey, the digestion process in sharks can take a long time, especially in cold-blooded species [90]p.45.

The small-spotted catshark feeds on a variety of small, benthic invertebrates, molluscs, crustaceans, small cephalopods, polychaete worms, and small bony fishes (Shimose et al., Thollot, 1996, Soares and Carvalho, 2019). They have been found to feed in shallow prey-rich areas with soft sediment or areas covered with filamentous algae (Sims et al., 2006, Soares and Carvalho, 2019). The diet of Greenland sharks is different. They feed on a diverse range of prey (Leclerc et al., 2012, Yano et al., 2007, Nielsen et al., 2014, Nielsen, 2017, McMeans et al., 2010) and on benthic and pelagic species (MacNeil et al., 2012). Their food includes bony and cartilagous fishes, cephalopods, crustaceans, and other vertebrates, as well as marine mammals

including seals and small cetaceans (Ebert et al., 2021), and pinniped species, as well as several groups of invertebrates (molluscs, echinoderms, decapods) (Yano et al., 2007). Their potential active predation and broad distribution suggests a high influence on marine food webs, despite their slow metabolism and low consumption rates. The Greenland shark is considered as an apex predator with a high trophic level (Edwards et al., 2019, Nielsen et al., 2014, Ebert et al., 2021). Their high trophic position has been confirmed by stable isotopes, fatty acids, and biomagnifying contaminants that show the consumption of diverse prey (McMeans et al., 2010, Fisk et al., 2002, Hussey et al., 2015). Besides that they are thought to be able to undergo a flexible response to variation in prey availability since they have a geographical variation in their diet (Nielsen et al., 2014, McMeans et al., 2013).

Metabolism of sharks

Only few studies have focused on the metabolism of elasmobranchs, the subclass of chondrichthyans to which sharks belong (Hara et al., 2018, Ebert et al., 2021). In sharks, it is common to classify muscles as red, white and pink, as described later.

Fatty acid oxidation is limited or absent in cardiac and skeletal muscle of elasmobranchs. Their energy metabolism rather relies on ketone bodies and amino acids as oxidative fuels in these tissues. Similar to other vertebrates, carbohydrates appear to be utilized as a fuel source in elasmobranchs. They have relatively low plasma levels of non-esterified fatty acids (NEFA) and plasma levels of the ketone body ß-hydroxybutyrate as high as those of fasted mammals. This possibly can be explained by the assumption that fatty acid oxidation in muscle was lost within this lineage or by the fact that the ancestral metabolic state of fishes involves negligible fatty acid oxidation in muscle (Speers-Roesch and Treberg, 2010). The metabolic rate (rate at which they use energy, which is closely related to their oxygen consumption) is closely related to the shark´s swimming speed. The size of a shark´s heart depends on their level of activeness. For benthic species the average heart rate lies at 40bpm, whereas fast swimmers have rates around 60-70bpm (Ebert et al., 2021). Gills extract oxygen from seawater. Oxygen is used during aerobic metabolism to release energy from glucose, with water and carbon dioxide as by-products.

Most studies on metabolism display a lower rate of anaerobic metabolism for deep-sea elasmobranch than for shallow-water species (Pinte et al., 2021). Generally, it is difficult to study animals living in the deep-sea since most of them are dying after capture. Therefore, directly measuring the whole animal metabolism of deep-sea sharks is nearly impossible. Indirect metabolism measurements for deep-sea animals can be used instead. Enzyme activity assays are a commonly used method (Drazen and Seibel, 2007) and can be measured under in vitro conditions. In combination with other metabolic proxies one can better understand the in vivo metabolism (Pinte et al., 2021). Also the Greenland shark has a very low field metabolic rate (Knight, 2022, Ste-Marie et al., 2022). The metabolic rate for Greenland sharks was calculated in a study that used 30 individuals. They measured their length, temperature and motion via attached sensors and calculated the animal´s body mass based on the length. The determined metabolic rate for the Greenland shark was 21.67±2.30 mg O_2 h^{-1} $kg^{-0.84}$ (*n*=30; 1–4 day accelerometer package deployments) in the late summer and 25.48±0.47 mg O_2 h^{-1} $kg^{-0.84}$ (*n*=6; PSATs) over an entire year. In comparison, the metabolic rate of bull sharks is 187–506 mg O_2 h^{-1} $kg^{-0.86}$. The determined value for Greenland sharks can be translated into 164–193g of fish or mammal for an average 224kg shark to be consumed daily to provide it with that energy. They may also survive periods without eating (Knight, 2022, Ste-Marie et al., 2022). The low mass-specific metabolic rates of the Greenland shark are a result of slow growth, long life spans (Nielsen et al., 2016), and slow swimming speeds (Watanabe et al., 2012). The metabolic rate has also been shown to be a determinant of life span based on the temperature and body size (Gillooly et al., 2001). It is also important to measure the metabolic rate and aerobic and anaerobic scope during resting, swimming and digestion of the Greenland shark to understand its trophic position in the ecosystem (Edwards et al., 2019). Besides that it is also important for understanding their survival strategy, as it is necessary to understand their energy requirements to calculate how much food they need (Ste-Marie et al., 2022, Knight, 2022). No work has been published on the metabolism of the small-spotted catshark yet. However, the species is not very active and often rests on the seabed.

Muscles of sharks

The muscular system of sharks is comprised of myomeres. The anatomical position of shark´s muscles is shown in figure 10. Many myomeres along each side of

their body, one per vertebra, form three-dimensionally folded structures with one main anterior-projecting cone and two posterior-projecting cones (NURSALL, 1956, Gemballa et al., 2003, Greene, 1913, Alexander, 1969). Each myomere spans over many vertebral segments by nesting of the cones (Shadwick and Goldbogen, 2012). Myofibers of sharks are segmented and are ordered in a characteristic zigzag. The myofibers are arranged in long bundles, attached to the skin, that run from head to tail of the shark (Ebert et al., 2021). The skeletal muscle of sharks is comprised of red and white muscle tissue with different characteristics (figure 10) (Ebert et al., 2021).

The different colour of red and white muscles in sharks arises from differences in vascularization and myoglobin content (Kryvi et al., 1981). Slow swimming in sharks mostly is powered by red fibers, fast or burst swimming by white fibers (Kryvi and Totland, 1977, Bone, 1978, Shadwick and Goldbogen, 2012). Red muscles rely on the aerobic metabolism activity (Watanabe et al., 2012, Ryan et al., 2015). The work of the red muscle is limited by oxygen (Ebert et al., 2021). It is highly vascularized and contains many mitochondria (Kryvi and Totland, 1977, Bone et al., 1986, Kryvi and Eide, 1977). It supports slow, continual movements (Watanabe et al., 2012, Ryan et al., 2015) and can provide more oxygen for aerobic processes than white muscles (Kryvi and Totland, 1977). White muscle has few blood capillaries, a lower level of mitochondria and relies on aerobic metabolism in resting and recovering situations and the anaerobic metabolism in high intensity activities (Watanabe et al., 2012, Ryan et al., 2015). It supports fast movements (Watanabe et al., 2012, Ryan et al., 2015). The anaerobic metabolism is important for sharks that need to suddenly swim at high speeds and use energy at a faster rate than oxygen can be re-supplied into the muscles (Ebert et al., 2021). Activities of aerobic enzymes are significantly lower than in red muscles (Childress and Somero, 1979, Sullivan and Somero, 1980, Drazen et al., 2011, Condon et al., 2012, Treberg et al., 2003, Pinte et al., 2021). White muscle cells are larger, have greater myofibrillar content, larger force and faster contraction velocities. The muscle power output, the product of force and shortening velocity, is higher than for red muscle (Bone, 1978). Red and white myofibers also have differences in the myonuclear content and gene expression which could explain the difference of enzyme activities (Moyes et al., 1992).Pink fibers, which are intermediate are located between red and white muscles (Kryvi and Totland, 1977, Bone et al., 1986, Kiessling et al., 2006).The proportion of white

muscle varies between species. Warm blooded sharks have big amounts (Ebert et al., 2021). Red muscle proportion is significantly different in different shark species. The proportion, as well as aerobic enzyme activities are positively related to the cruise swimming speed of sharks. Sharks with a slow cruise swimming speed have a lower aerobic metabolic phenotype and less red muscle (Childress and Somero, 1979, Sullivan and Somero, 1980, Drazen et al., 2011, Condon et al., 2012, Treberg et al., 2003). Besides that, biochemical assays and work loops as force vs. length curves used to determine the mechanical work of myofibers indicate that red and white skeletal myofibers both have very slow metabolic capacities and contraction (twitch) rates (Edwards et al., 2019). This leads to the assumption that they are unable to sustain high levels of either anaerobic or aerobic muscle contraction for extended periods (Fisk et al., 2012, MacNeil et al., 2012, Nielsen et al., 2014).

Not much has been published yet on skeletal muscles of sharks, especially myosin isomers in sharks. In sharks, not many MHC isoforms have been identified yet. Slow cardiac MHC isoform and fast MHC isoforms 1, 2, 3 and 4 have been identified for the Great white shark, Carcharodon carcharias. Cardiac MHC 6 alpha isoform has been identified for Shark mullet, Squalomugil nasutus. Beta cardiac MHC 7 and slow MHC 2 have been identified for the Ghost shark, callorhinchus milii (UniProt, 2022). Therefore, it was difficult to predict the fiber types and characteristics of the Greenland shark and the small-spotted catshark. The proportion of myofiber types in these muscles is unknown. S. canicula, has a five to six times higher mass-specific power output in white muscle than in red muscle. Their white muscle mass is 10 times greater (Shadwick and Goldbogen, 2012).

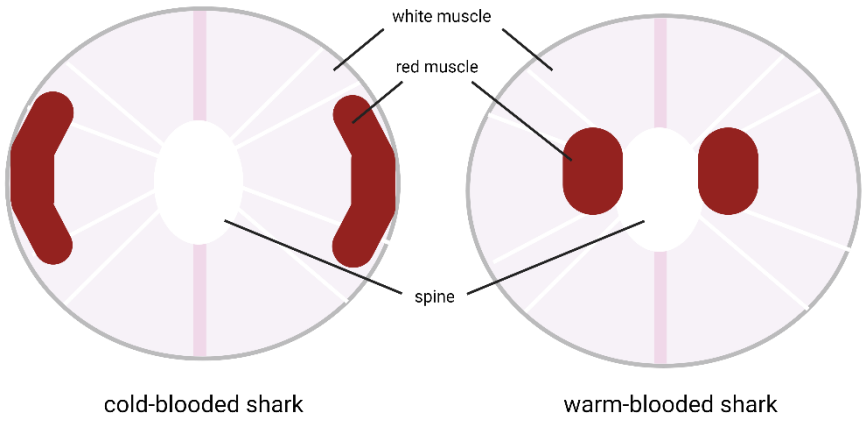

Figure 10: Muscle types and localisation in sharks. *The red muscles of warm-blooded (left) are located in the body core, rather than under the skin as in cold-blooded sharks (right). Created with BioRender.com.*

Movement of sharks

The frequency of contraction of the muscles, as well as the stiffness of the shark´s body define the swimming style of sharks. Sharks undergo two types of movement: steady swimming and burst swimming (Shadwick and Goldbogen, 2012). Alternate contraction of the muscles on both sides of the body produces forward, sinuous swimming, powered by the caudal fin. The degree of bend in the shark´s body is correlated with how much energy is used and efficiency of the movement, as better swimmers have stiffer bodies and undulate only the posterior half of their body with less than one wave in the body. Inefficient swimmers, as for example small-spotted catsharks use a form of swimming that is called “anguilliform”, which is an eel-like movement with undulation of their entire trunk and tail laterally. Anguilliform propulsion is often correlated with a long upper caudal lobe and small lower lobe. Besides that, tail shape and presence or absence of a precaudal pit also are important for swimming mode and speed. Shark fins help to stabilise the shark when moving. Sharks have stiff and unfoldable, fins. The large paired pectoral fins reduce rolling to the side and provide lift to the shark, which counters the negative buoyancy of the shark. Adjustments to the angle of the pectoral fins controls pitching (up and down movement), as well as yawing (lateral side to side motion) (Ebert et al., 2021).

Since sharks do not have a swim bladder, the main struggle for sharks that do not live on the seabed is to maintain the position in the water. The relatively light cartilaginous skeleton helps to provide buoyancy, however, low density oils stored in the liver (represent up to 25% of the total weight) provide most of it. Some sharks help themselves by additionally gulping air at the surface to store it in their stomachs, whereas others have to move continuously to not sink. Sharks that live on the seabed do not have problems with negative buoyancy. Sharks also move differently depending on the time of the day. The small-spotted catshark, only rests on the seabed throughout the day (Ebert et al., 2021)021.

Tail-beat frequencies vary in different shark species. Brief but symmetrical contractions of the lateral musculature enable burst sprints with tail-beat frequencies higher than in steady swimming. Burst speeds are dependent on tail-beat frequency (Bainbridge, 1958, Fierstine, 1965). The highest burst speeds reported are for I. oxyrinchus with up to 8 – 9 m s−1 (6·4–6·6LTs−1) (Peter Klimley et al., 2002). Tail-beat frequencies have also been measured for the Greenland shark.

The sharks swim with 0.34 m·s− 1 with a tail-beat frequency of 0.15 Hz. These are the lowest values for fish their size measured. Since locomotory muscle function of ectodermic fishes is depressed in cold waters, Greenland sharks are vulnerable to avian and mammalian predators with high body temperature. The Greenland shark reverses this pattern since they also hunt for example seals in Arctic waters. The mean and maximum speed (0.74 $m \cdot s^{-1}$) and acceleration during burst swimming (0.008 $m \cdot s^{-1}$) were much lower than those of seals (Watanabe et al., 2012). This indicates that the swimming performance of Greenland sharks is limited by cold waters (~2 °C) and that they are only able to catch seals while they sleep in the water to avoid other predators (Watanabe et al., 2012).

The Greenland shark as a model of successful aging

The Greenland shark is a good model of successful aging, as indicated by several factors. It´s exceptional longevity with up to at least 272 years for Greenland sharks with more than 500 cm in length (Nielsen et al., 2016). Possible reasons for the longevity of the Greenland shark could be negligible senescence, which is common in long-lived animals (Stenvinkel and Shiels, 2019), their low metabolism coming with a slow speed of life (Knight, 2022, Ste-Marie et al., 2022), their expected low productivity since they have extended longevity and low productivity relative to teleosts (Edwards et al., 2019, Musick, 1999), their indeterminate growth since they are sharks (Laforest et al., 2020), or a combination. The free radical theory of aging does not apply to the Greenland shark (Costantini et al., 2017). A possible correlation between exceptional longevity and its specific resistance to oxidative damage was tested (Costantini et al., 2017).

Case of research

Healthy aging, longevity and increasing life expectancy are topics that become more and more important over time. The Greenland shark is a great model for aging research since it is the longest lived vertebrate (Edwards et al., 2019) with a lifespan of at least 272 years with a maturity at about 150 years of age (Nielsen et al., 2016). Muscles are such a big part of the body that animals with longer lifespans need to be more efficient at muscle specific energy mechanisms. There have not been done studies on the muscle of the Greenland shark yet. Muscle is important but wastes away during aging with mechanisms of this not entirely known, and metabolic changes may be important. The regulation of organs such as muscle is well-known to be deteriorated over time in aged vertebrates contributing to the end of life (Francis et al., 2017). Thus, getting insights into muscle regulation in the Somniosus microcephalus would then be very informative and potentially usable for 'treating' the aging vertebrate muscle. Muscle aging, sarcopenia, muscle weakness or atrophy, is one of the main reasons for decrease in life quality among humans worldwide since so many people are affected (Frontera and Ochala, 2015). Some animals, as for example sharks, are good at aging and may be useful models to study sarcopenia and investigate underlying molecular mechanisms. Besides that, aging is also thought to potentially change the behaviour and properties of the key sarcomeric protein myosin, for example changes in the SRX/DRX state equilibrium (Colson et al., 2015, Phung et al., 2018). Therefore, it would be interesting to investigate the SRX/DRX ratio for red and white muscles of the long-lived Greenland shark, versus for the shorter-lived small-spotted catshark. We will also analyze cryosections of Greenland shark and small-spotted catshark red and white muscles and characterise different features of the muscles after immunofluorescent staining. The results then can later be compared to other vertebrates, mammals, and humans. Mant-ATP Chase Experiments will be done on the Greenland shark and small-spotted catshark to look at ATP- consumption in red and white myofibers and therefore be able to analyze the ratio of SRX/DRX content of myosin heads in the muscles. We hypothesize that muscle characteristics, as well as the ATP- consumption of the muscles, are different in both species.

Results

Cryosections

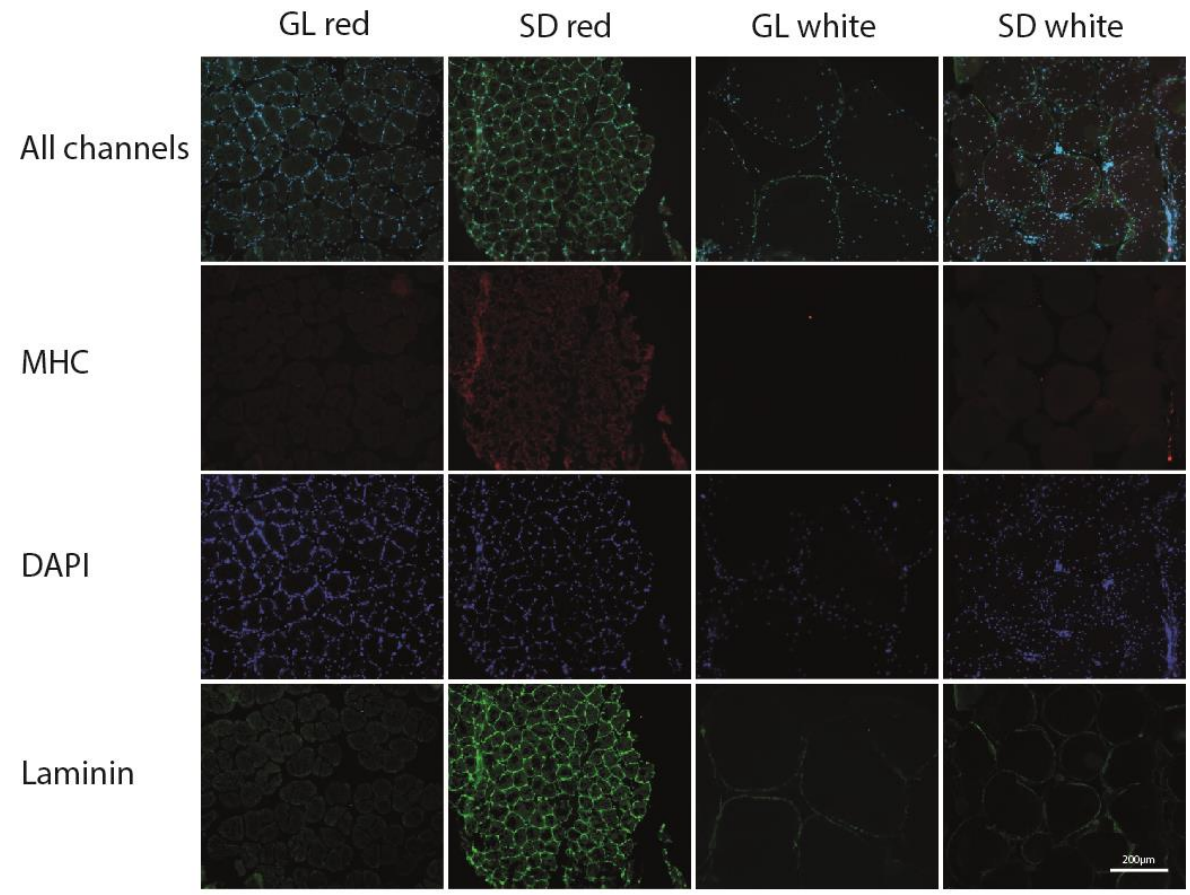

Figure 11: Channel separation of Greenland (GL) and Small-spotted Catshark (SD) white and red muscle, 10x images. *For each of the samples, a representative merged image, as well as the single channel for MHC (red), DAPI (showing the nuclei, blue) and laminin (showing the cell membranes, green) are shown. Images were taken with ZEISS Stereo-Microscope Stemi 508.*

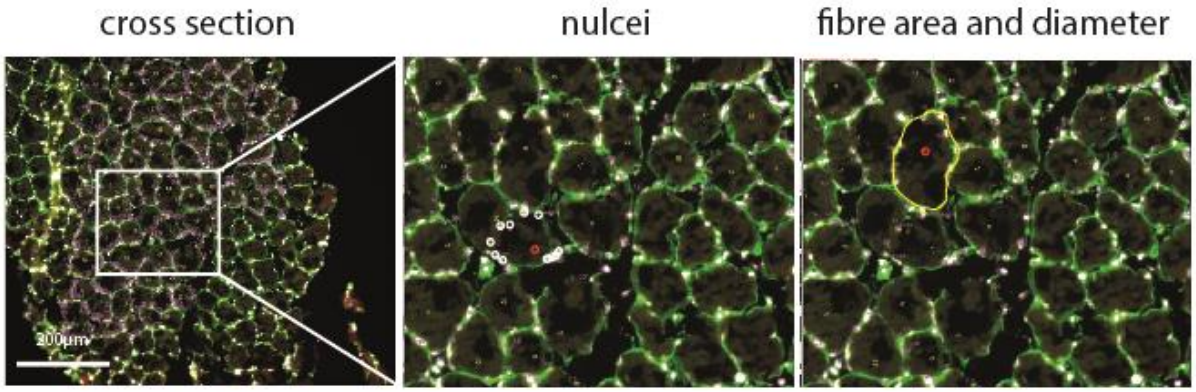

Figure 12: Sample measurement of Small-spotted Catshark red muscle cross section in 10x in Fiji/ImageJ with ObjectJ, with nuclei count, fiber area and diameter measurements (white= nuclei, red= fiber, yellow= fiber border). *Images were taken with ZEISS Stereo-Microscope Stemi 508.*

Cryosection of red and white muscles of the Greenland shark and of the small-spotted catshark merged, as well as the red, blue and green channel seperately are shown in figure 11. The red channel shows the MHC, the blue channel (DAPI) the nuclei and the green channel laminin, visualizing the cell membranes. Figure 12 shows the measurement of the fiber area and diameter, as well as the nuclei counting in Fiji/ImageJ with ObjectJ. Nuclei are shown in white, fibers in red and one fiber is surrounded in yellow.

Nuclei

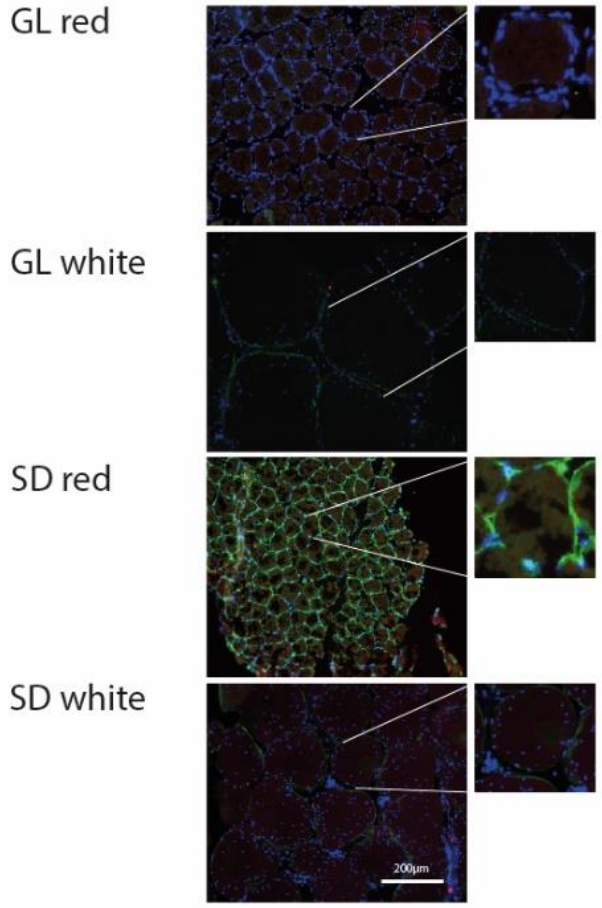

Figure 13: Nuclei pattern of one sample image per tissue (Greenland shark and Small-spotted Catshark red and white muscle). *Nuclei are displayed in blue (DAPI channel). Images were taken with ZEISS Stereo-Microscope Stemi 508.*

I also looked at the nuclei pattern for each tissue of both species, the Greenland shark and small-spotted catshark (figure 13). The nuclei pattern varied per tissue. In Greenland shark and small-spotted catshark red muscle the nuclei were located outside of the fibers. In Greenland shark white tissue at the borders of the fibers but outside and inside. In the small-spotted catshark, white muscles the nuclei are located outside and inside the cell membranes. In white muscles the nuclei also clustered between the fibers.

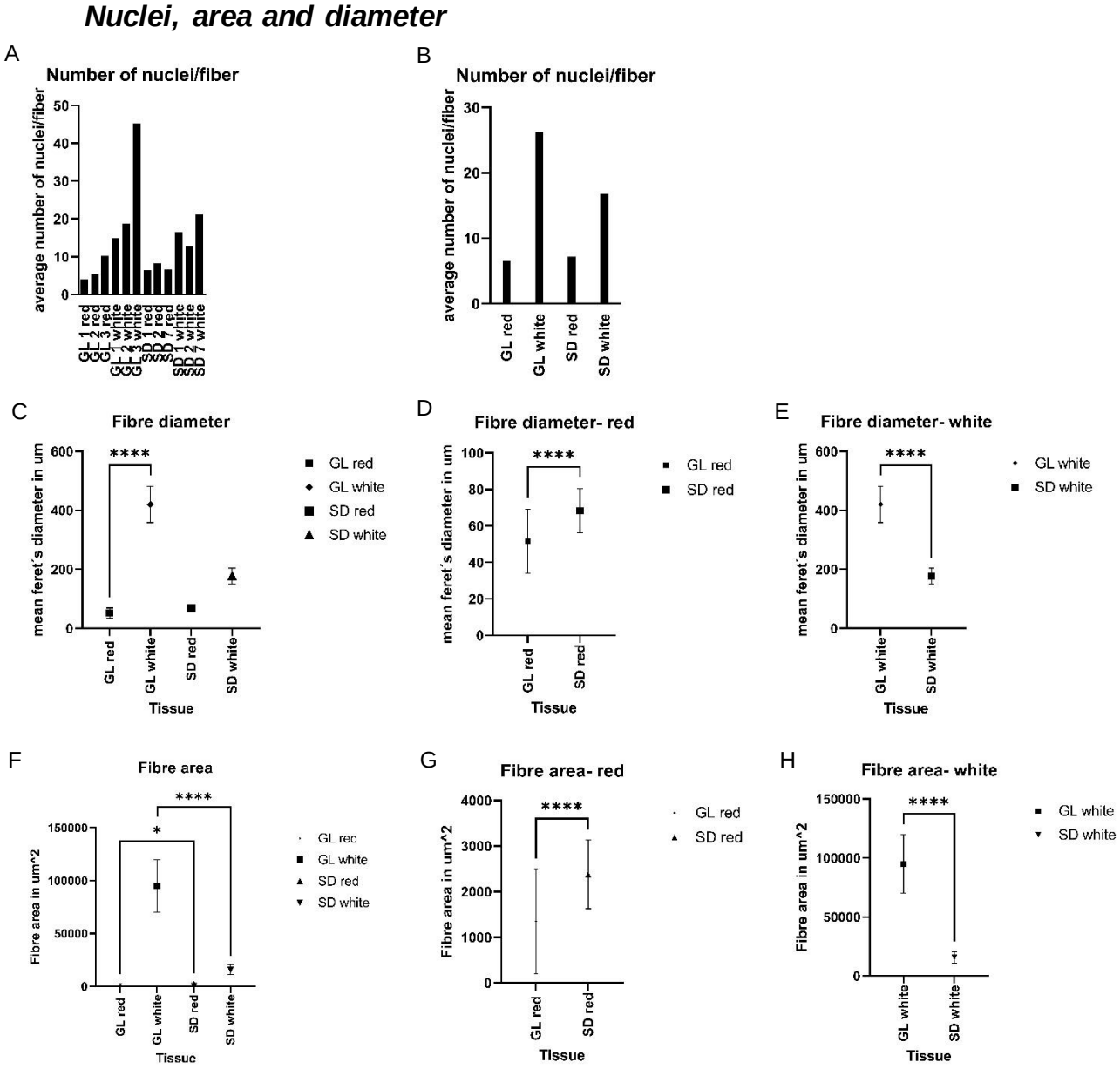

Figure 14: Mean nuclei count, fiber area and diameter per fiber/ sample and tissue. *A) Average number of nuclei per fiber per sample; B) Average number of nuclei per tissue (divided by shark species (Greenland shark/ small-spotted catshark) and tissue type (red/ white)); C) Mean feret´s diameter for a fiber per sample; D) Mean feret´s diameter for a fiber per sample for red tissue; E) Mean feret´s diameter for a fiber per sample for white tissue; F) Mean fiber area in um^2; G) Mean fiber area in um^2 for red tissue; H) Mean fiber area in um^2 for white tissue. GL=Greenland shark, SD= small-spotted catshark, Error bars show standard deviation. Significance is shown with asterisk in graphs.*

Furthermore, I also looked at the mean nuclei count, mean fiber area and mean feret´s diameter per fiber (figure 14). The significance for the number of nuclei per fiber could not be calculated because only the average number of nuclei per myofiber was calculated instead of counting the number of nuclei per myofiber. The average nuclei count per tissue varied. In both sharks, white muscles had more nuclei than the red muscles, as figure 14AB show. Greenland shark white muscles had more nuclei than small-spotted catshark white muscles. The mean varied with

~26 nuclei/fiber for the Greenland shark and ~17 nuclei/fiber for the small-spotted catshark. One Greenland shark sample has a very high average number of nuclei (45). For red muscles the number of nuclei/fiber was ~7 for both species.

The mean fiber area was significantly different between both species for red tissue (p value <0.0001), and white tissue (p value <0.0001), and varied per tissue and sample, as shown in figure 14CDE. On average, white myofibers were bigger for both species than red myofibers. Greenland shark white myofibers on average were bigger (94976um^2) than small-spotted catshark white muscles (15710um^2). Red myofibers were of similar size for both species.

I also looked at the feret´s diameter per sample and tissue, which was significantly different between both species for red (p value <0.0001) and white (p value <0.0001) muscle tissue (figure 14FGH). The mean diameter of red myofibers is lower than for white myofibers. Mean red myofiber diameter is similar in the Greenland shark and small-spotted catshark (51.57 and 68.38µm, respectively). However, the myofiber diameter is more homogenous in the small-spotted catshark. In the Greenland shark the values have a greater variability. White myofibers have on average a bigger diameter than red fibers. Greenland shark white muscles have bigger diameters (420.3µm) than small-spotted catshark white myofibers (177.4µm). However, small-spotted catshark white muscles contain fibers with a smaller diameter than some red fibers. Greenland shark white fibers all had bigger diameters than Greenland shark red fibers.

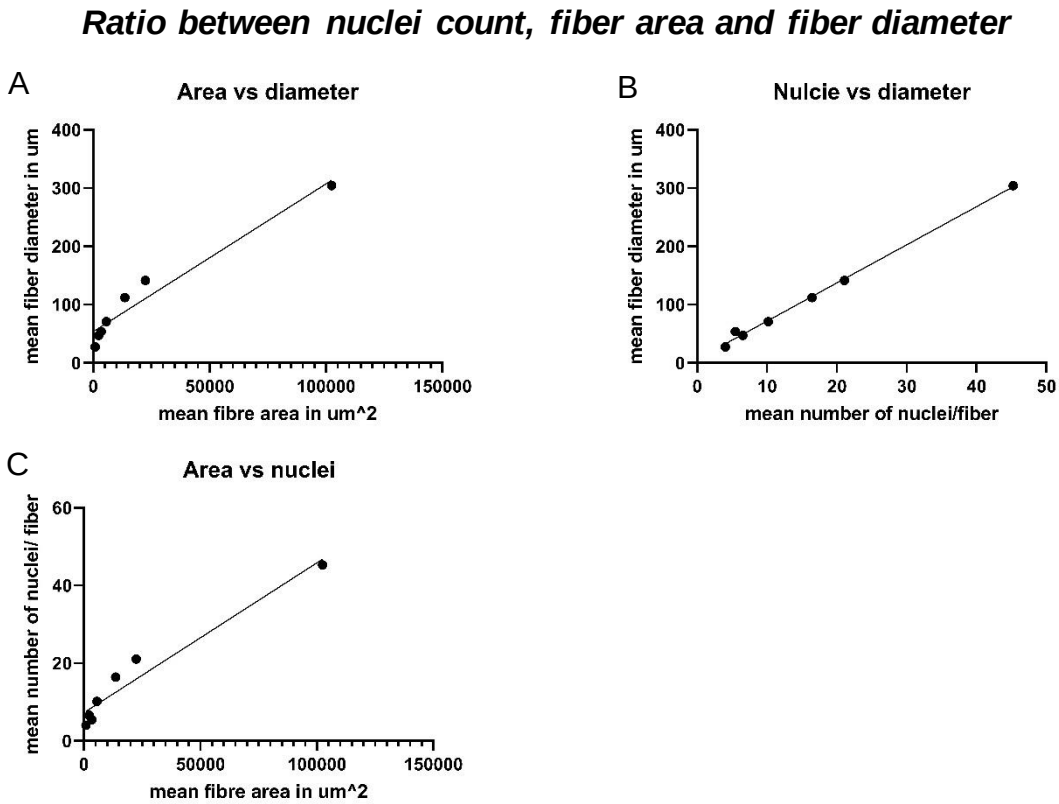

Figure 15: Relationship between different measurements per sample. *A) Mean nuclei count per fiber/sample vs. mean fiber area/ sample; B) Mean fiber area/ sample vs. mean fiber diameter/sample; C) Mean nuclei count per fiber/sample vs. mean fiber diameter/ sample.*

I looked at a possible correlation between fiber area and diameter, number and nuclei and diameter, as well as fiber area and number of nuclei, respectively. For all three comparisons the slope is significantly non- zero. An almost linear relation could be shown between the fiber area and the diameter (p value= 0.0002, R squared= 0.9509), the fiber area and the number of nuclei (p value= 0.0003, R squared= 0.9441), as well as the number of nuclei and the fiber diameter (p value= <0.0001, R squared 0.9966). Figure 15 shows the relationship between mean nuclei count, mean feret´s diameter and mean area per fiber.

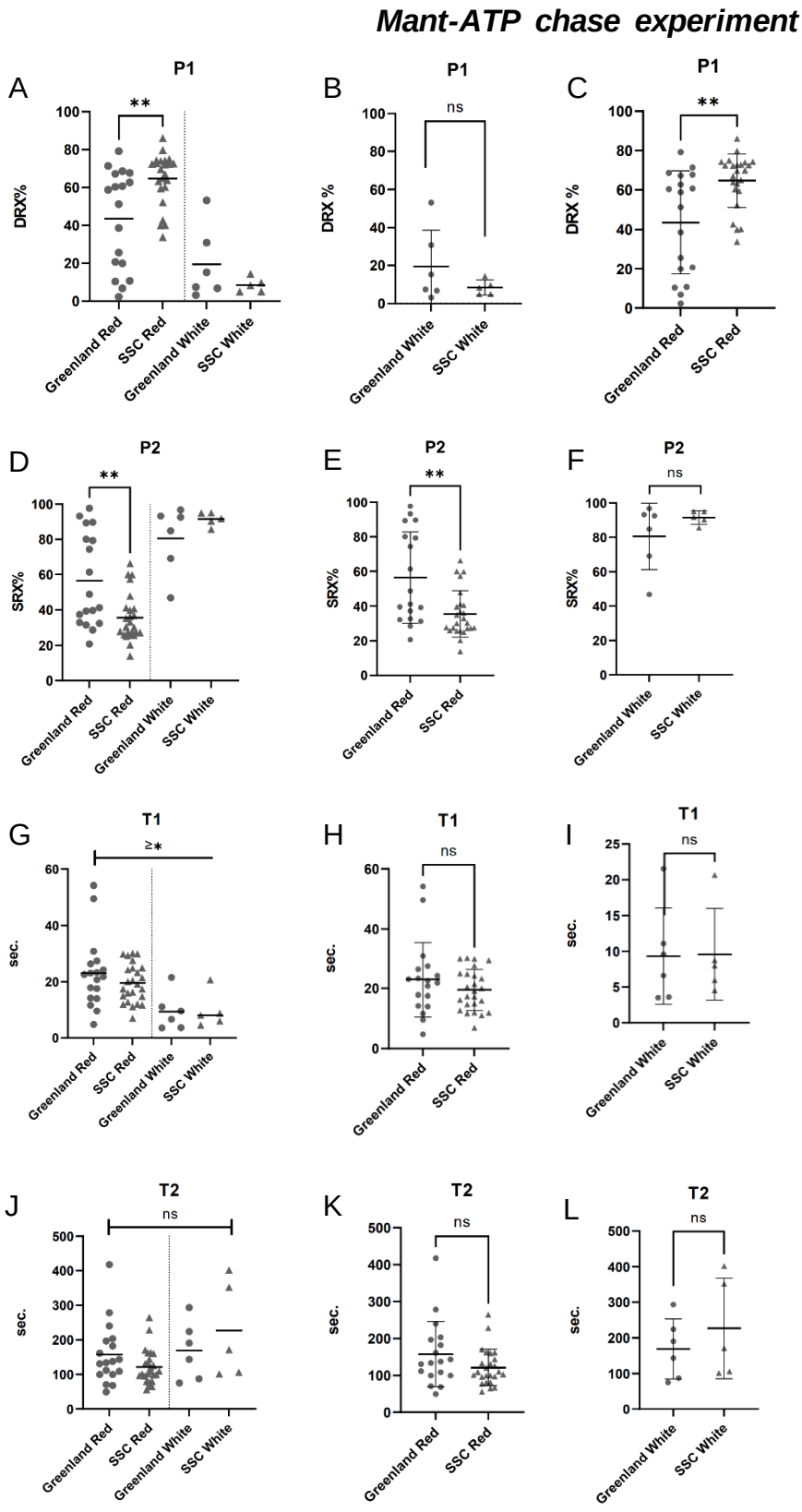

Figure 16: Myosin relaxed states in individual myofibers (P1-Percentage of myosin molecules in DRX state, P2- Percentage of myosin molecules in SRX state, T1-ATP hydrolysation time for myosin molecules in DRX state, T2- ATP hydrolysation time for myosin molecules in SRX state,). *A) Percentage of DRX state for red/white muscle of Greenland shark and small-spotted catshark respectively; B) Percentage of DRX state for white muscle of Greenland shark versus white muscle of the small-spotted catshark; C) Percentage of DRX state for red muscle of Greenland shark versus red muscle of the small-spotted catshark; D) Percentage of SRX state for red/white muscle of Greenland shark and small-spotted catshark respectively; E) Percentage of SRX state for*

red muscle of Greenland shark versus red muscle of the small-spotted catshark; F) Percentage of SRX state for white muscle of Greenland shark versus white muscle of the small-spotted catshark; G) Time for ATP hydrolysis in DRX state for red/white muscle of Greenland shark and small-spotted catshark respectively; H) Time for ATP hydrolysis in DRX state for red muscle of Greenland shark versus red muscle of the small-spotted catshark; I) Time for ATP hydrolyzation/hydrolysis in DRX state for white muscle of Greenland shark versus white muscle of the small-spotted catshark; J) Time for ATP hydrolysis in SRX state for red/white muscle of Greenland shark and small-spotted catshark respectively; K) Time for ATP hydrolysis in SRX state for red muscle of Greenland shark versus red muscle of the small-spotted catshark; L) Time for ATP hydrolysis in SRX state for white muscle of Greenland shark versus white muscle of the small-spotted catshark. Fibers with interrupted or HIT measurements or with r2 below 0.95 were excluded. Means and standard deviations also appear on histograms. Significance is shown with asterisk in graphs.

Figure 16 shows Mant-ATP chase experiment data. The proportion of myosin molecules in the super-relaxed state or disordered relaxed states as well as their ATP turnover lifetime were estimated from the equation presented in the methods section. Exponential decays for myofibers isolated from control sharks (small-spotted catshark) and the Greenland shark are shown.

I looked at P1, which was significantly different between Greenland shark and small-spotted catshark red muscle (p value= 0.0046), but not significantly different between the white muscle of both species (p value= 0.2267). P1 is the amplitude of the initial rapid decay approximating the 'disordered-relaxed state' (DRX) and is an estimate of the fraction of myosin heads in the DRX conformation. Of the Greenland shark red fibers, on average 43.51% of the myosin heads per fiber were in DRX conformation. However, the percentage of myosin heads in the DRX state varied between 2.3 and 71.4% between the red Greenland shark fibers. Of the small-spotted catshark red fibers, on average 64.69% of the myosin heads were in DRX conformation. The percentage of red small-spotted catshark fibers having myosin heads in DRX conformation varied between 33.7 and 86%. Of the Greenland shark white fibers, on average 19,45% of the myosin heads were in DRX conformation. The percentage of the Greenland shark white fibers having myosin in DRX conformation varied between 3.1 and 53.2%. Of the small-spotted catshark white fibers, on average 8.47% of the myosin heads per fiber were in DRX conformation. The percentage of red small-spotted catshark fibers having myosin heads in DRX conformation varied between 5 and 14.4%. The average percentage of fibers with myosin heads in the DRX state varied by 21.18% for red fibers between Greenland shark and small-spotted catshark and by 10.98% for white fibers between Greenland shark and small-spotted catshark. The values for the red myofibers were significant, whereas the white myofibers did not show significant results.

Furthermore, I also looked at P2, which was significantly different between Greenland shark and small-spotted catshark red muscle (p value= 0.0049), but not significantly different between the white muscle of both species (p value >0.05). P2 is the slower second decay approximating the proportion of myosin heads in the 'super-relaxed state (SRX) and is an estimate of the fraction of myosin heads in the SRX conformation. Of the Greenland shark red fibers, on average 56.49% of the myosin heads per fiber were in SRX conformation. The percentage of Greenland shark red fibers having myosin heads in SRX conformation varied between 20.8 and 93.2%. Of the small-spotted catshark red fibers, on average 35.54% of the myosin heads were in SRX conformation per fiber. The percentage of red small-spotted catshark fibers having myosin heads in SRX conformation varied between 20.3 and 66.2%. Of the Greenland shark white fibers, on average 80.55% of the myosin heads per fiber were in SRX conformation. The percentage of Greenland shark white fibers having myosin heads in SRX conformation varied between 46.8 and 96.8%. Of the small-spotted catshark white fibers, on average 91.53% of the myosin heads were in SRX conformation. The percentage of white small-spotted catshark fibers having myosin heads in SRX conformation varied between 85.6 and 95%. The average SRX percentage varied by 20.95% for red fibers between Greenland shark and small-spotted catshark and by 10.98% for white fibers between Greenland shark and small-spotted catshark.

Besides that, I also have calculated T1, which is the time constant for the decay. It describes how fast one ATP molecule gets hydrolyzed in the P1 (DRX) state. It was not significantly different, for white muscle (p value > 0.05) and red muscle (p value= 0.2944), of both shark species respectively. It is calculated by the equation 1/k fast. In red myofibers having myosin in DRX state, one ATP molecule on average gets hydrolyzed faster in the small-spotted catshark (19.53s) than in the Greenland shark (23). In white myofibers having myosin in DRX state, one ATP molecule on average gets hydrolyzed faster in the small-spotted catshark (9.58s) than in the Greenland shark (9.33s).

Also T2 has been calculated and was not significantly different for white muscle (p value > 0.05) and red muscle, of both shark species respectively (p value= 0.1334). It is the time constant associated with P2, describing how fast one ATP molecule gets hydrolyzed in the P2 (SRX) state and is calculated by the equation 1/k slow. In red myofibers having myosin in SRX state, one ATP molecule on average gets hydrolyzed faster in the small-spotted catshark (121.6s) than in the Greenland shark (157.5s). In white myofibers having myosin in SRX state, one ATP molecule on average gets hydrolyzed slower in the small-spotted catshark (226.7s) than in the Greenland shark (169s).

Discussion

The main focus and aims of the study was to determine characteristics and try to understand the functionality of Somniosus microcephalus muscle, compared to a control shark (small-spotted catshark), as well as its metabolic characteristics. For that, cryosections of red and white muscles will be analyzed and different features of the muscles will be characterised after immunofluorescent staining. With the help of Mant-ATP Chase Experiments the ATP- consumption in red and white muscle fibers as well as the SRX/DRX content of myosin heads in the muscles, will be determined.

The most interesting finding was that both tissues, red and white muscles, of both sharks respectively, had a low rate of myosin heads in the disordered relaxed state and high rate of myosin heads in the super-relaxed state. Also the finding that white muscle fibers of the Greenland shark are extraordinary big and have a different nuclei pattern than the other examined tissues was important.

In this thesis of work, we aimed to analyse the behavioural characteristics of Greenland sharks and small-spotted catsharks. These species were used as due to the unique, and successful, ability for Greenland sharks to largely defy conventional aging. Herein, muscle samples were isolated from these species and subjected to Mant-ATP chase experiments to understand how differentially myosin acts in these species.

The main finding of the study were the results of the Mant-ATP chase experiment. The data shows a low disordered relaxed state and high super-relaxed state percentage of myosin head states for both species and tissues. For both species, the percentage of myosin heads being in the disordered relaxed state was higher for red muscle than for white. However, the difference was smaller for the Greenland shark red and white muscle. The small-spotted catshark had a higher discrepancy in the disordered relaxed state fraction between red and white fibers. The respective ATP turnover time is also different between the muscle tissues. For fibers with myosin heads in the disordered relaxed state the corresponding ATP turnover time is lower for white fibers than for red. There is a slight difference between the species. For fibers with myosin heads in the super-relaxed state the corresponding ATP turnover time is lower for red fibers than for white. However, Greenland shark red and white fibers have similar ATP hydrolysis times for fibers with myosin heads in the SRX state. The ATP turnover times in this study also

correlated with the published data by (Nag and Trivedi, 2021), which said that for the DRX state the ATP turnover state of myosin in the absence of actin had a very slow ATP turnover time of <30 s and the SRX state has ATP turnover times of more than 100 s.

These changes and differences to a normal SRX/DRX ratio seen in the results of the Mant-ATP Chase Experiment are affecting the ATP consumption within the muscle and maybe the energy demand of muscles and the whole body. The active cycling state of myosin has a rapid ATP turnover time, whereas myosin in the DRX and SRX state need longer to hydrolyse ATP. However, myosin in the SRX state has a 10-fold slower ATP turnover rate than the non-actin-bound, disordered relaxes (DRX) state (Stewart et al., 2010). Myosin in the SRX state are held 'in-reserve'. Studies showed that ~ 50–60% of the myosin heads are in the SRX state (Stewart et al., 2010, Hooijman et al., 2011). This ratio can be shifted through physiological, pathophysiological, and non-physiological factors. The results of the Mant-ATP Chase Experiments showed a different SRX/DRX ratio. Only red muscle of the Greenland shark was between 50 and 60%, with 56.49%. Small-spotted catshark red muscle had less than 50% of the myosin heads in SRX state (35.54%), and for both species the fraction of myosin heads in the SRX state was higher than 60% with 80.55% for the Greenland shark and 91.53% for the small-spotted catshark. The fraction of myosin heads in the SRX state influences the ATP turnover rate. This means that the ATP consumption in the muscle is lower and gets hydrolyzed with a slower rate, especially because the majority of skeletal muscle of sharks is white. The muscle metabolism is therefore lower, as well as the energy demand of the muscle. Therefore, also the whole body has a slower metabolism, which can also influence the aging process. This would go in line with the fact that the Greenland shark has a very low field metabolic rate (Knight, 2022, Ste-Marie et al., 2022) and biochemical assays and work loops as force vs. length curves used to determine the mechanical work of myofibers indicate that red and white skeletal myofibers of sharks have very slow metabolic capacities and contraction (twitch) rates (Edwards et al., 2019). Also the fact that the main cause of accelerated aging in mammals is energy excess. Therefore, caloric restriction without malnutrition is currently the most effective non-genetic intervention to delay aging phenotypes in a wide range of mammals from flies to primates (Pifferi et al., 2019, Lian et al., 2018). This says that the metabolism influences the aging process. Since also the small-spotted catshark, that has a lower

life expectancy than the Greenland shark, has a higher fraction of SRX in the white muscle, similar to the Greenland shark, it cannot be the only reason for the extraordinary longevity of the Greenland shark. However, there is a difference between the small-spotted catshark and the Greenland shark since the Greenland shark has a “normal” SRX fraction in the red muscle, whereas the small-spotted catshark has a lower percentage than usual. Since aging can influence the SRX/DRX ratio towards more DRX heads in female mice, it is important to look at the age of the used individuals (Colson et al., 2015, Phung et al., 2018). A shift in the SRX/DRX ratio through aging is unlikely for the Greenland shark because we only worked with young individuals. For the small-spotted catsharks we worked with older (9 year old) individuals. Since the estimated life expectancy for this species is 17 years, we do not expect a shift in the SRX/DRX ratio through aging yet. Overall, this means that it could be beneficial for healthy aging to have a slower ATP concumption in the muscle.

Besides that, also the characteristics of white muscle tissue from the Greenland shark were interesting, especially the size and the nuclei pattern. In the white muscles of the Greenland shark, nuclei clustered between fibers. It looks similar to connective tissue (endo- or perimysium in muscles). One can also see perimysium, that surrounds the bundles in the Greenland shark white muscle. Furthermore, also the size of the white fibers was extraordinary big for the Greenland shark. The massive fiber size of Greenland shark white muscle, and hence the long transportation distances of transcripts, might be the reason for the nuclei distribution inside the fibers. For red muscles of the Greenland shark and the small-spotted catshark the nuclei distribution looked as expected, with nuclei similarly distributed at the cell membranes of the myofibers. Red fibers were approximately of the same size in both species, but the white fiber size differed for both species.

Another interesting finding was that the anti-laminin stainings in the first individuum of the Greenland shark red muscle also stained inside the cell membrane. The red and white fibers of this individuum generally had smaller diameters. An explanation for this could be that the first individuum of the Greenland shark was still in a developmental phase and smaller than the other Greenland sharks. For the first individual the size of the animal was not given. One does not know how old the Greenland sharks were since the age was not given. However, the size was given for

two of the three sharks with 386cm and 398cm in length. One study done on ageing of the Greenland shark suggested a maximum life expectancy of up to at least 272 years for Greenland sharks with more than 500 cm in length (Nielsen et al., 2016). Therefore, our smaller individual might not be that old yet since sharks also have indeterminate growth (Laforest et al., 2020).

Furthermore, it was also shown that both, red and white fibers, were mainly round and organised in bundles. The fiber diameter grows with fiber size. Although some samples of the Greenland shark white muscle had a very high number of nuclei per fiber, the fibers were also bigger in these samples. A linear relation could be shown between the fiber area and the diameter, between the fiber diameter and nuclei count, as well as the fiber area and nuclei count. This indicates that bigger fibers have more nuclei and the number of nuclei increases with fiber size.

The next steps in the line of work would be to do de novo sequencing of the transcriptome of the Greenland shark using RNA sequencing, to make more progressions in the research and field. It would be a useful approach to map transcriptomic differences in muscle cells between the two species. We hypothesize that the Somniosus microcephalus muscle transcriptome has marked differences in contractile and metabolic genes when compared with other marine vertebrates. Pilot and initial work has been done by me, as the isolation of the RNA and the preparation of the sequencing libraries. However, the data has not yet been fully generated and analysed and is therefore beyond the timeline of this thesis.

Some flaws in the study were that the fiber type classification did not work because the myosin antibody is probably not working so well in sharks. It has not been tested before. Besides that, also the high fat content might have influenced and interfered with the staining. However, the laminin staining, as well as the DAPI staining worked most of the time. For future studies the protocol could be optimised.

However, also the results of the cryosection- experiment led to interesting findings. As described above, possible reasons for the longevity of the Greenland shark could be negligible senescence, which is common in long-lived animals, their low metabolism coming with a slow speed of life, their expected low productivity since they have extended longevity and low productivity relative to teleosts (Musick, 1999), or their indeterminate growth since they are sharks (Laforest et al., 2020). We looked

at a potential correlation of its longevity with muscle metabolism and found differences in the white muscle characteristics, which might be a sign for a different muscle metabolism or substrate delivery to the muscle.

Conclusion and future outlook

The results show some differences between the two species, especially for the white muscle. The reason for this might be a different lifestyle and therefore different functions of the muscles. However, both species are cold-blooded. Also the metabolism of the two shark species might be different. The Greenland shark has a very low field metabolic rate (Ste-Marie et al., 2022, Knight, 2022), which might interfere with the white muscle structure. The low mass-specific metabolic rates of the Greenland shark are a result of slow growth, long life spans (Nielsen et al., 2016), and slow swimming speeds (Watanabe et al., 2012). The metabolic rate has also been shown to be a determinant of life span based on the temperature and body size (Gillooly et al., 2001). The Mant-ATP chase experiment data combined with the staining results of the cryosections indicates that the white tissue has a different function than to work as a normal muscle. The red tissue looks like regular skeletal muscle. For future research it would be interesting to study the Greenland shark´s proteome, transcriptome and genome, as well as Sirtuin levels, or negligible senescense. We hypothesize that something in the Greenland shark genome is remodelled in genes that are related to the metabolism or they might have a cluster of metabolic genes and that the Greenland shark muscle has differences in contractile and metabolic genes compared to the small-spotted catshark.

Materials and Methods

Animals

Red and white muscle of one male and two female Greenland sharks *Somniosus microcephalus* were supplied by Holly Shiels from the University of Manchester, UK. The sharks were caught in Greenland in 2019 and 2021, two of them at Dec. Longitudes N of 60.671 and 60.6912, and Dec. Longitudes W of 46.187 and 46.085 . The conversion and location of the coordinates is shown in figure 17. Samples of the small-spotted catshark *Scyliorhinus canicula* were supplied by captive breeding at the Fiskeri- og Søfartsmuseet (translation from Danish: Fishing and Maritime Museum) in Esbjerg, Denmark. Age estimation for the Greenland shark was not provided. The age of the small-spotted catsharks was provided by the Fiskeri- og Søfartsmuseet and was performed according to recorded data. Seven individuals of the small-spotted catshark with sizes of 50-80cm in length, five males and three females were provided by the aquarium. They were around nine years old. For the experiments, one male (length not given) and two females (386cm and 398cm in length) of the Greenland sharks were compared with one male and two females of the small-spotted catshark. Transcriptome sequencing, cryosectioning, as well as Mant-ATP chase experiments were performed using red and white muscle samples. Animal handling and sample collections at the Fiskeri- og Søfartsmuseet, as well as the catching of the Greenland shark was conducted by professionals.

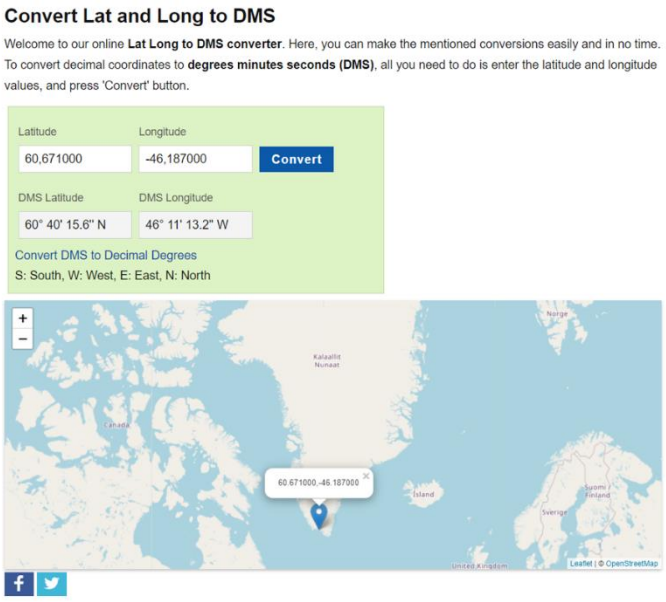

Figure 17: Convertion tool for lateral and longitudinal to DMS latitude *(LatLong, 2022).*

Cryosection and immunofluorescence staining

White and red muscles of the Greenland shark and small-spotted catshark were cut in 10 µm sections. Before sectioning the Greenland shark, muscle chunks were hardened in 4% PFA over night at 4°C. For the small-spotted catshark, sections were cut at optical temperatures of -20°C and chamber temperatures of 22°C. Muscle sections of the Greenland shark were cut at -30°C optical temperature and chamber temperature. The slides were stored at -80°C after cutting. Before staining, the sections were air dried, rehydrated in PBS and fixed in 4% PFA for 15 minutes. After three washes in PBS they were permeabilized with 0.1% Triton X-100 for 10 minutes and after another three washes in PBS, blocked with goat serum for 1 h. The sections were incubated in primary antibodies over night at 4°C (Anti-Laminin antibody produced in rabbit, L9393, Sigma-Aldrich, 1:20 in goat serum together with one of the myosin heavy chain antibodies, 1:25 in goat serum: Myosin Type I, mouse, A4.951, DSHB; Myosin Type IIA, mouse, SC71-S, DSHB; Myosin Type IIB, mouse, BF-F3, DSHB; Myosin Type IIX, mouse, 6H 1-S, DSHB). On the next day, the sections were washed three times in PBS and secondary antibodies were added (1:500 in goat serum: Alexa Fluor 488 goat anti-rabbit IgG (H+L), A11034, Thermo Fisher; AlexaFluor 647 F(ab´)2 fragment of goat anti-mouse IgG (H+L), A21237, Thermo Fisher) for one hour at room temperature in a dark room. After three washes in PBS, the nuclei were counterstained with DAPI (1:1000 in PBS; 62248, Sigma-Aldrich) for 5 minutes. The sections were washed in PBS one more time before mounting with Vectashield, and the images were captured using a Stereo-Microscope Stemi 508 (ZEISS).

Mant-ATP Chase Experiments

The Mant-ATP chase experiments were conducted as follows (Ochala et al., 2021). First, single myofibers were isolated from a muscle chunk for each sample. For this, the samples were slowly defrosted (glycerol:relaxing buffer 1:1, 24h in -20C and 24h in 4h), after which the samples were stored in -20C. The day of the experiment the samples were put in relaxing solution and the single myofibers were isolated under the microscope. The ends of the single myofibers were individually clamped to half-split copper meshes (SPI G100 2010C-XA, width, 3 mm) glued to a glass slide (Academy, 26 × 76 mm, thickness 1.00–1.20 mm). For the white muscle, 2 fibers were mounted per slide, and for the red muscle 6 fibers. After that, flow

chambers were created via attaching cover slips to the top of the glass slide (Menzel-Gläser, Braunschweig, Germany, 22 × 22 mm, thickness 0.13–0.16 mm) [18,19]. At 25 °C, fibers were subjected to the Mant-ATP chase protocol. Each fiber was first incubated for 5 min with a rigor buffer. Then, a solution containing the rigor buffer with 250 µM Mant-ATP, a fluorescently labelled ATP analogue was flushed and kept in the chamber for 5 min. After that, a solution made of rigor buffer with 4 mM ATP was added with simultaneous acquisition of the Mant-ATP chase images. The fluorescence decay was recorded with a Zeiss Axio Scope A1 microscope with a Plan-Apochromat 20x/0.8 objective and a Zeiss AxioCam ICm 1 camera. Images were taken for 5 min, every 5 s. The acquisition/exposure time was 20 ms and a DAPI filter set was used. The fluorescence decay was assessed at one region per individual myofiber using the ROI manager in ImageJ as previously published [18,19]. To calculate the results, the mean background fluorescence intensity was subtracted from the average of the fiber fluorescence intensity for each image that was taken. The time points were then normalized by the fluorescence intensity of the final Mant-ATP image before the washout (T = 0). These data were then fit to an unconstrained double exponential decay using Graphpad Prism:

$$Normalised\ Fluorescence\ = 1 - P1\ (1 - exp(-t/T1)) - P2\ (1 - exp(-t/T2))$$

P1 is the amplitude of the initial rapid decay approximating the ‘disordered-relaxed state’ (DRX), with T1 being the time constant for the decay. P2 is the slower second decay approximating the proportion of myosin heads in the ‘super-relaxed state’ (SRX) and T2 is the time constant associated with P2. P1 and P2 were adjusted for the level of non-specific binding found to be 40% in skeletal muscle [16], to obtain DRX and SRX values. The analysis for the Mant-ATP chase experiments was conducted via ImageJ and Graphpad Prism. Ratios of SRX/DRX were determined for each tissue.

List of Supplies

Table 2: List of supplies.

Supply	Company
10% Normal Goat serum	Life technologies
A11034 Alexa Fluor 488 goat anti-rabbit IgG (H+L)	Invitrogen by Thermo Fisher Scientific
AlexaFluor 647 F(ab´)2 fragment of goat anti-mouse IgG (H+L)	Invitrogen by Thermo Fisher Scientific
Anti-Laminin antibody produced in rabbit L9393	Sigma-Aldrich
Barcodes: NEBNext Multiplex Oligos for Illumina (Methylated Adaptor)	New England BioLabs
Cell Culture 6 well plate Non-Pyrogenic Polystyrene	Costar Corning incorporated
Centrifuge 5415R	Eppendorf
Chloroform	Sigma-Aldrich
Collagenase from Clostridium histolyticum C0130-100MG	Sigma-Aldrich
Cryochamber Kummefryser FB100A	Wasco
Cryostat CM3050 S	Leica
DAPI Ref:62248	Thermo scientific
DNaseI (RNase free) Catalog # M0303S	New England BioLabs
Glycogen	Qiagen
HB-500 Minidizer Hybridization Oven	UVP
IMDM with L-Glutamine and HEPES Catalog #: 12-722F IMDM with L-Glutamine and 25 mM HEPES, 500 mL	Lonza
Isopropanol/ 2-Propanol	Sigma-Aldrich
MyCycler thermal cycler	BIO-RAD
Myosin Type I-mouse antibody (A4.951)	Developmental Studies Hybridoma Bank
Myosin Type IIA-mouse antibody (SC71-S)	Developmental Studies Hybridoma Bank
Myosin Type IIB-mouse antibody (BF-F3)	Developmental Studies Hybridoma Bank
Myosin Type IIX-mouse antibody (6H 1-S)	Developmental Studies Hybridoma Bank
NEBNext Poly(A) mRNA Magnetic Isolation Module (NEB #E7490)	New England BioLabs
NEBNext Ultra II Directional RNA Library Prep Kit for Illumina E7760S Lot: 10126607	New England BioLabs

Nuclease-free H_2O	New England BioLabs
O.C.T. Compound LOT 2105609810	Sakura Tissue-Tek
Paraformaldehyde, 4% in PBS, Ready-to-Use Fixative	Biotium
Qubit Fluorometric Quantification Machine	ThermoFisher Scientific
Qubit™ RNA High Sensitivity (HS) and Broad Range (BR) Assay Kits. Catalog number: Q10211	ThermoFisher Scientific
RNaseZAP	Sigma-Aldrich
Stereo-Microscope Stemi 305	ZEISS
Stereo-Microscope Stemi 508	ZEISS
Superfrost™Plus Adhesion Microscope Slides White Tab	Epredia
TissueLyser II	QIAGEN Retsch
TRIzol RNA Isolation Reagent	ThermoFisher Scientific
Tweezers	Dumont switzerland
Vectashield Antifade Mounting Medium	VECTOR Laboratories

Reference List

Books

EBERT, D. A., DANDO, M. & FOWLER, S. 2021. *Sharks of the world*, Princeton University Press, p. 11, 16, 22, 24, 31-34, 48-53, 105, 192, 199, 324, 439.

EBERT, D. A. & FOWLER, S. L. 2014. *A pocket guide to sharks of the world,* New Jersey, Princeton University Press Wild Nature Press Walter de Gruyter GmbH, p.147, 192.

GUEST, P. C. 2019. `Of Mice, Whales, Jellyfish and Men: In Pursuit of Increased Longevity`. *Reviews on Biomarker Studies in Aging and Anti-Aging Research.* Springer, pp 1-24.

Periodicals

ACEVEDO, L. M. & RIVERO, J. L. 2006. New insights into skeletal muscle fibre types in the dog with particular focus towards hybrid myosin phenotypes. *Cell Tissue Res,* 323**,** 283-303.

ADAMS, P. D. 1980. Life history patterns in marine fishes and their consequences for management. *Fishery Bulletin- National Oceanic and Atmospheric Administration*.

ALEXANDER, R. M. 1969. The orientation of muscle fibres in the myomeres of fishes. *Journal of the Marine Biological Association of the United Kingdom,* 49**,** 263 - 290.

ANDERSEN, P. 1975. Capillary density in skeletal muscle of man. *Acta Physiol Scand,* 95**,** 203-5.

ANTON, B., VITETTA, L., CORTIZO, F. & SALI, A. 2005. Can we delay aging? The biology and science of aging. *Annals of the New York Academy of Sciences,* 1057**,** 525-535.

AZEMIN, M. Z. C., KUMAR, D. K., WONG, T. Y., WANG, J. J., MITCHELL, P., KAWASAKI, R. & WU, H. 2012. Age-related rarefaction in the fractal dimension of retinal vessel. *Neurobiology of aging,* 33**,** 194. e1-194. e4.

BADA, J. L., VROLIJK, C. D., BROWN, S., DRUFFEL, E. R. M. & HEDGES, R. E. M. 1987. Bomb radiocarbon in metabolically inert tissues from terrestrial and marine mammals. *Geophysical Research Letters,* 14**,** 1065-1067.

BAINBRIDGE, R. 1958. The speed of swimming of fish as related to size and to the frequency and amplitude of the tail beat. *Journal of experimental biology,* 35**,** 109-133.

BARBOSA-SILVA, T. G., BIELEMANN, R. M., GONZALEZ, M. C. & MENEZES, A. M. 2016. Prevalence of sarcopenia among community-dwelling elderly of a medium-sized South American city: results of the COMO VAI? study. *J Cachexia Sarcopenia Muscle,* 7**,** 136-43.

BAREJA, A., HOLT, J. A., LUO, G., CHANG, C., LIN, J., HINKEN, A. C., FREUDENBERG, J. M., KRAUS, W. E., EVANS, W. J. & BILLIN, A. N. 2014. Human and mouse skeletal muscle stem cells: convergent and divergent mechanisms of myogenesis. *PLoS One,* 9**,** e90398.

BARNARD, R., EDGERTON, V., FURUKAWA, T. & PETER, J. 1971. Histochemical, biochemical, and contractile properties of red, white, and intermediate fibers. *American Journal of Physiology-Legacy Content,* 220**,** 410-414.

BASSNETT, S., SHI, Y. & VRENSEN, G. F. J. M. 2011. Biological glass: structural determinants of eye lens transparency. *Philosophical Transactions of the Royal Society B: Biological Sciences,* 366**,** 1250-1264.

BEHNKE, B. J., MCDONOUGH, P., PADILLA, D. J., MUSCH, T. I. & POOLE, D. C. 2003. Oxygen exchange profile in rat muscles of contrasting fibre types. *J Physiol,* 549**,** 597-605.

BEIN, M. A., UNLUCAN, D., OLOWU, G. & KALIFA, W. 2017. Healthcare spending and health outcomes: evidence from selected East African countries. *Afr Health Sci,* 17**,** 247-254.

BERG, J. S., POWELL, B. C. & CHENEY, R. E. 2001. A millennial myosin census. *Mol Biol Cell,* 12**,** 780-94.

BICER, S. & REISER, P. J. 2004. Myosin light chain isoform expression among single mammalian skeletal muscle fibers: species variations. *J Muscle Res Cell Motil,* 25**,** 623-33.

BIOLO, G., CEDERHOLM, T. & MUSCARITOLI, M. 2014. Muscle contractile and metabolic dysfunction is a common feature of sarcopenia of aging and chronic diseases: from sarcopenic obesity to cachexia. *Clin Nutr,* 33**,** 737-48.

BLUMENTHAL, D. K., TAKIO, K., EDELMAN, A. M., CHARBONNEAU, H., TITANI, K., WALSH, K. A. & KREBS, E. G. 1985. Identification of the calmodulin-binding domain of skeletal muscle myosin light chain kinase. *Proc Natl Acad Sci U S A,* 82**,** 3187-91.

BONE, Q., CHUBB, A.D. 1978. The histochemical demonstration of myofibrillar ATPase in elasmobranch muscle. *Histochemical Journal*.

BONE, Q., JOHNSTON, I., PULSFORD, A. & RYAN, K. 1986. Contractile properties and ultrastructure of three types of muscle fibre in the dogfish myotome. *Journal of Muscle Research & Cell Motility,* 7**,** 47-56.

BOTTINELLI, R., BETTO, R., SCHIAFFINO, S. & REGGIANI, C. 1994. Maximum shortening velocity and coexistence of myosin heavy chain isoforms in single skinned fast fibres of rat skeletal muscle. *J Muscle Res Cell Motil,* 15**,** 413-9.

BRENNER, B. & EISENBERG, E. 1986. Rate of force generation in muscle: correlation with actomyosin ATPase activity in solution. *Proc Natl Acad Sci U S A,* 83**,** 3542-6.

BROOKS, J. L., GUTTRIDGE, T. L., FRANKS, B. R., GRUBBS, R. D., CHAPMAN, D. D., GRUBER, S. H., DIBATTISTA, J. D. & FELDHEIM, K. A. 2016. Using genetic inference to re-evaluate the minimum longevity of the lemon shark Negaprion brevirostris. *Journal of Fish Biology,* 88**,** 2067-2074.

BUTLER, P. G., WANAMAKER, A. D., SCOURSE, J. D., RICHARDSON, C. A. & REYNOLDS, D. J. 2013. Variability of marine climate on the North Icelandic Shelf in a 1357-year proxy archive based on growth increments in the bivalve Arctica islandica. *Palaeogeography, Palaeoclimatology, Palaeoecology,* 373**,** 141-151.

C., B. A. A. 1881. An Introduction to the Study of Fishes. *Nature,* 23**,** 213-215.

CAMPANA, S. E. 2001. Accuracy, precision and quality control in age determination, including a review of the use and abuse of age validation methods. *Journal of Fish Biology,* 59**,** 197-242.

CAMPANA, S. E., FISK, A. T. & KLIMLEY, A. P. 2015. Movements of Arctic and northwest Atlantic Greenland sharks (Somniosus microcephalus) monitored with archival satellite pop-up tags suggest long-range migrations. *Deep Sea Research Part II: Topical Studies in Oceanography,* 115**,** 109-115.

CAMPANA, S. E., NATANSON, L. J. & MYKLEVOLL, S. 2002. Bomb dating and age determination of large pelagic sharks. *Canadian Journal of Fisheries and Aquatic Sciences,* 59**,** 450-455.

CAMPANA, S. E., SHELTON, P., SIMPSON, M. & LAWSON, J. 2008. *Status of basking sharks in Atlantic Canada*, Fisheries and Oceans.

CATIC, A. 2018. Cellular Metabolism and Aging. *In:* OTTINGER, M. A. (ed.) *Progress in Molecular Biology and Translational Science.* Academic Press.

CAVALIER-SMITH, T. 1982. Skeletal DNA and the evolution of genome size. *Annu Rev Biophys Bioeng,* 11**,** 273-302.

CHABOWSKI, A., CHATHAM, J. C., TANDON, N. N., CALLES-ESCANDON, J., GLATZ, J. F. C., LUIKEN, J. J. F. P. & BONEN, A. 2006. Fatty acid transport and FAT/CD36 are increased in red but not in white skeletal muscle of ZDF rats. *American Journal of Physiology-Endocrinology and Metabolism,* 291**,** E675-E682.

CHESSER, B. 2015. Senescence in Humans. ML Books International New Delhi, India.

CHILDRESS, J. & SOMERO, G. 1979. Depth-related enzymic activities in muscle, brain and heart of deep-living pelagic marine teleosts. *Marine Biology,* 52**,** 273-283.

CHRISTIAN, C. J. & BENIAN, G. M. 2020. Animal models of sarcopenia. *Aging Cell,* 19**,** e13223.

COLSON, B. A., PETERSEN, K. J., COLLINS, B. C., LOWE, D. A. & THOMAS, D. D. 2015. The myosin super-relaxed state is disrupted by estradiol deficiency. *Biochem Biophys Res Commun,* 456**,** 151-5.

CONCEIÇÃO, M. S., VECHIN, F. C., LIXANDRÃO, M., DAMAS, F., LIBARDI, C. A., TRICOLI, V., ROSCHEL, H., CAMERA, D. & UGRINOWITSCH, C. 2018. Muscle Fiber Hypertrophy and Myonuclei Addition: A Systematic Review and Meta-analysis. *Medicine & Science in Sports & Exercise,* 50.

CONDON, N. E., FRIEDMAN, J. R. & DRAZEN, J. C. 2012. Metabolic enzyme activities in shallow-and deep-water chondrichthyans: implications for metabolic and locomotor capacity. *Marine Biology,* 159**,** 1713-1731.

COOKE, R. 2011. The role of the myosin ATPase activity in adaptive thermogenesis by skeletal muscle. *Biophys Rev,* 3**,** 33-45.

COSTANTINI, D., SMITH, S., KILLEN, S. S., NIELSEN, J. & STEFFENSEN, J. F. 2017. The Greenland shark: A new challenge for the oxidative stress theory of ageing? *Comp Biochem Physiol A Mol Integr Physiol,* 203**,** 227-232.

CRESSEY, D. 2017. Sharks can live a lot longer than researchers realized. *Nature,* 549**,** 316-317.

CRUZ-JENTOFT, A. J., BAEYENS, J. P., BAUER, J. M., BOIRIE, Y., CEDERHOLM, T., LANDI, F., MARTIN, F. C., MICHEL, J. P., ROLLAND, Y., SCHNEIDER, S. M., TOPINKOVA, E., VANDEWOUDE, M. & ZAMBONI, M. 2010. Sarcopenia: European consensus on definition and diagnosis: Report of the European Working Group on Sarcopenia in Older People. *Age Ageing,* 39**,** 412-23.

CRUZ-JENTOFT, A. J. & SAYER, A. A. 2019. Sarcopenia. *The Lancet,* 393**,** 2636-2646.

CURCIO, F., FERRO, G., BASILE, C., LIGUORI, I., PARRELLA, P., PIROZZI, F., DELLA-MORTE, D., GARGIULO, G., TESTA, G., TOCCHETTI, C. G., BONADUCE, D. & ABETE, P. 2016. Biomarkers in sarcopenia: A multifactorial approach. *Experimental Gerontology,* 85**,** 1-8.

D'ANTONA, G., PELLEGRINO, M. A., ADAMI, R., ROSSI, R., CARLIZZI, C. N., CANEPARI, M., SALTIN, B. & BOTTINELLI, R. 2003. The effect of ageing and immobilization on structure and function of human skeletal muscle fibres. *J Physiol,* 552**,** 499-511.

DA COSTA, J. P., VITORINO, R., SILVA, G. M., VOGEL, C., DUARTE, A. C. & ROCHA-SANTOS, T. 2016. A synopsis on aging-Theories, mechanisms and future prospects. *Ageing Res Rev,* 29**,** 90-112.

DAHL, R., LARSEN, S., DOHLMANN, T. L., QVORTRUP, K., HELGE, J. W., DELA, F. & PRATS, C. 2015. Three-dimensional reconstruction of the human skeletal muscle mitochondrial network as a tool to assess mitochondrial content and structural organization. *Acta Physiologica,* 213**,** 145-155.

DAO, T., GREEN, A. E., KIM, Y. A., BAE, S. J., HA, K. T., GARIANI, K., LEE, M. R., MENZIES, K. J. & RYU, D. 2020. Sarcopenia and Muscle Aging: A Brief Overview. *Endocrinol Metab (Seoul),* 35**,** 716-732.

DAWSON, J. M., TYLER, K. R. & HUDLICKA, O. 1987. A comparison of the microcirculation in rat fast glycolytic and slow oxidative muscles at rest and during contractions. *Microvasc Res,* 33**,** 167-82.

DE MAGALHÃES, J. P., COSTA, J. & CHURCH, G. M. 2007. An analysis of the relationship between metabolism, developmental schedules, and longevity using phylogenetic independent contrasts. *J Gerontol A Biol Sci Med Sci,* 62**,** 149-60.

DENARDI, C., AUSONI, S., MORETTI, P., GORZA, L., VELLECA, M., BUCKINGHAM, M. & SCHIAFFINO, S. 1993. Type 2X-myosin heavy chain is coded by a muscle fiber type-specific and developmentally regulated gene. *J Cell Biol,* 123**,** 823-35.

DEVINE, B. M., WHEELAND, L. J. & FISHER, J. A. 2018. First estimates of Greenland shark (Somniosus microcephalus) local abundances in Arctic waters. *Scientific reports,* 8**,** 1-10.

DOLLEMORE, D. 2002. *Aging under the microscope : a biological quest,* Bethesda, MD, National Institute on Aging, National Institutes of Health, Office of Communications and Public Liason.

DRAZEN, J. C. & SEIBEL, B. A. 2007. Depth-related trends in metabolism of benthic and benthopelagic deep-sea fishes. *Limnology and Oceanography,* 52**,** 2306-2316.

DRAZEN, J. C., YEH, J., FRIEDMAN, J. & CONDON, N. 2011. Metabolism and enzyme activities of hagfish from shallow and deep water of the Pacific Ocean. *Comparative Biochemistry and Physiology Part A: Molecular & Integrative Physiology,* 159**,** 182-187.

DURAN-ORTIZ, S., LIST, E. O., BASU, R. & KOPCHICK, J. J. 2021. Extending lifespan by modulating the growth hormone/insulin-like growth factor-1 axis: coming of age. *Pituitary,* 24**,** 438-456.

ECKHARDT, F., KAPPELER, P. M. & KRAUS, C. 2017. Highly variable lifespan in an annual reptile, Labord's chameleon (Furcifer labordi). *Sci Rep,* 7**,** 11397.

EDWARDS, J. E., HILTZ, E., BROELL, F., BUSHNELL, P. G., CAMPANA, S. E., CHRISTIANSEN, J. S., DEVINE, B. M., GALLANT, J. J., HEDGES, K. J., MACNEIL, M. A., MCMEANS, B. C., NIELSEN, J., PRÆBEL, K., SKOMAL, G. B., STEFFENSEN, J. F., WALTER, R. P., WATANABE, Y. Y., VANDERZWAAG, D. L. & HUSSEY, N. E. 2019. Advancing Research for the Management of Long-Lived Species: A Case Study on the Greenland Shark. *Frontiers in Marine Science,* 6.

ELLIS, J. R. & SHACKLEY, S. E. 1997. The reproductive biology of Scyliorhinus canicula in the Bristol Channel, U.K. *Journal of Fish Biology,* 51**,** 361-372.

ESSÉN, B., JANSSON, E., HENRIKSSON, J., TAYLOR, A. W. & SALTIN, B. 1975. Metabolic characteristics of fibre types in human skeletal muscle. *Acta Physiol Scand,* 95**,** 153-65.

FIERSTINE, H. L. 1965. *Studies in locomotion and anatomy of scombroid fishes*, University of California, Los Angeles.

FISK, A. T., LYDERSEN, C. & KOVACS, K. M. 2012. Archival pop-off tag tracking of Greenland sharks Somniosus microcephalus in the High Arctic waters of Svalbard, Norway. *Marine Ecology Progress Series,* 468**,** 255-265.

FISK, A. T., TITTLEMIER, S. A., PRANSCHKE, J. L. & NORSTROM, R. J. 2002. Using anthropogenic contaminants and stable isotopes to assess the feeding ecology of Greenland sharks. *Ecology,* 83**,** 2162-2172.

FOLCH, J., BUSQUETS, O., ETTCHETO, M., SÁNCHEZ-LÓPEZ, E., PALLÀS, M., BEAS-ZARATE, C., MARIN, M., CASADESUS, G., OLLOQUEQUI, J., AULADELL, C. & CAMINS, A. 2018. Experimental Models for Aging and their Potential for Novel Drug Discovery. *Curr Neuropharmacol,* 16**,** 1466-1483.

FONTANA, L., PARTRIDGE, L. & LONGO, V. D. 2010. Extending healthy life span--from yeast to humans. *Science,* 328**,** 321-6.

FORTIN, M., VIDEMAN, T., GIBBONS, L. E. & BATTIÉ, M. C. 2014. Paraspinal Muscle Morphology and Composition: A 15-yr Longitudinal Magnetic Resonance Imaging Study. *Medicine & Science in Sports & Exercise,* 46**,** 893-901.

FRANCIS, M. P., CAMPANA, S. E. & JONES, C. M. 2007. Age under-estimation in New Zealand porbeagle sharks (Lamna nasus): is there an upper limit to ages that can be determined from shark vertebrae? *Marine and Freshwater Research,* 58**,** 10-23.

FRANCIS, P., LYONS, M., PIASECKI, M., MCPHEE, J., HIND, K. & JAKEMAN, P. 2017. Measurement of Muscle Health in Aging. *Biogerontology,* 18.

FRONTERA, W. R., HUGHES, V. A., FIELDING, R. A., FIATARONE, M. A., EVANS, W. J. & ROUBENOFF, R. 2000a. Aging of skeletal muscle: a 12-yr longitudinal study. *J Appl Physiol (1985),* 88**,** 1321-6.

FRONTERA, W. R. & OCHALA, J. 2015. Skeletal muscle: a brief review of structure and function. *Calcif Tissue Int,* 96**,** 183-95.

FRONTERA, W. R., REID, K. F., PHILLIPS, E. M., KRIVICKAS, L. S., HUGHES, V. A., ROUBENOFF, R. & FIELDING, R. A. 2008. Muscle fiber size and function in elderly humans: a longitudinal study. *J Appl Physiol (1985),* 105**,** 637-42.

FRONTERA, W. R., SUH, D., KRIVICKAS, L. S., HUGHES, V. A., GOLDSTEIN, R. & ROUBENOFF, R. 2000b. Skeletal muscle fiber quality in older men and women. *American Journal of Physiology-Cell Physiology,* 279**,** C611-C618.

FUSHAN, A. A., TURANOV, A. A., LEE, S. G., KIM, E. B., LOBANOV, A. V., YIM, S. H., BUFFENSTEIN, R., LEE, S. R., CHANG, K. T., RHEE, H., KIM, J. S., YANG, K. S. & GLADYSHEV, V. N. 2015. Gene expression defines natural changes in mammalian lifespan. *Aging Cell,* 14**,** 352-65.

GALLANT, J. J., RODRIGUEZ, M. A., STOKESBURY, M. J. & HARVEY-CLARK, C. 2016. Influence of environmental variables on the diel movements of the greenland shark (Somniosus microcephalus) in the St. Lawrence Estuary. *The Canadian Field-Naturalist,* 130**,** 1-14.

GARCÍA, V. B., LUCIFORA, L. O. & MYERS, R. A. 2008. The importance of habitat and life history to extinction risk in sharks, skates, rays and chimaeras. *Proceedings of the Royal Society B: Biological Sciences,* 275**,** 83-89.

GAUTHIER, G. F. 1979. Ultrastructural identification of muscle fiber types by immunocytochemistry. *J Cell Biol,* 82**,** 391-400.

GEMBALLA, S., EBMEYER, L., HAGEN, K., HANNICH, T., HOJA, K., ROLF, M., TREIBER, K., VOGEL, F. & WEITBRECHT, G. 2003. Evolutionary transformations of myoseptal tendons in gnathostomes. *Proceedings of the Royal Society of London. Series B: Biological Sciences,* 270**,** 1229-1235.

GEORGE, J. C., BADA, J., ZEH, J., SCOTT, L., BROWN, S. E., O'HARA, T. & SUYDAM, R. 1999. Age and growth estimates of bowhead whales (Balaena mysticetus) via aspartic acid racemization. *Canadian Journal of Zoology,* 77**,** 571-580.

GILLOOLY, J. F., BROWN, J. H., WEST, G. B., SAVAGE, V. M. & CHARNOV, E. L. 2001. Effects of size and temperature on metabolic rate. *science,* 293**,** 2248-2251.

GIRALDO, Y. M. & TRANIELLO, J. F. 2014. Worker senescence and the sociobiology of aging in ants. *Behav Ecol Sociobiol,* 68**,** 1901-1919.

GOLDBERGER, A. L., PENG, C.-K. & LIPSITZ, L. A. 2002. What is physiologic complexity and how does it change with aging and disease? *Neurobiology of aging,* 23**,** 23-26.

GOLDMAN, K. J., CAILLIET, G. M., ANDREWS, A. H. & NATANSON, L. J. Assessing the Age and Growth of Chondrichthyan Fishes. 2012.

GOLLNICK, P. D., KARLSSON, J., PIEHL, K. & SALTIN, B. 1974. Selective glycogen depletion in skeletal muscle fibres of man following sustained contractions. *J Physiol,* 241**,** 59-67.

GORZA, L. 1990. Identification of a novel type 2 fiber population in mammalian skeletal muscle by combined use of histochemical myosin ATPase and anti-myosin monoclonal antibodies. *J Histochem Cytochem,* 38**,** 257-65.

GOSS, R. J. 1974. Aging versus growth. *Perspect Biol Med,* 17**,** 485-94.

GREENE, C. W. 1913. An undescribed longitudinal differentiation of the great lateral muscle of the king salmon. *The Anatomical Record,* 7**,** 99-101.

GREENHAFF, P. L., SÖDERLUND, K., REN, J. M. & HULTMAN, E. 1993. Energy metabolism in single human muscle fibres during intermittent contraction with occluded circulation. *J Physiol,* 460**,** 443-53.

GRIFFITH, O. L., MOODIE, G. E. E. & CIVETTA, A. 2003. Genome size and longevity in fish. *Experimental gerontology,* 38**,** 333-337.

GUARENTE, L. 2014. Aging research—where do we stand and where are we going? *Cell,* 159**,** 15-19.

GUARENTE, L. & KENYON, C. 2000. Genetic pathways that regulate ageing in model organisms. *Nature,* 408**,** 255-62.

GUNNARSDOTTIR, R. & JØRGENSEN, M. W. Utilization possibilites of waste products from fishing and hunting to biogas and bio-oil production in Uummannaq County. Sustainable Energy Supply in the Arctic-sun, wind, water etc.: ARTEK Event, 2008. Arctic Technology Centre, Department of Civil Engineering, 52-58.

GUNNING, P., PONTE, P., BLAU, H. & KEDES, L. 1983. alpha-skeletal and alpha-cardiac actin genes are coexpressed in adult human skeletal muscle and heart. *Mol Cell Biol,* 3**,** 1985-95.

GUTH, L. & SAMAHA, F. J. 1969. Qualitative differences between actomyosin ATPase of slow and fast mammalian muscle. *Exp Neurol,* 25**,** 138-52.

HAMADY, L. L., NATANSON, L. J., SKOMAL, G. B. & THORROLD, S. R. 2014. Vertebral bomb radiocarbon suggests extreme longevity in white sharks. *PloS one,* 9**,** e84006.

HANDSCHIN, C. 2016. Caloric restriction and exercise "mimetics": Ready for prime time? *Pharmacol Res,* 103**,** 158-66.

HANSSON, K. A., EFTESTØL, E., BRUUSGAARD, J. C., JUVKAM, I., CRAMER, A. W., MALTHE-SØRENSSEN, A., MILLAY, D. P. & GUNDERSEN, K. 2020. Myonuclear content regulates cell size with similar scaling properties in mice and humans. *Nat Commun,* 11**,** 6288.

HARA, Y., YAMAGUCHI, K., ONIMARU, K., KADOTA, M., KOYANAGI, M., KEELEY, S. D., TATSUMI, K., TANAKA, K., MOTONE, F., KAGEYAMA, Y., NOZU, R., ADACHI, N., NISHIMURA, O., NAKAGAWA, R., TANEGASHIMA, C., KIYATAKE, I., MATSUMOTO, R., MURAKUMO, K., NISHIDA, K., TERAKITA, A., KURATANI, S., SATO, K., HYODO, S. & KURAKU, S. 2018. Shark genomes provide insights into elasmobranch evolution and the origin of vertebrates. *Nat Ecol Evol,* 2**,** 1761-1771.

HARRIDGE, S. D., BOTTINELLI, R., CANEPARI, M., PELLEGRINO, M. A., REGGIANI, C., ESBJÖRNSSON, M. & SALTIN, B. 1996. Whole-muscle and single-fibre contractile properties and myosin heavy chain isoforms in humans. *Pflugers Arch,* 432**,** 913-20.

HAUSDORFF, J. M., MITCHELL, S. L., FIRTION, R., PENG, C.-K., CUDKOWICZ, M. E., WEI, J. Y. & GOLDBERGER, A. L. 1997. Altered fractal dynamics of gait: reduced stride-interval correlations with aging and Huntington's disease. *Journal of applied physiology,* 82**,** 262-269.

HERDENDORF, C. E. & BERRA, T. M. 1995. A Greenland shark from the wreck of the SS Central America at 2,200 meters. *Transactions of the American Fisheries Society,* 124**,** 950-953.

HILL, T. R., MENDONÇA, N., GRANIC, A., SIERVO, M., JAGGER, C., SEAL, C. J., KERSE, N., WHAM, C., ADAMSON, A. J. & MATHERS, J. C. 2016. What do we know about the nutritional status of the very old? Insights from three cohorts of advanced age from the UK and New Zealand. *Proc Nutr Soc,* 75**,** 420-30.

HOLM, S., DAVIS, R. B., JAVOIŠ, J., ÕUNAP, E., KAASIK, A., MOLLEMAN, F. & TAMMARU, T. 2016. A comparative perspective on longevity: the effect of body size dominates over ecology in moths. *J Evol Biol,* 29**,** 2422-2435.

HOLMES, B. J., PEDDEMORS, V. M., GUTTERIDGE, A. N., GERAGHTY, P. T., CHAN, R. W. K., TIBBETTS, I. R. & BENNETT, M. B. 2015. Age and growth of the tiger shark Galeocerdo cuvier off the east coast of Australia. *Journal of Fish Biology,* 87**,** 422-448.

HOLTZE, S., GORSHKOVA, E. A., BRAUDE, S., CELLERINO, A., DAMMANN, P., HILDEBRANDT, T. B., HOEFLICH, A., HOFFMANN, S., KOCH, P., TERZIBASI TOZZINI, E., SKULACHEV, M. V., SKULACHEV, V. P. & SAHM, A. 2021. Alternative Animal Models of Aging Research. *Frontiers in Molecular Biosciences,* 8.

HOOIJMAN, P., STEWART, MELANIE A. & COOKE, R. 2011. A New State of Cardiac Myosin with Very Slow ATP Turnover: A Potential Cardioprotective Mechanism in the Heart. *Biophysical Journal,* 100**,** 1969-1976.

HOPPELER, H., LÜTHI, P., CLAASSEN, H., WEIBEL, E. R. & HOWALD, H. 1973. The ultrastructure of the normal human skeletal muscle. A morphometric analysis on untrained men, women and well-trained orienteers. *Pflugers Arch,* 344**,** 217-32.

HOWALD, H., HOPPELER, H., CLAASSEN, H., MATHIEU, O. & STRAUB, R. 1985. Influences of endurance training on the ultrastructural composition of the different muscle fiber types in humans. *Pflugers Arch,* 403**,** 369-76.

HUA, X., COWMAN, P., WARREN, D. & BROMHAM, L. 2015. Longevity Is Linked to Mitochondrial Mutation Rates in Rockfish: A Test Using Poisson Regression. *Molecular biology and evolution,* 32**,** 2633-2645.

HUSSEY, N. E., COSANDEY-GODIN, A., WALTER, R. P., HEDGES, K. J., VANGERWEN-TOYNE, M., BARKLEY, A. N., KESSEL, S. T. & FISK, A. T. 2015. Juvenile Greenland sharks Somniosus microcephalus (Bloch & Schneider, 1801) in the canadian arctic. *Polar biology,* 38**,** 493-504.

HUXLEY, A. F. & NIEDERGERKE, R. 1954. Structural changes in muscle during contraction; interference microscopy of living muscle fibres. *Nature,* 173**,** 971-3.

HUXLEY, H. & HANSON, J. 1954. Changes in the cross-striations of muscle during contraction and stretch and their structural interpretation. *Nature,* 173**,** 973-6.

IANNUZZI-SUCICH, M., PRESTWOOD, K. M. & KENNY, A. M. 2002. Prevalence of sarcopenia and predictors of skeletal muscle mass in healthy, older men and women. *J Gerontol A Biol Sci Med Sci,* 57**,** M772-7.

JACKMAN, M. R. & WILLIS, W. T. 1996. Characteristics of mitochondria isolated from type I and type IIb skeletal muscle. *American Journal of Physiology-Cell Physiology,* 270**,** C673-C678.

JAVAN, R., HORVATH, J. J., CASE, L. E., AUSTIN, S., CORDERI, J., DUBROVSKY, A., KISHNANI, P. S. & BASHIR, M. R. 2013. Generating color-coded anatomic muscle maps for correlation of quantitative magnetic resonance imaging analysis with clinical examination in neuromuscular disorders. *Muscle & Nerve,* 48**,** 293-295.

JAYASINGHE, I. D. & LAUNIKONIS, B. S. 2013. Three-dimensional reconstruction and analysis of the tubular system of vertebrate skeletal muscle. *J Cell Sci,* 126**,** 4048-58.

JUEL, C. & PILEGAARD, H. 1998. Lactate/H+ transport kinetics in rat skeletal muscle related to fibre type and changes in transport capacity. *Pflugers Arch,* 436**,** 560-4.

JUNNILA, R. K., LIST, E. O., BERRYMAN, D. E., MURREY, J. W. & KOPCHICK, J. J. 2013. The GH/IGF-1 axis in ageing and longevity. *Nat Rev Endocrinol,* 9**,** 366-376.

KALINKOVICH, A. & LIVSHITS, G. 2015. Sarcopenia--The search for emerging biomarkers. *Ageing Res Rev,* 22**,** 58-71.

KALISH, J. M. 1993. Pre-and post-bomb radiocarbon in fish otoliths. *Earth and Planetary Science Letters,* 114**,** 549-554.

KAMEL, H. K. 2003. Sarcopenia and Aging. *Nutrition Reviews,* 61**,** 157-167.

KAPLAN, D. T., FURMAN, M. I., PINCUS, S. M., RYAN, S. M., LIPSITZ, L. A. & GOLDBERGER, A. L. 1991. Aging and the complexity of cardiovascular dynamics. *Biophysical journal,* 59**,** 945-949.

KARATZAFERI, C., DE HAAN, A., VAN MECHELEN, W. & SARGEANT, A. J. 2001. Metabolism changes in single human fibres during brief maximal exercise. *Exp Physiol,* 86**,** 411-5.

KARSTEN, K. B., ANDRIAMANDIMBIARISOA, L. N., FOX, S. F. & RAXWORTHY, C. J. 2008. A unique life history among tetrapods: an annual chameleon living mostly as an egg. *Proc Natl Acad Sci U S A,* 105**,** 8980-4.

KIESSLING, A., RUOHONEN, K. & BJØRNEVIK, M. 2006. Muscle fibre growth and quality in fish.

KIRKWOOD, T. B. 2005. Understanding the odd science of aging. *Cell,* 120**,** 437-447.

KNIGHT, K. 2022. Sluggish metabolism keeps Greenland sharks going on meagre meals. *Journal of Experimental Biology,* 225.

KOTAS, J., MASTROCHIRICO, V. & PETRERE, M. 2011. Age and growth of the Scalloped Hammerhead shark, Sphyrna lewini (Griffith and Smith, 1834), from the southern Brazilian coast. *Brazilian journal of biology = Revista brasleira de biologia,* 71**,** 755-61.

KRAEGEN, E. W., SOWDEN, J. A., HALSTEAD, M. B., CLARK, P. W., RODNICK, K. J., CHISHOLM, D. J. & JAMES, D. E. 1993. Glucose transporters and in vivo glucose uptake in skeletal and cardiac muscle: fasting, insulin stimulation and immunoisolation studies of GLUT1 and GLUT4. *Biochem J,* 295 (Pt 1)**,** 287-93.

KRYVI, H. & EIDE, A. 1977. Morphometric and autoradiographic studies on the growth of red and white axial muscle fibres in the shark Etmopterus spinax. *Anat Embryol (Berl),* 151**,** 17-28.

KRYVI, H., FLATMARK, T., FLATMARK, T. & TOTLAND, G. K. 1981. The myoglobin content in red, intermediate and white fibres of the swimming muscle sin three species of shark—a comparative study using high-performance liquid chromatography. *Journal of Fish Biology,* 18.

KRYVI, H. & TOTLAND, G. K. 1977. Histochemical studies with microphotometric determinations of the lateral muscles in the sharks Etmopterus spinax and Galeus melastomus. *Journal of the Marine Biological Association of the United Kingdom,* 57**,** 261-271.

LAFOREST, K. V., PEELE, E. E. & YOPAK, K. E. 2020. Ontogenetic Shifts in Brain Size and Brain Organization of the Atlantic Sharpnose Shark, Rhizoprionodon terraenovae. *Brain Behav Evol,* 95**,** 162-180.

LAMBOLEY, C. R., MURPHY, R. M., MCKENNA, M. J. & LAMB, G. D. 2014. Sarcoplasmic reticulum Ca2+ uptake and leak properties, and SERCA isoform expression, in type I and type II fibres of human skeletal muscle. *J Physiol,* 592**,** 1381-95.

LAPLANTE, M. & SABATINI, D. M. 2012. mTOR signaling in growth control and disease. *Cell,* 149**,** 274-93.

LARSSON, L., EDSTROM, L., LINDEGREN, B., GORZA, L. & SCHIAFFINO, S. 1991. MHC composition and enzyme-histochemical and physiological properties of a novel fast-twitch motor unit type. *American Journal of Physiology-Cell Physiology,* 261**,** C93-C101.

LARSSON, L. & MOSS, R. L. 1993. Maximum velocity of shortening in relation to myosin isoform composition in single fibres from human skeletal muscles. *The Journal of Physiology,* 472**,** 595-614.

LAURETANI, F., BAUTMANS, I., DE VITA, F., NARDELLI, A., CEDA, G. P. & MAGGIO, M. 2014. Identification and treatment of older persons with sarcopenia. *Aging Male,* 17**,** 199-204.

LEBERER, E. & PETTE, D. 1984. Lactate dehydrogenase isozymes in type I, IIA and IIB fibres of rabbit skeletal muscles. *Histochemistry,* 80**,** 295-8.

LECLERC, L.-M. E., LYDERSEN, C., HAUG, T., BACHMANN, L., FISK, A. T. & KOVACS, K. M. 2012. A missing piece in the Arctic food web puzzle? Stomach contents of Greenland sharks sampled in Svalbard, Norway. *Polar biology,* 35**,** 1197-1208.

LEE, B. C., KAYA, A. & GLADYSHEV, V. N. 2016. Methionine restriction and life-span control. *Annals of the New York Academy of Sciences,* 1363**,** 116-124.

LEE, S.-H., LEE, J.-H., LEE, H.-Y. & MIN, K.-J. 2019. Sirtuin signaling in cellular senescence and aging. *BMB reports,* 52**,** 24-34.

LIAN, T., WU, Q., HODGE, B. A., WILSON, K. A., YU, G. & YANG, M. 2018. Drosophila Gut—A Nexus Between Dietary Restriction and Lifespan. *International Journal of Molecular Sciences,* 19**,** 3810.

LONGO, V. D., ANTEBI, A., BARTKE, A., BARZILAI, N., BROWN-BORG, H. M., CARUSO, C., CURIEL, T. J., DE CABO, R., FRANCESCHI, C., GEMS, D., INGRAM, D. K., JOHNSON, T. E., KENNEDY, B. K., KENYON, C., KLEIN, S., KOPCHICK, J. J., LEPPERDINGER, G., MADEO, F., MIRISOLA, M. G., MITCHELL, J. R., PASSARINO, G., RUDOLPH, K. L., SEDIVY, J. M., SHADEL, G. S., SINCLAIR, D. A., SPINDLER, S. R., SUH, Y., VIJG, J., VINCIGUERRA, M. & FONTANA, L. 2015. Interventions to Slow Aging in Humans: Are We Ready? *Aging Cell,* 14**,** 497-510.

LÓPEZ-OTÍN, C., BLASCO, M. A., PARTRIDGE, L., SERRANO, M. & KROEMER, G. 2013. The hallmarks of aging. *Cell,* 153**,** 1194-1217.

LOWRY, C. V., KIMMEY, J. S., FELDER, S., CHI, M. M., KAISER, K. K., PASSONNEAU, P. N., KIRK, K. A. & LOWRY, O. H. 1978. Enzyme patterns in single human muscle fibers. *J Biol Chem,* 253**,** 8269-77.

LUTHER, P. K. 2009. The vertebrate muscle Z-disc: sarcomere anchor for structure and signalling. *J Muscle Res Cell Motil,* 30**,** 171-85.

LYNNERUP, N., KJELDSEN, H., HEEGAARD, S., JACOBSEN, C. & HEINEMEIER, J. 2008. Radiocarbon Dating of the Human Eye Lens Crystallines Reveal Proteins without Carbon Turnover throughout Life. *PLOS ONE,* 3**,** e1529.

MACALUSO, F. & MYBURGH, K. H. 2012. Current evidence that exercise can increase the number of adult stem cells. *J Muscle Res Cell Motil,* 33**,** 187-98.

MACNEIL, M. A., MCMEANS, B. C., HUSSEY, N. E., VECSEI, P., SVAVARSSON, J., KOVACS, K. M., LYDERSEN, C., TREBLE, M. A., SKOMAL, G. B., RAMSEY, M. & FISK, A. T. 2012. Biology of the Greenland shark Somniosus microcephalus. *J Fish Biol,* 80**,** 991-1018.

MALAFARINA, V., URIZ-OTANO, F., INIESTA, R. & GIL-GUERRERO, L. 2012. Sarcopenia in the elderly: diagnosis, physiopathology and treatment. *Maturitas,* 71**,** 109-14.

MANOR, B., COSTA, M. D., HU, K., NEWTON, E., STAROBINETS, O., KANG, H. G., PENG, C., NOVAK, V. & LIPSITZ, L. A. 2010. Physiological complexity and system adaptability: evidence from postural control dynamics of older adults. *Journal of Applied Physiology,* 109**,** 1786-1791.

MCCANN, K. & SHUTER, B. 1997. Bioenergetics of life history strategies and the comparative allometry of reproduction. *Canadian Journal of Fisheries and Aquatic Sciences,* 54**,** 1289-1298.

MCCOMAS, A. J. & THOMAS, H. C. 1968. Fast and slow twitch muscles in man. *J Neurol Sci,* 7**,** 301-7.

MCMEANS, B. C., ARTS, M. T., LYDERSEN, C., KOVACS, K. M., HOP, H., FALK-PETERSEN, S. & FISK, A. T. 2013. The role of Greenland sharks (Somniosus microcephalus) in an Arctic ecosystem: assessed via stable isotopes and fatty acids. *Marine Biology,* 160**,** 1223-1238.

MCMEANS, B. C., SVAVARSSON, J., DENNARD, S. & FISK, A. T. 2010. Diet and resource use among Greenland sharks (Somniosus microcephalus) and teleosts sampled in Icelandic waters, using δ13C, δ15N, and mercury. *Canadian Journal of fisheries and aquatic sciences,* 67**,** 1428-1438.

MIKHAILOVA, M. V., BELYAEVA, N. F., KOZLOVA, N. I., ZOLOTAREV, K. V., MIKHAILOV, A. N., BERMAN, A. E. & ARCHAKOV, A. I. 2017. [Protective action of fish muscle extracts against cellular senescence induced by oxidative stress]. *Biomed Khim,* 63**,** 351-355.

MILLER, M. S. & TOTH, M. J. 2013. Myofilament protein alterations promote physical disability in aging and disease. *Exercise and sport sciences reviews,* 41**,** 93.

MITTELDORF, J. 2017. *Aging is a group-selected adaptation: theory, evidence, and medical implications*, CRC Press.

MITTELDORF, J. 2019. What Is Antagonistic Pleiotropy? *Biochemistry (Mosc),* 84**,** 1458-1468.

MOEN, R. J., KLEIN, J. C. & THOMAS, D. D. 2014. Electron paramagnetic resonance resolves effects of oxidative stress on muscle proteins. *Exerc Sport Sci Rev,* 42**,** 30-6.

MONAGHAN, P. & METCALFE, N. B. 2000. Genome size and longevity. *Trends Genet,* 16**,** 331-2.

MOORE, R. L. & STULL, J. T. 1984. Myosin light chain phosphorylation in fast and slow skeletal muscles in situ. *American Journal of Physiology-Cell Physiology,* 247**,** C462-C471.

MOYES, C. D., SCHULTE, P. M. & HOCHACHKA, P. W. 1992. Recovery metabolism of trout white muscle: role of mitochondria. *American Journal of Physiology-Regulatory, Integrative and Comparative Physiology,* 262**,** R295-R304.

MUSICK, J. A. 1999. Criteria to Define Extinction Risk in Marine Fishes: The American Fisheries Society Initiative. *Fisheries,* 24**,** 6-14.

MUUS, B. J., NIELSEN, J. G. & DAHLSTRÖM, P. 1999. *Die Meeresfische Europas in Nordsee, Ostsee und Atlantik*, Kosmos.

MYTILINEOU, C., POLITOU, C.-Y., PAPACONSTANTINOU, C., KAVADAS, S., D ONGHIA, G. & SION, L. 2005. Deep-water fish fauna in the Eastern Ionian Sea. *Belgian Journal of Zoology,* 135**,** 229.

NAG, S. & TRIVEDI, D. V. 2021. To lie or not to lie: Super-relaxing with myosins. *Elife,* 10.

NEEDHAM, D. M. 1926. RED AND WHITE MUSCLE. *Physiological Reviews,* 6**,** 1-27.

NIELSEN, J., HEDEHOLM, R. B., SIMON, M. & STEFFENSEN, J. F. 2014. Distribution and feeding ecology of the Greenland shark (Somniosus microcephalus) in Greenland waters. *Polar biology,* 37**,** 37-46.

NIELSEN, J. 2017. *The Greenland Shark (Somniosus Microcephalus): Diet, Tracking and Radiocarbon Age Estimates Reveal the World's Oldest Vertebrate.* University of Copenhagen, Faculty of Science,[Department of Biology, Marine ….

NIELSEN, J., HEDEHOLM, R. B., HEINEMEIER, J., BUSHNELL, P. G., CHRISTIANSEN, J. S., OLSEN, J., RAMSEY, C. B., BRILL, R. W., SIMON, M., STEFFENSEN, K. F. & STEFFENSEN, J. F. 2016. Eye lens radiocarbon reveals centuries of longevity in the Greenland shark (Somniosus microcephalus). *Science,* 353**,** 702-4.

NORSE, E. A., BROOKE, S., CHEUNG, W. W. L., CLARK, M. R., EKELAND, I., FROESE, R., GJERDE, K. M., HAEDRICH, R. L., HEPPELL, S. S., MORATO, T., MORGAN, L. E., PAULY, D., SUMAILA, R. & WATSON, R. 2012. Sustainability of deep-sea fisheries. *Marine Policy,* 36**,** 307-320.

NURSALL, J. R. 1956. THE LATERAL MUSCULATURE AND THE SWIMMING OF FISH. *Proceedings of the Zoological Society of London,* 126**,** 127-144.

OCHALA, J., FINNO, C. J. & VALBERG, S. J. 2021. Myofibre Hyper-Contractility in Horses Expressing the Myosin Heavy Chain Myopathy Mutation, MYH1(E321G). *Cells,* 10.

OGATA, T. & MORI, M. 1964. HISTOCHEMICAL STUDY OF OXIDATIVE ENZYMES IN VERTEBRATE MUSCLES. *J Histochem Cytochem,* 12**,** 171-82.

OHNO, S. 1972. So much "junk" DNA in our genome. *Brookhaven Symp Biol,* 23**,** 366-70.

OSTLER, E. 2012. Chemistry of ageing. *Chemistry Central,* 2**,** 433-6.

OTTENHEIJM, C. A. & GRANZIER, H. 2010. Lifting the nebula: novel insights into skeletal muscle contractility. *Physiology (Bethesda),* 25**,** 304-10.

PADYKULA, H. A. & GAUTHIER, G. F. 1967. Morphological and cytochemical characteristics of fiber types in normal mammalian skeletal muscle. *Exploratory concepts in muscular dystrophy and related disorders.* Excerpta Medica Foundation Amsterdam.

PAGEL, M. & JOHNSTONE, R. A. 1992. Variation across species in the size of the nuclear genome supports the junk-DNA explanation for the C-value paradox. *Proceedings of the Royal Society of London. Series B: Biological Sciences,* 249**,** 119-124.

PAN, H. & FINKEL, T. 2017. Key proteins and pathways that regulate lifespan. *J Biol Chem,* 292**,** 6452-6460.

PARTRIDGE, L. & BARTON, N. H. 1993. Optimality, mutation and the evolution of ageing. *Nature,* 362**,** 305-11.

PASCUAL-FERNÁNDEZ, J., FERNÁNDEZ-MONTERO, A., CÓRDOVA-MARTÍNEZ, A., PASTOR, D., MARTÍNEZ-RODRÍGUEZ, A. & ROCHE, E. 2020. Sarcopenia: Molecular Pathways and Potential Targets for Intervention. *International Journal of Molecular Sciences,* 21**,** 8844.

PATNAIK, B. K., MAHAPATRO, N. & JENA, B. S. 1994. Ageing in fishes. *Gerontology,* 40**,** 113-32.

PEDERSEN, B. K. & FEBBRAIO, M. A. 2012. Muscles, exercise and obesity: skeletal muscle as a secretory organ. *Nature Reviews Endocrinology,* 8**,** 457-465.

PENG, C.-K., MIETUS, J. E., LIU, Y., LEE, C., HAUSDORFF, J. M., STANLEY, H. E., GOLDBERGER, A. L. & LIPSITZ, L. A. 2002. Quantifying fractal dynamics of human respiration: age and gender effects. *Annals of biomedical engineering,* 30**,** 683-692.

PETER, J. B., BARNARD, R. J., EDGERTON, V. R., GILLESPIE, C. A. & STEMPEL, K. E. 1972. Metabolic profiles of three fiber types of skeletal muscle in guinea pigs and rabbits. *Biochemistry,* 11**,** 2627-33.

PETER, J. B., SAWAKI, S., BARNARD, R. J., EDGERTON, V. R. & GILLESPIE, C. A. 1971. Lactate dehydrogenase isoenzymes: distribution in fast-twitch red, fast-twitch white, and slow-twitch intermediate fibers of guinea pig skeletal muscle. *Arch Biochem Biophys,* 144**,** 304-7.

PETER KLIMLEY, A., BEAVERS, S. C., CURTIS, T. H. & JORGENSEN, S. J. 2002. Movements and swimming behavior of three species of sharks in La Jolla Canyon, California. *Environmental biology of fishes,* 63**,** 117-135.

PETTE, D. & STARON, R. S. 1990. Cellular and molecular diversities of mammalian skeletal muscle fibers. *Rev Physiol Biochem Pharmacol,* 116**,** 1-76.

PHUNG, L. A., KARVINEN, S. M., COLSON, B. A., THOMAS, D. D. & LOWE, D. A. 2018. Age affects myosin relaxation states in skeletal muscle fibers of female but not male mice. *PLOS ONE,* 13**,** e0199062.

PIANKA, E. R. 1970. On r- and K-Selection. *The American Naturalist,* 104**,** 592 - 597.

PIFFERI, F., TERRIEN, J., PERRET, M., EPELBAUM, J., BLANC, S., PICQ, J. L., DHENAIN, M. & AUJARD, F. 2019. Promoting healthspan and lifespan with caloric restriction in primates. *Commun Biol,* 2**,** 107.

PINTE, N., COUBRIS, C., JONES, E. & MALLEFET, J. 2021. Red and white muscle proportions and enzyme activities in mesopelagic sharks. *Comparative Biochemistry and Physiology Part B: Biochemistry and Molecular Biology,* 256**,** 110649.

PIRAINO, S., BOERO, F., AESCHBACH, B. & SCHMID, V. 1996. Reversing the Life Cycle: Medusae Transforming into Polyps and Cell Transdifferentiation in Turritopsis nutricula (Cnidaria, Hydrozoa). *Biol Bull,* 190**,** 302-312.

PORTEIRO, F. M., SUTTON, T. T., BYRKJEDAL, I., ORLOV, A., HEINO, M. P., MENEZES, G. M. M. & BERGSTAD, O. A. 2017. Fishes of the Northern Mid-Atlantic Ridge collected during the MAR-ECO Cruise in June-July 2004. An annotated checklist.

PROTHERO, J. & JÜRGENS, K. D. 1987. Scaling of maximal life span in mammals: a review. *Basic Life Sci,* 42**,** 49-74.

PYLE, W. G. & SOLARO, R. J. 2004. At the crossroads of myocardial signaling: the role of Z-discs in intracellular signaling and cardiac function. *Circ Res,* 94**,** 296-305.

RAMAMURTHY, B., HÖÖK, P. & LARSSON, L. 1999. An overview of carbohydrate-protein interactions with specific reference to myosin and ageing. *Acta Physiol Scand,* 167**,** 327-9.

REBBECK, R. T., KARUNASEKARA, Y., BOARD, P. G., BEARD, N. A., CASAROTTO, M. G. & DULHUNTY, A. F. 2014. Skeletal muscle excitation-contraction coupling: who are the dancing partners? *Int J Biochem Cell Biol,* 48**,** 28-38.

REID, K. F., DOROS, G., CLARK, D. J., PATTEN, C., CARABELLO, R. J., CLOUTIER, G. J., PHILLIPS, E. M., KRIVICKAS, L. S., FRONTERA, W. R. & FIELDING, R. A. 2012. Muscle power failure in mobility-limited older adults: preserved single fiber function despite lower whole muscle size, quality and rate of neuromuscular activation. *Eur J Appl Physiol,* 112**,** 2289-301.

REID, K. F., PASHA, E., DOROS, G., CLARK, D. J., PATTEN, C., PHILLIPS, E. M., FRONTERA, W. R. & FIELDING, R. A. 2014. Longitudinal decline of lower extremity muscle power in healthy and mobility-limited older adults: influence of muscle mass, strength, composition, neuromuscular activation and single fiber contractile properties. *Eur J Appl Physiol,* 114**,** 29-39.

RODRIGUEZ-CABELLO, C., SÁNCHEZ, F. & VELASCO, F. 2005. Growth of lesser spotted dogfish (Scyliorhinus canicula L., 1758) in the Cantabrian Sea, based on tag-recapture data. *J Northwest Atl Fish Sci,* 37**,** 131-140.

ROLLAND, Y., ABELLAN VAN KAN, G., GILLETTE-GUYONNET, S. & VELLAS, B. 2011. Cachexia versus sarcopenia. *Curr Opin Clin Nutr Metab Care,* 14**,** 15-21.

ROMIJN, J. A., COYLE, E. F., SIDOSSIS, L. S., GASTALDELLI, A., HOROWITZ, J. F., ENDERT, E. & WOLFE, R. R. 1993. Regulation of endogenous fat and carbohydrate metabolism in relation to exercise intensity and duration. *American Journal of Physiology-Endocrinology and Metabolism,* 265**,** E380-E391.

ROSE, M. R. 1991. *Evolutionary biology of aging*, Oxford University Press on Demand.

ROSENBERG, I. H. 1997. Sarcopenia: origins and clinical relevance. *J Nutr,* 127**,** 990s-991s.

ROSSI, A. C., MAMMUCARI, C., ARGENTINI, C., REGGIANI, C. & SCHIAFFINO, S. 2010. Two novel/ancient myosins in mammalian skeletal muscles: MYH14/7b and MYH15 are expressed in extraocular muscles and muscle spindles. *J Physiol,* 588**,** 353-64.

ROTH, G., BLANKE, J. & WAKE, D. B. 1994. Cell size predicts morphological complexity in the brains of frogs and salamanders. *Proc Natl Acad Sci U S A,* 91**,** 4796-800.

RUSHTON, J. P. 1987. Toward a theory of human multiple birthing: sociobiology and r/K reproductive strategies. *Acta Genet Med Gemellol (Roma),* 36**,** 289-96.

RUSSELL, D. A., VANDERZWAAG, D. L., RUSSELL, D. A. & VANDERZWAAG, D. L. 2011. Recasting Transboundary Fisheries Management Arrangements in Light of Sustainability Principles: Canadian and International Perspectives. *Chapter 2. The International Law And Policy Seascape Governing Transboundary Fisheries.* Brill | Nijhoff.

RYAN, L. A., MEEUWIG, J. J., HEMMI, J. M., COLLIN, S. P. & HART, N. S. 2015. It is not just size that matters: shark cruising speeds are species-specific. *Marine Biology,* 162**,** 1307-1318.

S. HIKIDA, R. 2011. Aging Changes in Satellite Cells and Their Functions. *Current Aging Science,* 4**,** 279-297.

SAKUMA, K., AOI, W. & YAMAGUCHI, A. 2015. Current understanding of sarcopenia: possible candidates modulating muscle mass. *Pflugers Arch,* 467**,** 213-29.

SALTIN, B. 1983. Skeletal muscle adaptability: significance for metabolism and performance. *Skeletal muscle*.

SANTILLI, V., BERNETTI, A., MANGONE, M., PAOLONI, M. 2014. Clinical definition of sarcopenia. *Clinical Cases in Mineral and Bone Metabolism*

SANZ, A. & STEFANATOS, R. K. 2008. The mitochondrial free radical theory of aging: a critical view. *Curr Aging Sci,* 1**,** 10-21.

SCHIAFFINO, S., AUSONI, S., GORZA, L., SAGGIN, L., GUNDERSEN, K. & LOMO, T. 1988. Myosin heavy chain isoforms and velocity of shortening of type 2 skeletal muscle fibres. *Acta Physiol Scand,* 134**,** 575-6.

SCHIAFFINO, S., GORZA, L., SARTORE, S., SAGGIN, L., AUSONI, S., VIANELLO, M., GUNDERSEN, K. & LØMO, T. 1989. Three myosin heavy chain isoforms in type 2 skeletal muscle fibres. *J Muscle Res Cell Motil,* 10**,** 197-205.

SCHIAFFINO, S. & REGGIANI, C. 1994. Myosin isoforms in mammalian skeletal muscle. *Journal of Applied Physiology,* 77**,** 493-501.

SCHIAFFINO, S. & REGGIANI, C. 2011. Fiber types in mammalian skeletal muscles. *Physiol Rev,* 91**,** 1447-531.

SCHIAFFINO, S. A. R., C. 1996. Molecular Diversity of Myofibrillar Proteins: Gene Regulation and Functional Significance. *The American Naturalist*.

SCHUMANN, A. Y., BARTSCH, R. P., PENZEL, T., IVANOV, P. C. & KANTELHARDT, J. W. 2010. Aging effects on cardiac and respiratory dynamics in healthy subjects across sleep stages. *Sleep,* 33**,** 943-955.

SHADWICK, R. E. & GOLDBOGEN, J. A. 2012. Muscle function and swimming in sharks. *Journal of Fish Biology,* 80**,** 1904-1939.

SHIMOSE, T., YOKAWA, K., SAITO, H. & TACHIHARA, K. FAO species catalogue, vol 4. Sharks of the world. An annotated and illustrated catalogue of shark species known to date. Part 2. Carcharhiniformes FAO species catalogue, vol 4. Sharks of the world. An annotated and illustrated catalogue of shark species known to date. Part 2. Carcharhiniformes, 1984.

SIMPFENDORFER, C. A. & KYNE, P. M. 2009. Limited potential to recover from overfishing raises concerns for deep-sea sharks, rays and chimaeras. *Environmental Conservation,* 36**,** 97-103.

SIMS, D., NASH, J. & MORRITT, D. 2001. Movements and activity of male and female dogfish in a tidal sea lough: alternative behavioural strategies and apparent sexual segregation. *Marine Biology,* 139**,** 1165-1175.

SIMS, D. W., WEARMOUTH, V. J., SOUTHALL, E. J., HILL, J. M., MOORE, P., RAWLINSON, K., HUTCHINSON, N., BUDD, G. C., RIGHTON, D. & METCALFE, J. D. 2006. Hunt warm, rest cool: bioenergetic strategy underlying diel vertical migration of a benthic shark. *Journal of Animal Ecology,* 75**,** 176-190.

SJØGAARD, G. 1982. Capillary supply and cross-sectional area of slow and fast twitch muscle fibres in man. *Histochemistry,* 76**,** 547-55.

SMITH, S. E., AU, D. W. & SHOW, C. 1998. Intrinsic rebound potentials of 26 species of Pacific sharks. *Marine and Freshwater Research,* 49**,** 663-678.

SOARES, K. D. A. & CARVALHO, M. R. 2019. The catshark genus Scyliorhinus (Chondrichthyes: Carcharhiniformes: Scyliorhinidae): taxonomy, morphology and distribution. *Zootaxa,* 4601**,** zootaxa.4601.1.1.

SPAMER, C. & PETTE, D. 1977. Activity patterns of phosphofructokinase, glyceraldehydephosphate dehydrogenase, lactate dehydrogenase and malate dehydrogenase in microdissected fast and slow fibres from rabbit psoas and soleus muscle. *Histochemistry,* 52**,** 201-16.

SPEERS-ROESCH, B. & TREBERG, J. R. 2010. The unusual energy metabolism of elasmobranch fishes. *Comparative Biochemistry and Physiology Part A: Molecular & Integrative Physiology,* 155**,** 417-434.

STARK, G. & MEIRI, S. 2018. Cold and dark captivity: Drivers of amphibian longevity. *Global Ecology and Biogeography,* 27**,** 1384-1397.

STE-MARIE, E., WATANABE, Y. Y., SEMMENS, J. M., MARCOUX, M. & HUSSEY, N. E. 2020. A first look at the metabolic rate of Greenland sharks (Somniosus microcephalus) in the Canadian Arctic. *Sci Rep,* 10**,** 19297.

STE-MARIE, E., WATANABE, Y. Y., SEMMENS, J. M., MARCOUX, M. & HUSSEY, N. E. 2022. Life in the slow lane: field metabolic rate and prey consumption rate of the Greenland shark (Somniosus microcephalus) modelled using archival biologgers. *J Exp Biol,* 225.

STENVINKEL, P., AVESANI, C. M., GORDON, L. J., SCHALLING, M. & SHIELS, P. G. 2021. Biomimetics provides lessons from nature for contemporary ways to improve human health. *J Clin Transl Sci,* 5**,** e128.

STENVINKEL, P. & SHIELS, P. 2019. Long-lived animals with negligible senescence: Clues for ageing research. *Biochemical Society Transactions,* 47**,** BST20190105.

STEWART, M. A., FRANKS-SKIBA, K., CHEN, S. & COOKE, R. 2010. Myosin ATP turnover rate is a mechanism involved in thermogenesis in resting skeletal muscle fibers. *Proceedings of the National Academy of Sciences,* 107**,** 430-435.

SULLIVAN, K. & SOMERO, G. 1980. Enzyme activities of fish skeletal muscle and brain as influenced by depth of occurrence and habits of feeding and locomotion. *Marine Biology,* 60**,** 91-99.

SWEENEY, H. L. & STULL, J. T. 1990. Alteration of cross-bridge kinetics by myosin light chain phosphorylation in rabbit skeletal muscle: implications for regulation of actin-myosin interaction. *Proc Natl Acad Sci U S A,* 87**,** 414-8.

TACUTU, R., THORNTON, D., JOHNSON, E., BUDOVSKY, A., BARARDO, D., CRAIG, T., DIANA, E., LEHMANN, G., TOREN, D., WANG, J., FRAIFELD, V. E. & MAGALHÃES, J. P. D. 2018. Human Ageing Genomic Resources: New and updated databases. Oxford University Press.

TERRIER, P. & DÉRIAZ, O. 2011. Kinematic variability, fractal dynamics and local dynamic stability of treadmill walking. *Journal of neuroengineering and rehabilitation,* 8**,** 1-14.

THOLLOT, P. 1996. *Les poissons de mangrove du lagon sud-ouest de Nouvelle-Calédonie*, IRD Editions.

TIMSON, D. J. 2003. Fine tuning the myosin motor: the role of the essential light chain in striated muscle myosin. *Biochimie,* 85**,** 639-45.

TOWER, J. 2017. Sex-Specific Gene Expression and Life Span Regulation. *Trends Endocrinol Metab,* 28**,** 735-747.

TREBERG, J. R., MARTIN, R. A. & DRIEDZIC, W. R. 2003. Muscle enzyme activities in a deep-sea squaloid shark, Centroscyllium fabricii, compared with its shallow-living relative, Squalus acanthias. *Journal of Experimental Zoology Part A: Comparative Experimental Biology,* 300**,** 133-139.

TUMASIAN, R. A., 3RD, HARISH, A., KUNDU, G., YANG, J. H., UBAIDA-MOHIEN, C., GONZALEZ-FREIRE, M., KAILEH, M., ZUKLEY, L. M., CHIA, C. W., LYASHKOV, A., WOOD, W. H., 3RD, PIAO, Y., COLETTA, C., DING, J., GOROSPE, M., SEN, R., DE, S. & FERRUCCI, L. 2021. Skeletal muscle transcriptome in healthy aging. *Nat Commun,* 12**,** 2014.

VASTO, S., SCAPAGNINI, G., BULATI, M., CANDORE, G., CASTIGLIA, L., COLONNA-ROMANO, G., LIO, D., NUZZO, D., PELLICANO, M. & RIZZO, C. 2010. Biomarkes of aging. *Frontiers in Bioscience-Scholar,* 2**,** 392-402.

VÉLEZ-ZUAZO, X. & AGNARSSON, I. 2011. Shark tales: a molecular species-level phylogeny of sharks (Selachimorpha, Chondrichthyes). *Mol Phylogenet Evol,* 58**,** 207-17.

VINOGRADOV, A. E. 1997. NUCLEOTYPIC EFFECT IN HOMEOTHERMS: BODY-MASS INDEPENDENT RESTING METABOLIC RATE OF PASSERINE BIRDS IS RELATED TO GENOME SIZE. *Evolution,* 51**,** 220-225.

VØLLESTAD, N. K., TABATA, I. & MEDBØ, J. I. 1992. Glycogen breakdown in different human muscle fibre types during exhaustive exercise of short duration. *Acta Physiol Scand,* 144**,** 135-41.

VØLLESTAD, N. K., VAAGE, O. & HERMANSEN, L. 1984. Muscle glycogen depletion patterns in type I and subgroups of type II fibres during prolonged severe exercise in man. *Acta Physiol Scand,* 122**,** 433-41.

WADA M., K., S. Distribution of myosin isofoforms in skeletal muscle: various kinds, functional significance, and training-induced change.

WATANABE, Y. Y., LYDERSEN, C., FISK, A. T. & KOVACS, K. M. 2012. The slowest fish: Swim speed and tail-beat frequency of Greenland sharks. *Journal of Experimental Marine Biology and Ecology,* 426-427**,** 5-11.

WEIBEL, E. R. 2013. The structural conditions for oxygen supply to muscle cells: the Krogh cylinder model. *J Exp Biol,* 216**,** 4135-7.

WEISLEDER, N., BROTTO, M., KOMAZAKI, S., PAN, Z., ZHAO, X., NOSEK, T., PARNESS, J., TAKESHIMA, H. & MA, J. 2006. Muscle aging is associated with compromised Ca2+ spark signaling and segregated intracellular Ca2+ release. *J Cell Biol,* 174**,** 639-45.

WELLE, S. 2002. Cellular and Molecular Basis of Age-Related Sarcopenia. *Canadian Journal of Applied Physiology,* 27**,** 19-41.

WILKINS, J. T., KRIVICKAS, L. S., GOLDSTEIN, R., SUH, D. & FRONTERA, W. R. 2001. Contractile properties of adjacent segments of single human muscle fibers. *Muscle Nerve,* 24**,** 1319-26.

WILLIAMS, G. 1957. Pleiotropy, natural selection, and the evolution of senescence. Evolution (NY) 11: 398.

YAMADA, M., MORIGUCH, Y., MITANI, T., AOYAMA, T. & ARAI, H. 2014. Age-dependent changes in skeletal muscle mass and visceral fat area in Japanese adults from 40 to 79 years-of-age. *Geriatr Gerontol Int,* 14 Suppl 1**,** 8-14.

YAN, Z., LIRA, V. A. & GREENE, N. P. 2012. Exercise training-induced regulation of mitochondrial quality. *Exerc Sport Sci Rev,* 40**,** 159-64.

YANO, K., STEVENS, J. & COMPAGNO, L. 2007. Distribution, reproduction and feeding of the Greenland shark Somniosus (Somniosus) microcephalus, with notes on two other sleeper sharks, Somniosus (Somniosus) pacificus and Somniosus (Somniosus) antarcticus. *Journal of fish biology,* 70**,** 374-390.

YIN, D. & CHEN, K. 2005. The essential mechanisms of aging: Irreparable damage accumulation of biochemical side-reactions. *Experimental gerontology,* 40**,** 455-465.

ZHU, Y., TCHKONIA, T., PIRTSKHALAVA, T., GOWER, A. C., DING, H., GIORGADZE, N., PALMER, A. K., IKENO, Y., HUBBARD, G. B., LENBURG, M., O'HARA, S. P., LARUSSO, N. F., MILLER, J. D., ROOS, C. M., VERZOSA, G. C., LEBRASSEUR, N. K., WREN, J. D., FARR, J. N., KHOSLA, S., STOUT, M. B., MCGOWAN, S. J., FUHRMANN-STROISSNIGG, H., GURKAR, A. U., ZHAO, J., COLANGELO, D., DORRONSORO, A., LING, Y. Y., BARGHOUTHY, A. S., NAVARRO, D. C., SANO, T., ROBBINS, P. D., NIEDERNHOFER, L. J. & KIRKLAND, J. L. 2015. The Achilles' heel of senescent cells: from transcriptome to senolytic drugs. *Aging Cell,* 14**,** 644-58.

Other Sources

LATLONG. 2022. *Convert Lat and Long to DMS* [Online]. Available: https://www.latlong.net/lat-long-dms.html [Accessed 26.10. 2022,].

LEONARD P. GUARENTE, P. S., KARA ROGERS. 2022. *Aging at the molecular and cellular levels* [Online]. Available: https://www.britannica.com/science/aging-life-process/Changes-in-tissue-and-cell-morphology [Accessed 26.10. 2022,].

ORGANIZATION, W. H. 2019a. Available: http://apps.who.int/medicinedocs/en/m/abstract/Js18806en/ [Accessed 26.10. 2022,].

ORGANIZATION, W. H. 2019b. *The top 10 causes of death* [Online]. Available: https://www.who.int/news-room/fact-sheets/detail/the-top-10-causes-of-death [Accessed 26.10. 2022,].

UNIPROT. 2022. *Myosin heavy chain shark* [Online]. Available: https://www.uniprot.org/uniprotkb?dir=descend&query=myosin%20heavy%20chain%20shark&sort=organism_name [Accessed 26.10. 2022,].

List of figures

List of tables

Supplementary data

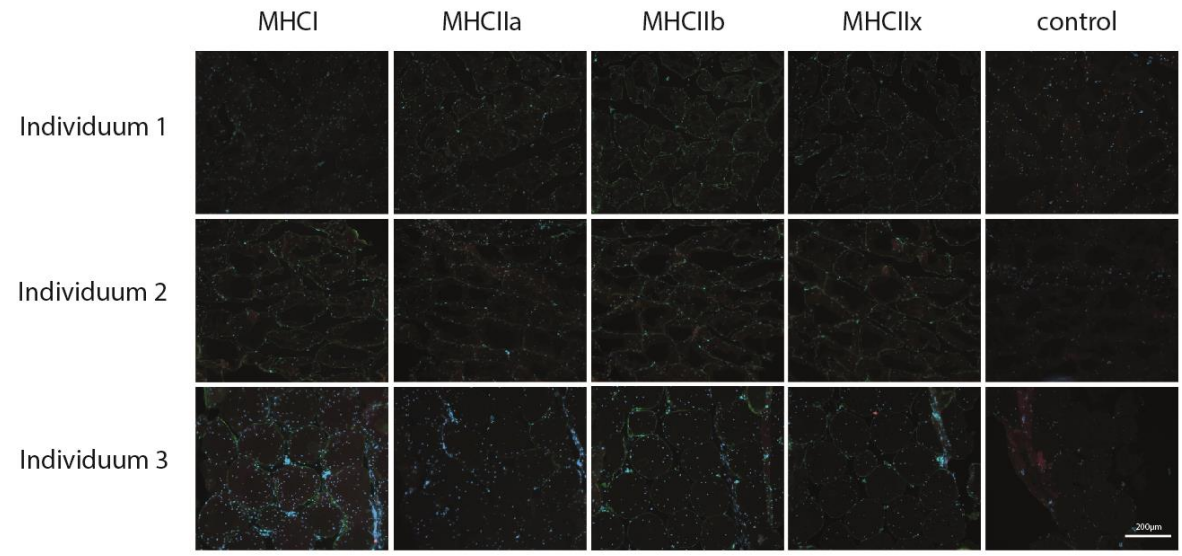

Smallspotted Catshark white muscle: 10x magnification:
blue channel: DAPI staining for nuclei; red channel: anti-MHC staining for myofibre typing;
green channel: anti-laminin staining for laminin as a cell membrane measurement.

Figure 18: Small-spotted catshark white muscle cryosections. *Images were taken with ZEISS Stereo-Microscope Stemi 508.*

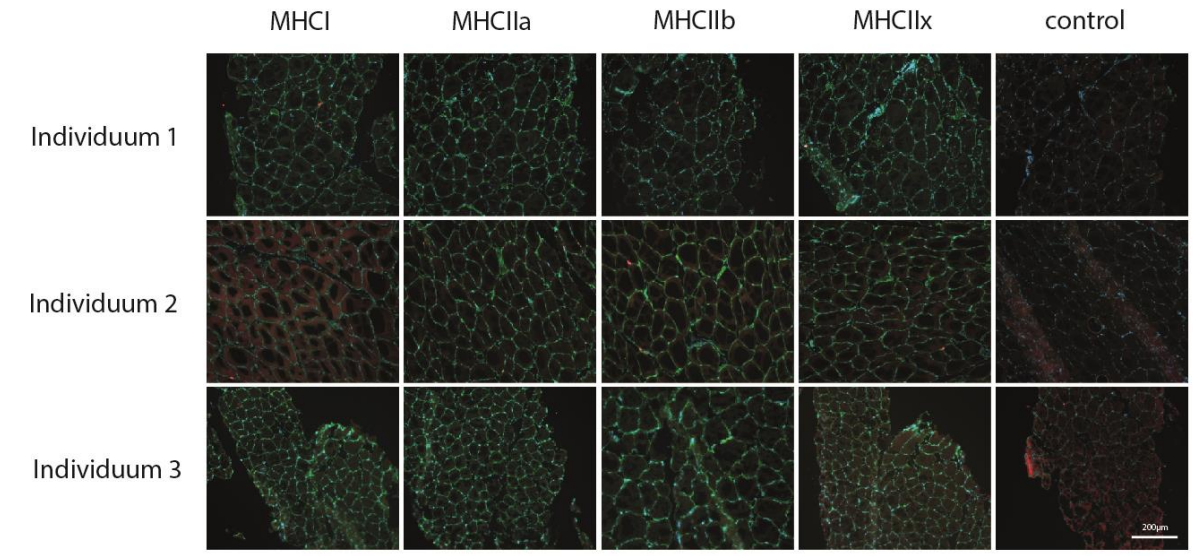

Smallspotted Catshark red muscle: 10x magnification (20x for individuum 3 MHCIIb):
blue channel: DAPI staining for nuclei; red channel: anti-MHC staining for myofibre typing;
green channel: anti-laminin staining for laminin as a cell membrane measurement.

Figure 19: Small-spotted catshark red muscle cryosections. *Images were taken with ZEISS Stereo-Microscope Stemi 508.*

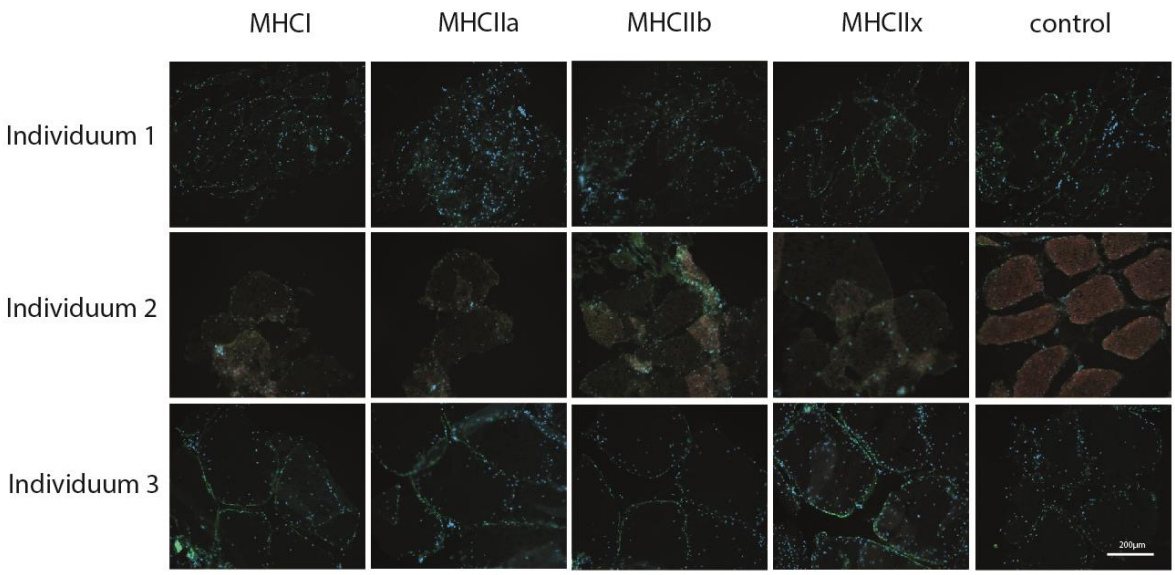

Greenland shark white muscle: 10x magnification:
blue channel: DAPI staining for nuclei; red channel: anti-MHC staining for myofibre typing;
green channel: anti-laminin staining for laminin as a cell membrane measurement.

Figure 20: Greenland shark white muscle cryosections. *Images were taken with ZEISS Stereo-Microscope Stemi 508.*

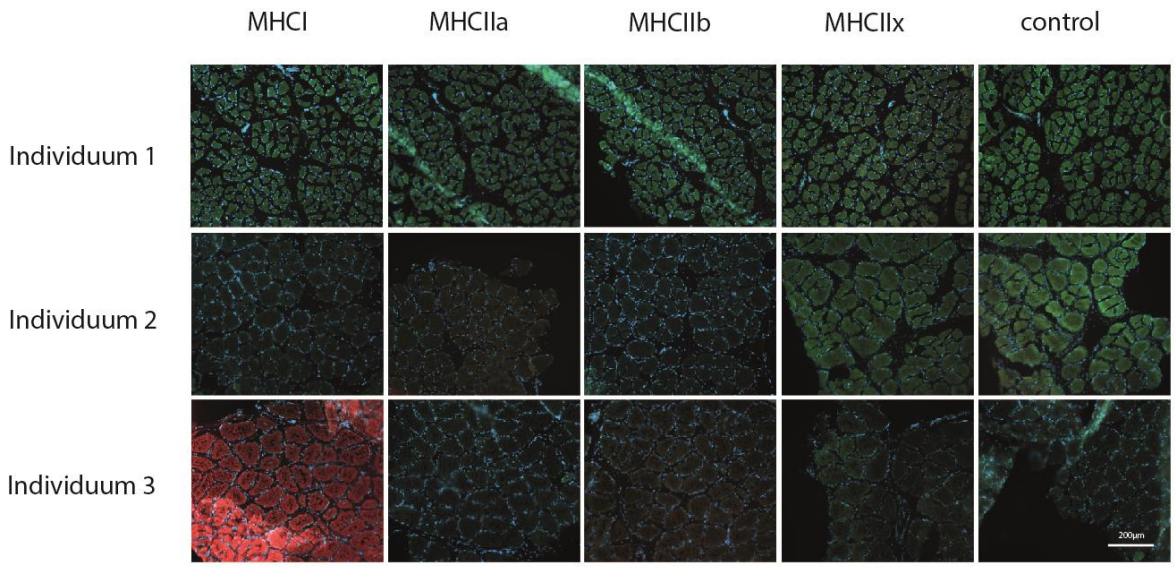

Greenlands shark red muscle: 10x magnification:
blue channel: DAPI staining for nuclei; red channel: anti-MHC staining for myofibre typing;
green channel: anti-laminin staining for laminin as a cell membrane measurement.

Figure 21: Greenland shark red muscle cryosections. *Images were taken with ZEISS Stereo-Microscope Stemi 508.*

Table 3: Average number of nuclei per fibre per sample.

	Average number of nuclei per myofiber
GL 1 red	4,027887
GL 2 red	5,470076
GL 3 red	10,16893
GL 1 white	14,85625
GL 2 white	18,69333
GL 3 white	45,25
SD 1 red	6,538026
SD 2 red	8,367683
SD 7 red	6,554546
SD 1 white	16,44626
SD 2 white	12,94872
SD 7 white	21,09558

Table 4: Average nuclei count per fibre per tissue.

	Average number of nuclei per myofiber
GL red	6,55563
GL white	26,26653
SD red	7,153418
SD white	16,83019

Table 5: Statistical test results for fiber area and diameter.

		P value	P value summary	Significantly different (P < 0.05)?	One- or two-tailed P value?	R squared (eta squared)	Test
Fiber area	SD red vs. GL red	<0.0001	****	Yes	Two-tailed	0.1174	Unpaired t-test
	SD white vs. GL white	<0.0001	****	Yes	Two-tailed	0.8778	Unpaired t-test
Fiber diameter	SD red vs. GL red	<0.0001	****	Yes	Two-tailed	0.1293	Unpaired t-test
	SD white vs. GL white	<0.0001	****	Yes	Two-tailed	0.8133	Unpaired t-test

Table 6: Mean fiber area per tissue.

	Mean fiber area in um^2
SD red	1351
GL red	2380
SD white	15710
GL white	94976

Table 7: Mean fiber area per tissue.

	Mean feret´s diameter/fiber in um
SD red	68.38

GL red	51.57
SD white	177.4
GL white	420.3

Ich habe mich bemüht, sämtliche Inhaber*innen der Bildrechte ausfindig zu machen und ihre Zustimmung zur Verwendung der Bilder in dieser Arbeit eingeholt. Sollte dennoch eine Urheberrechtsverletzung bekannt werden, ersuche ich um Meldung bei mir.